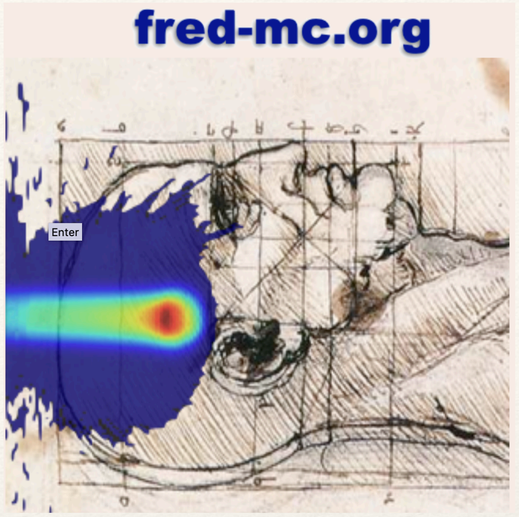

Development of tools for quality control on therapeutic carbon beams with a fast MC code (FRED)

Candidate: **Micol De Simoni**

Supervisor: **Prof. Vincenzo Patera**
Co-Supervisor: **Prof. Angelo Schiavi**

PhD "Accelerator Physics", XXXIII cycle
"Sapienza", University of Rome

Particle Therapy (PT)

PT is a non-invasive technique for deep or radio-resistant tumor treatments performed with protons or light ions, aiming to deliver a high precision treatment. Compared to conventional radiotherapy, ions allow for a higher dose deposition in the tumor region while sparing the surrounding healthy tissue.

The **biological damage** is related to the **absorbed energy**, **ionization density** and **type of projectile used**.

$$D = \frac{dE}{dm} \left[1Gy = 1\frac{J}{kg}\right]$$

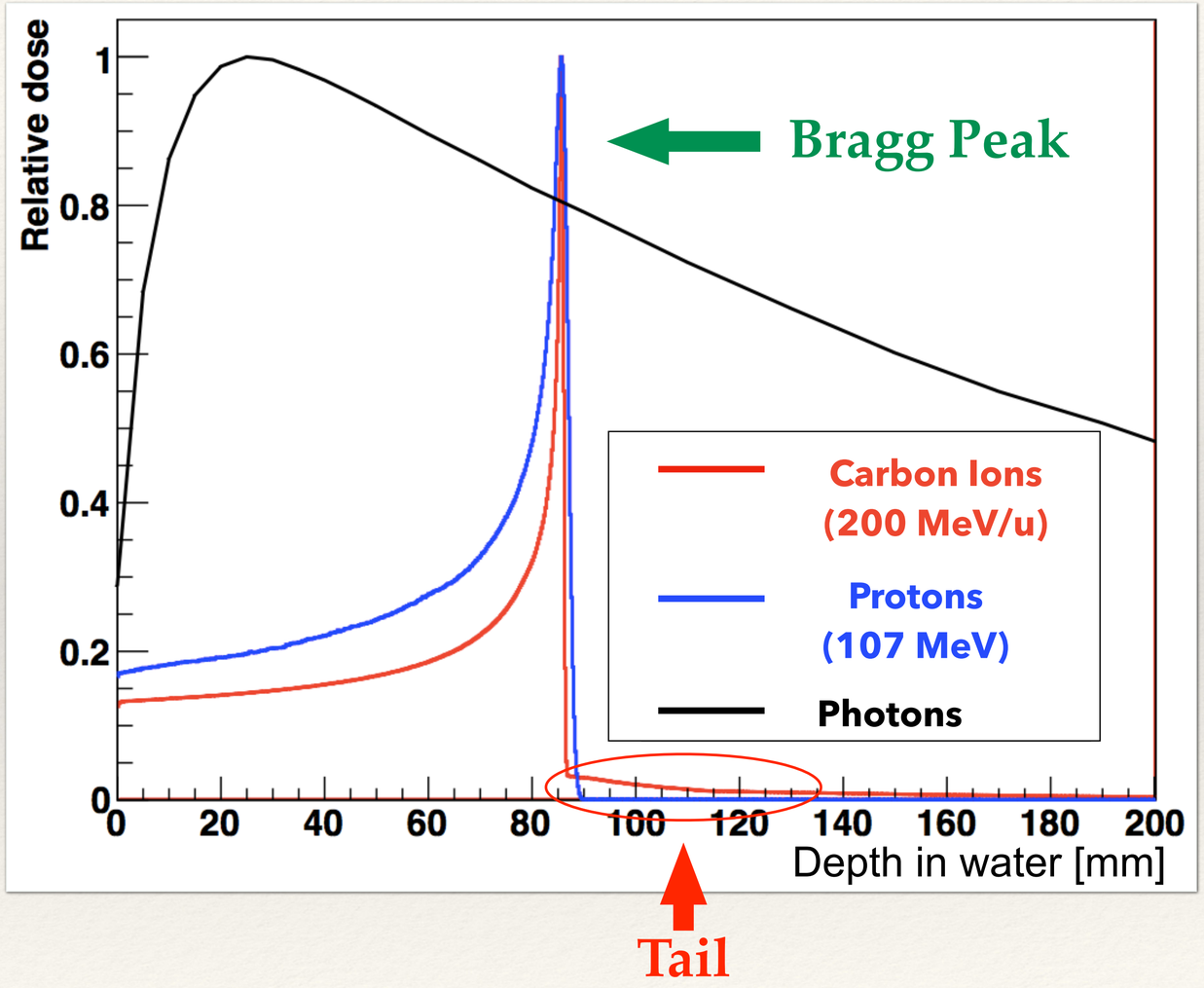

Particle Therapy (PT)

To cover the entire tumor volume, an overlap of beams at different energies is used obtaining a wider irradiation profile:

SOBP (Spread Out Bragg Peak)

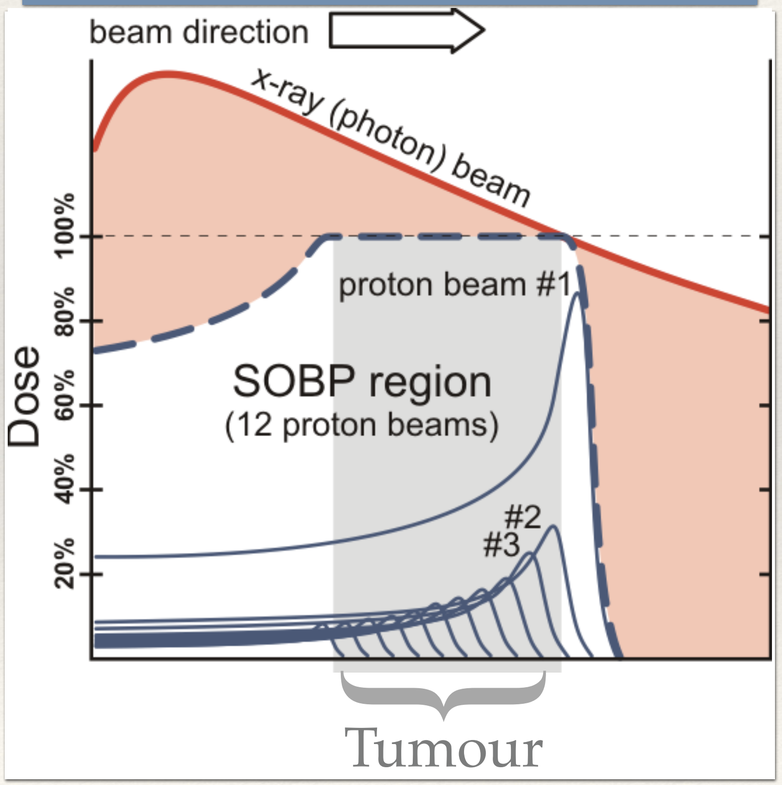

Dose release control at the min level demands for an **accelerator control system of absolute precision and reliability** since benefit for the patient can only be achieved if the treatment is delivered exactly as planned.

proton treatment
(2 proton beams)

photon treatment
(5 photon beams)

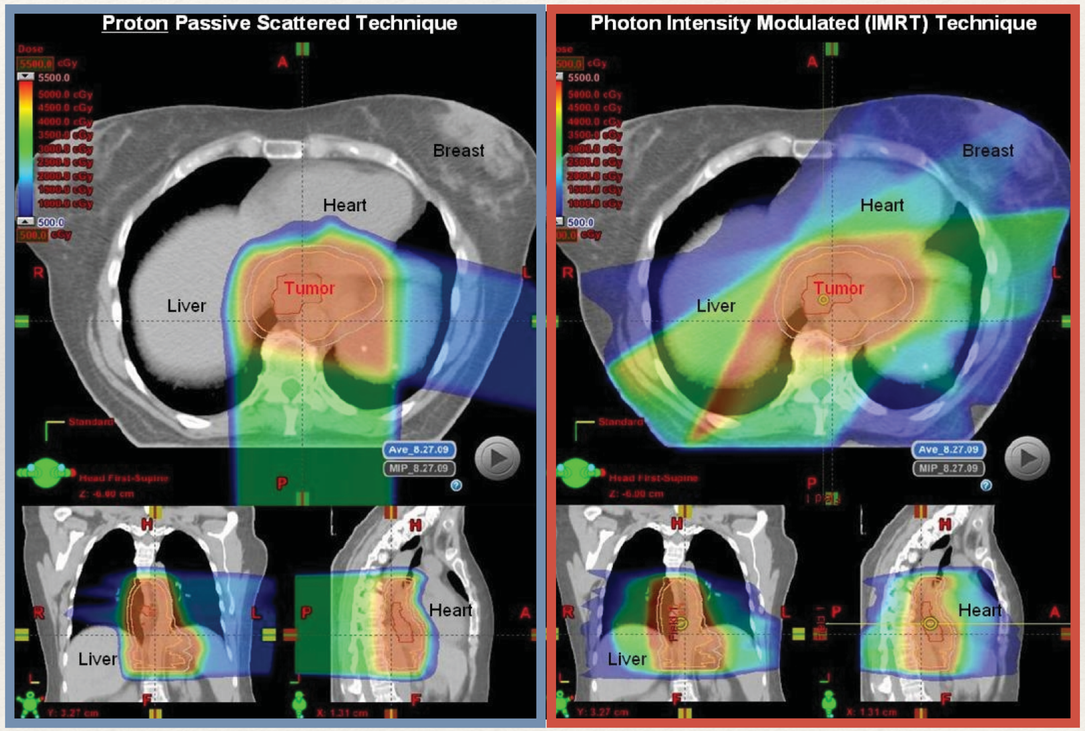

S. H. Lin, in Cancer, Volume 3 (2011), pp. 490-4101

Treatment Planning System

(required) Kinetic Energy (MeV)	Stopping Power (MeV cm²/g)			Range		
	Electronic	Nuclear	Total	CSDA (g/cm²)	Projected (g/cm²)	Detour Factor Projected / CSDA
1.000E-03	1.337E+02	4.315E+01	1.769E+02	6.319E-06	2.878E-06	0.4555
1.500E-03	1.638E+02	3.460E+01	1.984E+02	8.969E-06	4.400E-06	0.4906
2.000E-03	1.891E+02	2.927E+01	2.184E+02	1.137E-05	5.909E-06	0.5197
2.500E-03	2.114E+02	2.557E+01	2.370E+02	1.357E-05	7.380E-06	0.5440
3.000E-03	2.316E+02	2.281E+01	2.544E+02	1.560E-05	8.811E-06	0.5647
4.000E-03	2.675E+02	1.894E+01	2.864E+02	1.930E-05	1.155E-05	0.5986
5.000E-03	2.990E+02	1.631E+01	3.153E+02	2.262E-05	1.415E-05	0.6254
6.000E-03	3.276E+02	1.439E+01	3.420E+02	2.567E-05	1.661E-05	0.6473
7.000E-03	3.538E+02	1.292E+01	3.667E+02	2.849E-05	1.896E-05	0.6656
8.000E-03	3.782E+02	1.175E+01	3.900E+02	3.113E-05	2.121E-05	0.6813
9.000E-03	4.012E+02	1.080E+01	4.120E+02	3.363E-05	2.337E-05	0.6950
1.000E-02	4.229E+02	1.000E+01	4.329E+02	3.599E-05	2.545E-05	0.7070
1.250E-02	4.6					
1.500E-02	5					
1.750E-02	5					
2.000E-02	5					
2.250E-02	5					
2.500E-02	5					
2.750E-02	6					
3.000E-02	6					
3.500E-02	6					
4.000E-02	7					
4.500E-02	7					

Table of:

- dE vs E_{beam} , x, y, z
- RBE vs E_{beam}, dE, x, y, z

Patient anatomic data (CT, MRI, PET)

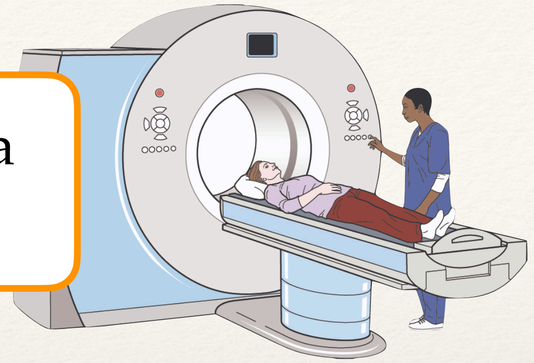

Physician Prescription

TPS

	% of Volume	Prescription/tolerance dose (Gy)	Relative importance
Prostate PTV	100	74.0	1.0
Prostate PTV	5.0	72.0	1.0
Prostate PTV	10.0	76.0	1.0
Rectum	90.0	10.0	0.5
Rectum	50.0	20.0	0.5
Rectum	10.0	30.0	0.5
Bladder	90.0	10.0	0.2
Bladder	50.0	20.0	0.2
Bladder	10.0	30.0	0.2
Femoral heads	90.0	10.0	0.2
Femoral heads	50.0	20.0	0.2
Femoral heads	10.0	40.0	0.2

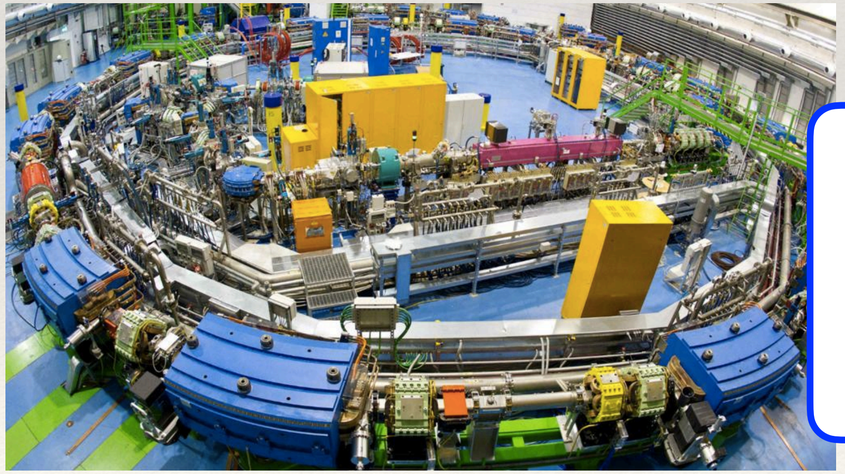

Accelerators Parameters: Fluences for each beam spot

Features of the accelerator

TPS provides to the accelerator control system an input file, called raster file, with information about:

- type of projectile (mostly protons or carbon ions);
- presence of ripplefilter (to scatter the beam);
- number of different energies needed;
- total number of particles;
- For each energy: number of particles, position, intensity, FWHM and direction of the beams.

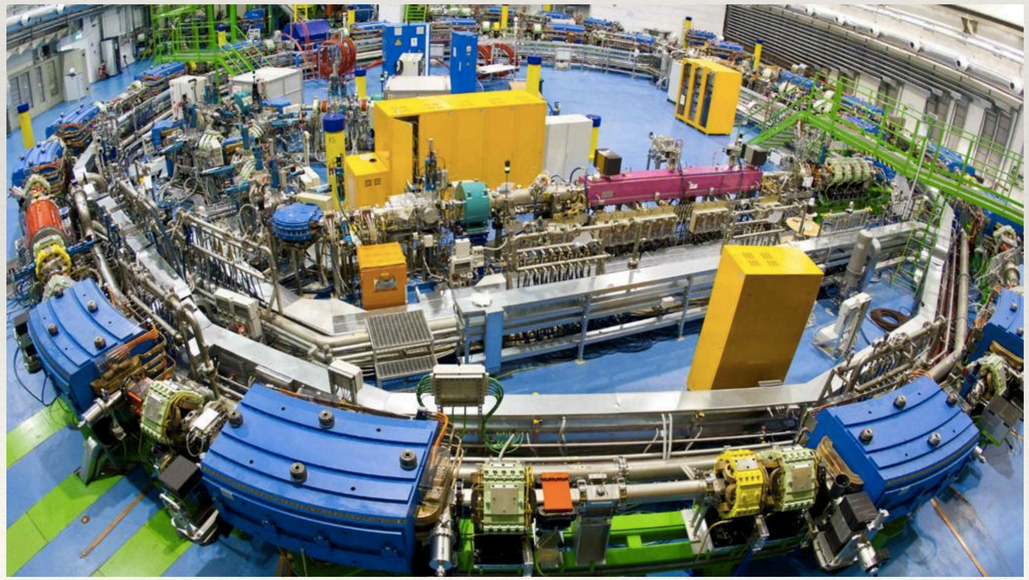

CNAO (Pavia) Synchrotron

```
patient_id none
machine# 0
projectile 12C
charge 6
mass 12
bolus 0
ripplefilter 0
#submachines 14
#particles 21531.5 333787 2.03959E+08
submachine# 57 186.57 2 6.9
#particles 32280.4 32280.4 7.2631E+06
stepsize 2 2
#points 225
14 14 32280.4
12 14 32280.4
10 14 32280.4
8 14 32280.4
6 14 32280.4
4 14 32280.4
2 14 32280.4
0 14 32280.4
-2 14 32280.4
-4 14 32280.4   • • •
```

Example of raster file of CNAO

~50 patients a day: for each one a patient-specific set of particle beams is needed.

Treatment Planning System

ANALYTIC TPS

- Fast (~ 1 h/core, minutes on GPU)
- Simplified beam-body interaction model using a 3D water equivalent representation of the patient morphology

Routinely used in PT treatment

MC TPS (for instance FLUKA and TOPAS/Geant4)

- Slow (~ days/core)
- Explicitly take into account the details in the interaction of particles with human tissues

Only used to check treatment plans for a restricted number of difficult cases

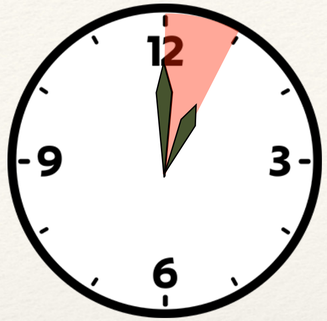

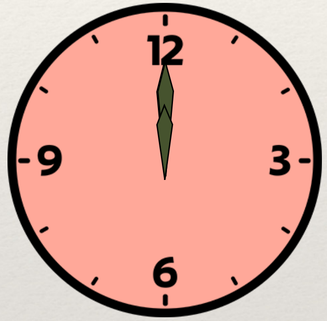

Treatment Planning System

ANALYTIC TPS

- Fast (~ 1 h/core, minutes on GPU)
- Simplified beam-body interaction model using a 3D water equivalent representation of the patient morphology

Routinely used in PT treatment

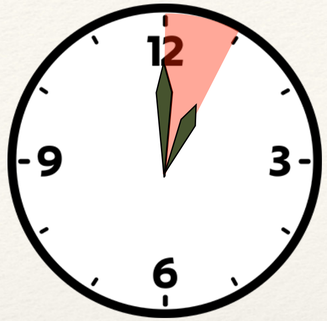

MC TPS (for instance FLUKA and TOPAS/Geant4)

- Slow (~ days/core)
- Explicitly take into account the details in the interaction of particles with human tissues

Only used to check treatment plans for a restricted number of difficult cases

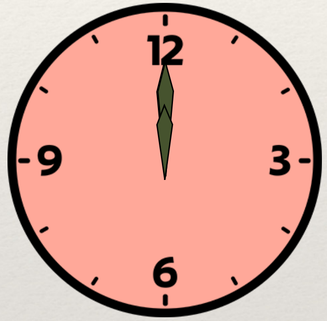

FAST MC: FRED
(Fast paRticle thErapy Dose evaluator)

NEW!!

- Fast (few minutes)
- Takes into account the details in the interaction of particles with human tissues that are needed for a TPS

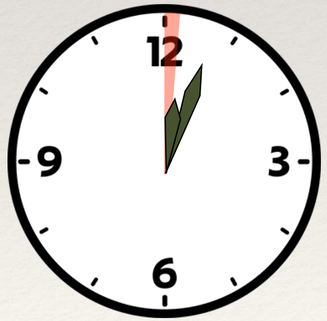

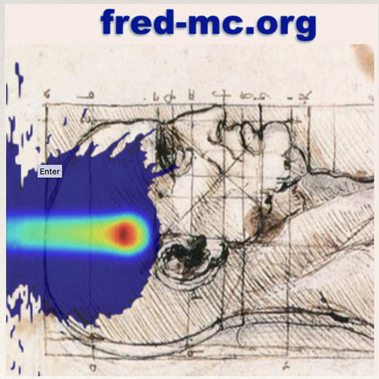

FRED as tool for quality control

Analytic TPS are periodically tested to verify the software.

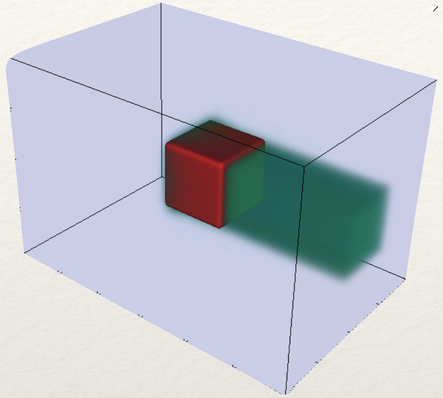

For this purpose, the accelerator delivers the beams in a tank full of water following the TPS instructions and the dose is measured in different points of the target with ionization chambers.

FRED can be used to verify that the analytic TPS is correct comparing the two simulations instead of delivering the beam with the accelerator.

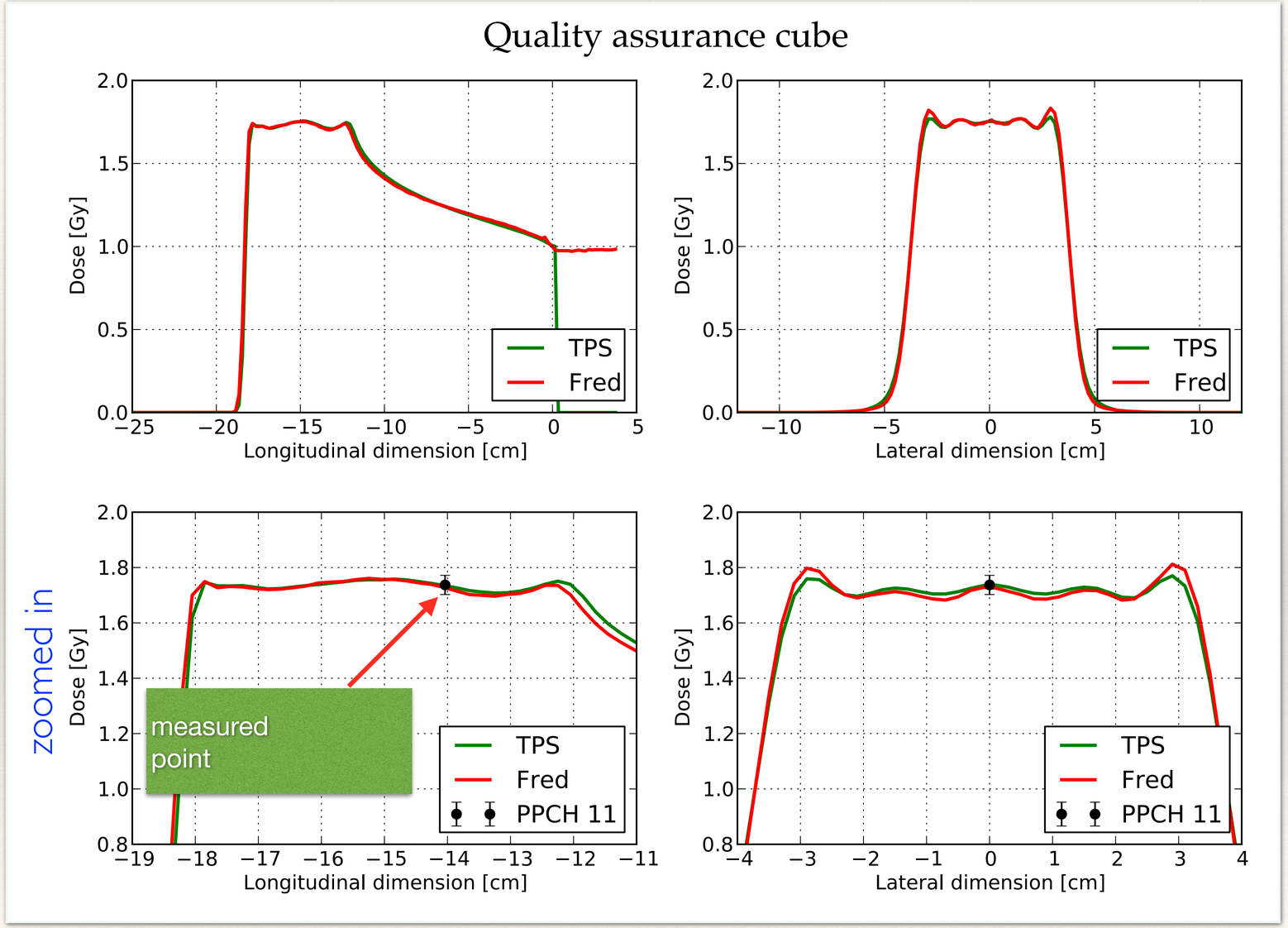

Carbon Therapy

FRED is already used in proton therapy as a quality assurance tool in the clinical center of Maastricht and Krakow and as a research tool at several clinical and research centers in Europe (Krakow, Trento, Maastricht, Lyon and PSI)

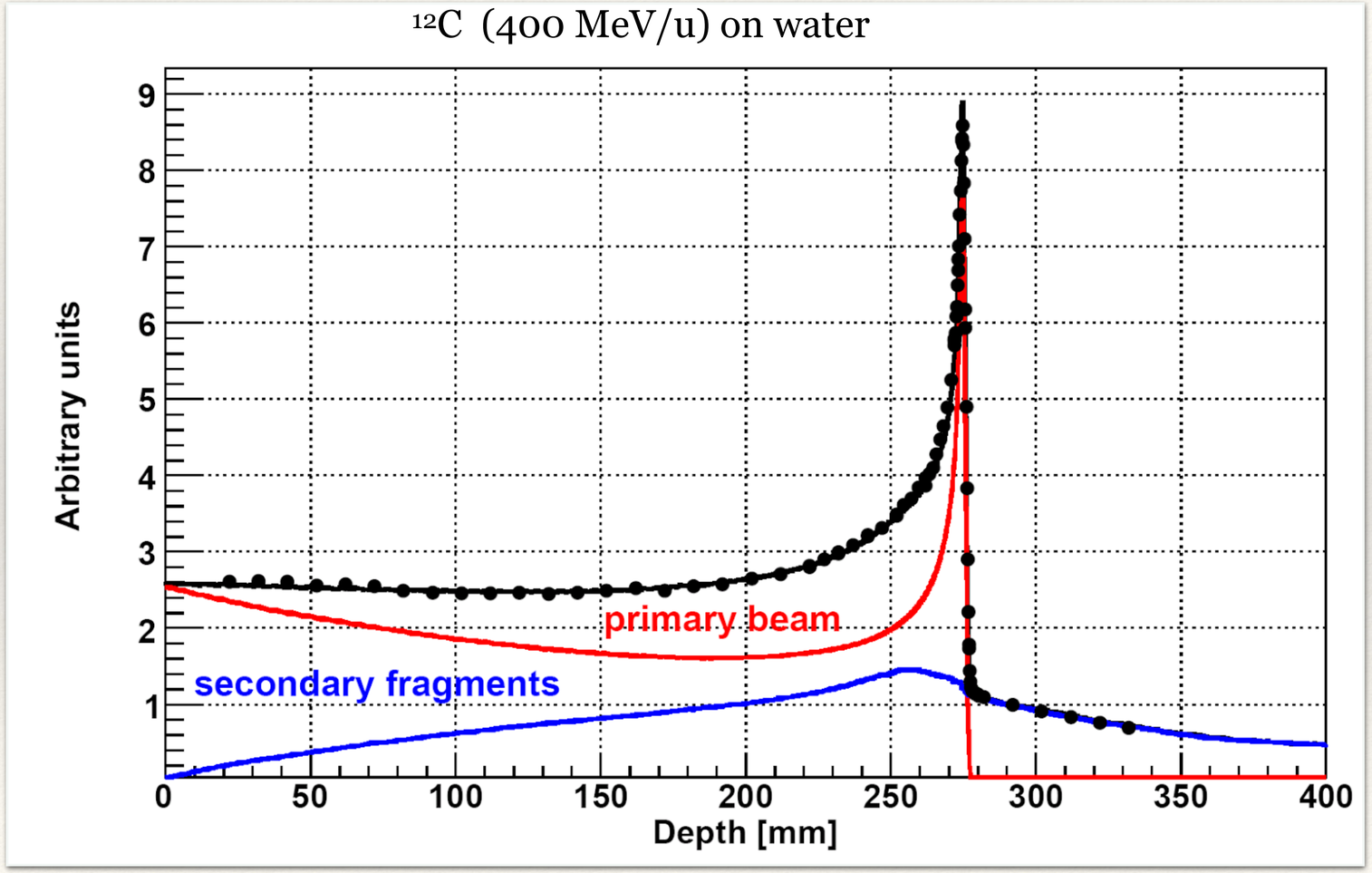

Interest of CNAO and MedAustron for the use of FRED in carbon Therapy

fondazione CNAO

MedAustron

My PhD thesis!

- Mitigation and attenuation of the primary beam
- Different biological effectiveness of the fragments wrt the beam
- Different fragment ranges

Features of a fast-MC code

I developed the code to balance dose release accuracy in the therapeutic energy, calculation time, and GPU execution guidelines:

Features of a fast-MC code

I developed the code to balance dose release accuracy in the therapeutic energy, calculation time, and GPU execution guidelines:

- Already existent full-MC can not run on GPU → **Code developed on scratch to run on GPU**

Features of a fast-MC code

I developed the code to balance dose release accuracy in the therapeutic energy, calculation time, and GPU execution guidelines:

- Already existent full-MC can not run on GPU → **Code developed on scratch to run on GPU**

- Where possible, the code was **based on data** → Easily updatable! (waiting for i.e. results of FOOT experimet)

Features of a fast-MC code

I developed the code to balance dose release accuracy in the therapeutic energy, calculation time, and GPU execution guidelines:

- Already existent full-MC can not run on GPU → **Code developed on scratch to run on GPU**

- Where possible, the code was **based on data** → Easily updatable! (waiting for i.e. results of FOOT experimet)

- Generation made for **different particles** and for **different energies** → Double differential cross-section needed

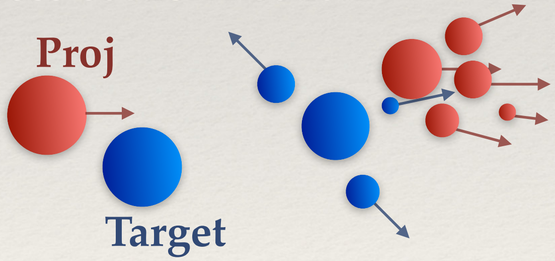

Features of a fast-MC code

I developed the code to balance dose release accuracy in the therapeutic energy, calculation time, and GPU execution guidelines:

- Already existent full-MC can not run on GPU → **Code developed on scratch to run on GPU**
- Where possible, the code was **based on data** → Easily updatable! (waiting for i.e. results of FOOT experimet)
- Generation made for **different particles** and for **different energies** → Double differential cross-section needed

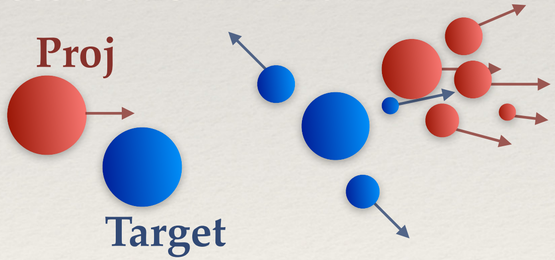

- **Lack of experimental data** at the energies of interest in medical physics → GANIL experiment

Dudouet. J. et al. Phys Rev C 88 (2013)

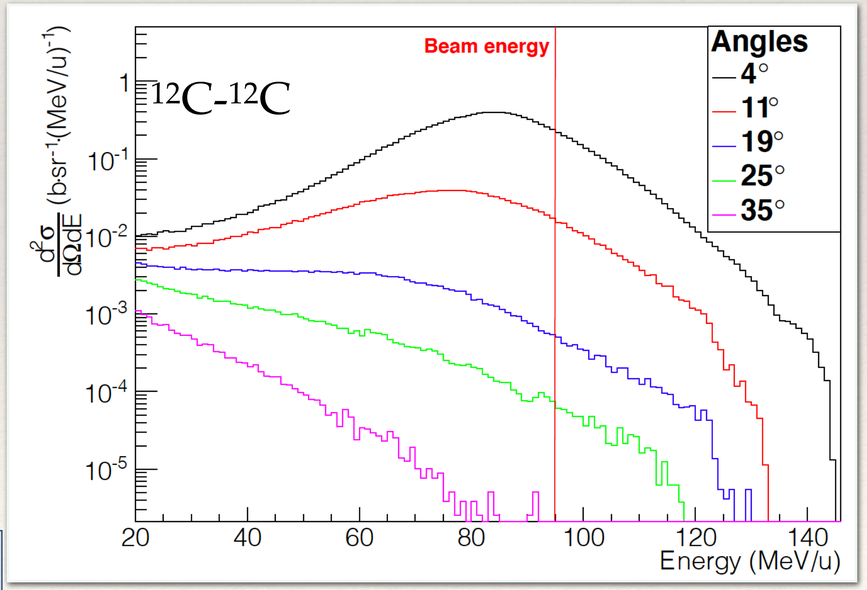

My PhD work

- **Ionization energy loss** (Bethe-Bloch, Gaussian approximation, Vavilov and Landau distributions)
- **Multiple Coulomb Scattering** (theory of Moliére adding a scaling factor following Fippel and Soukup approach)

- **Nuclear Model** (phenomenologic approach based on Ganil measurement at 95 MeV/u)**:**
  - **Coefficient of mass attenuation** to decide when there is an elastic and non-elastic event. Based on data found in literature;
  - **Sampling of the fragments** and their **energy and angle distributions**. Based on double differential cross-section measurements;

- **Biological Dose and Relative Biological Effectiveness** (LEM1 model)

My PhD work

Beam

- **Ionization energy loss** (Bethe-Bloch, Gaussian approximation, Vavilov and Landau distributions)
- **Multiple Coulomb Scattering** (theory of Moliére adding a scaling factor following Fippel and Soukup approach)

Beam and Frag.

- **Nuclear Model** (phenomenologic approach based on Ganil measurement at 95 MeV/u)**:**
  - **Coefficient of mass attenuation** to decide when there is an elastic and non-elastic event. Based on data found in literature;
  - **Sampling of the fragments** and their **energy and angle distributions**. Based on double differential cross-section measurements;

D_{bio} and RBE

- **Biological Dose and Relative Biological Effectiveness** (LEM1 model)

Result

Comparison with :

- full MC (FLUKA);
- experiments found in literature.

Coefficient of Mass Attenuation

$$\frac{\mu}{\rho} = \sum_i \frac{N_A w_i \sigma_i}{A_i}$$

Non-elastic cross-section
σ(C-C) and **σ(C-H)** obtained from a fit on data;

Zhang H. Y. et al. Nucl. Phys. 707 (2002)

Takechi M. et al. Phys. Rev. C 79.6 (2009)

Kox S. et al. Nucl. Phys. 420 (1984), Phys. Letters 159 (1985)

ICRU (International Commission on Radiation Units & Measurements)

Elastic cross-section
Obtained from a fit on data and using the *Ranft* model;

ENDF/B-VII Incident-Proton Data

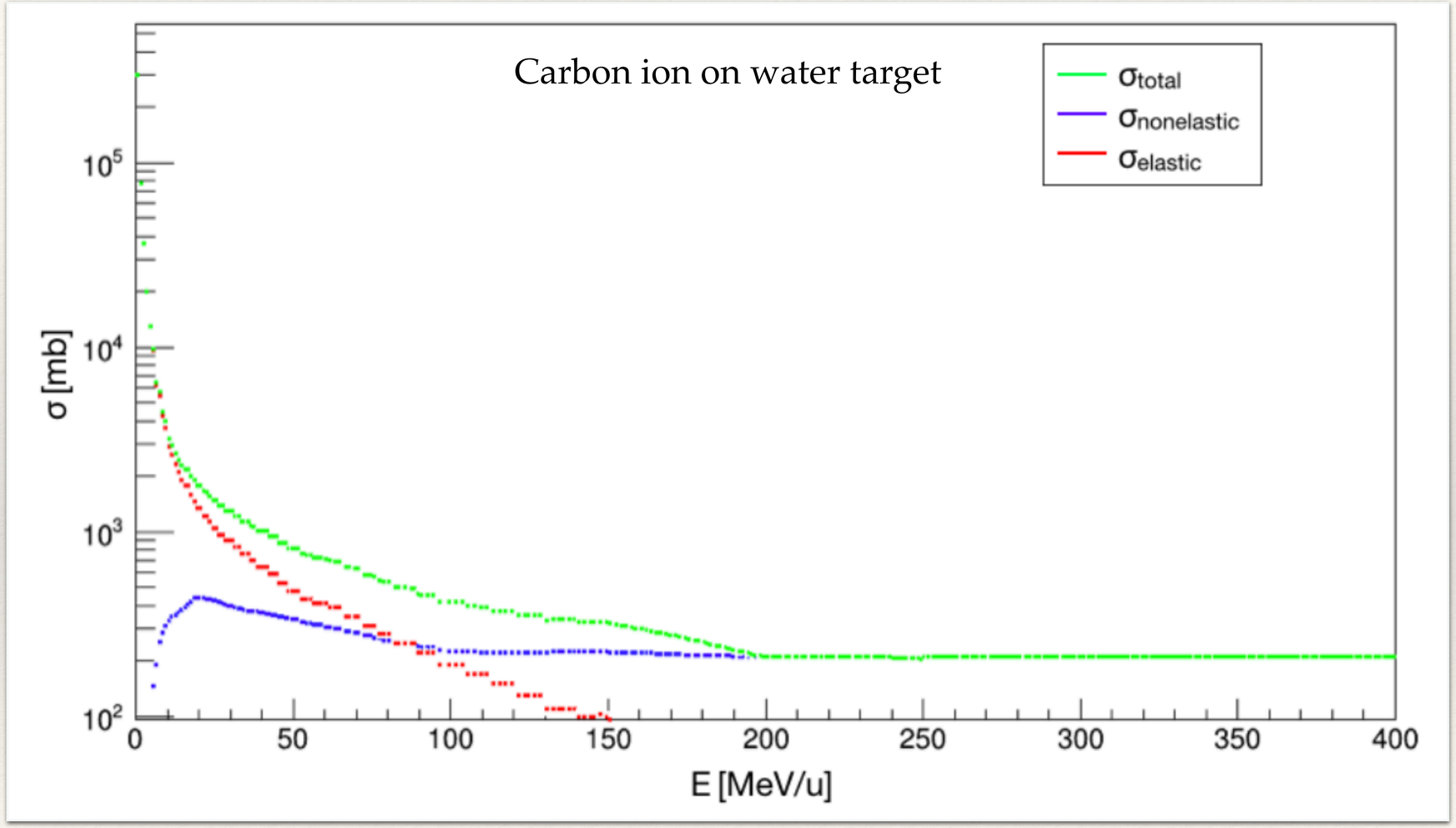

Non-elastic cross-section

$$\frac{\mu}{\rho} = \sum_i \frac{N_A w_i \sigma_i}{A_i}$$

Non-elastic cross-section σ(C-C) and σ(C-H) obtained from a fit on data;

- *Zhang H. Y. et al. Nucl. Phys. 707 (2002)*
- *Takechi M. et al. Phys. Rev. C 79.6 (2009)*
- *Kox S. et al. Nucl. Phys. 420 (1984), Phys. Letters 159 (1985)*
- *ICRU (International Commission on Radiation Units & Measurements)*

Fit on **σ(C-C)** data

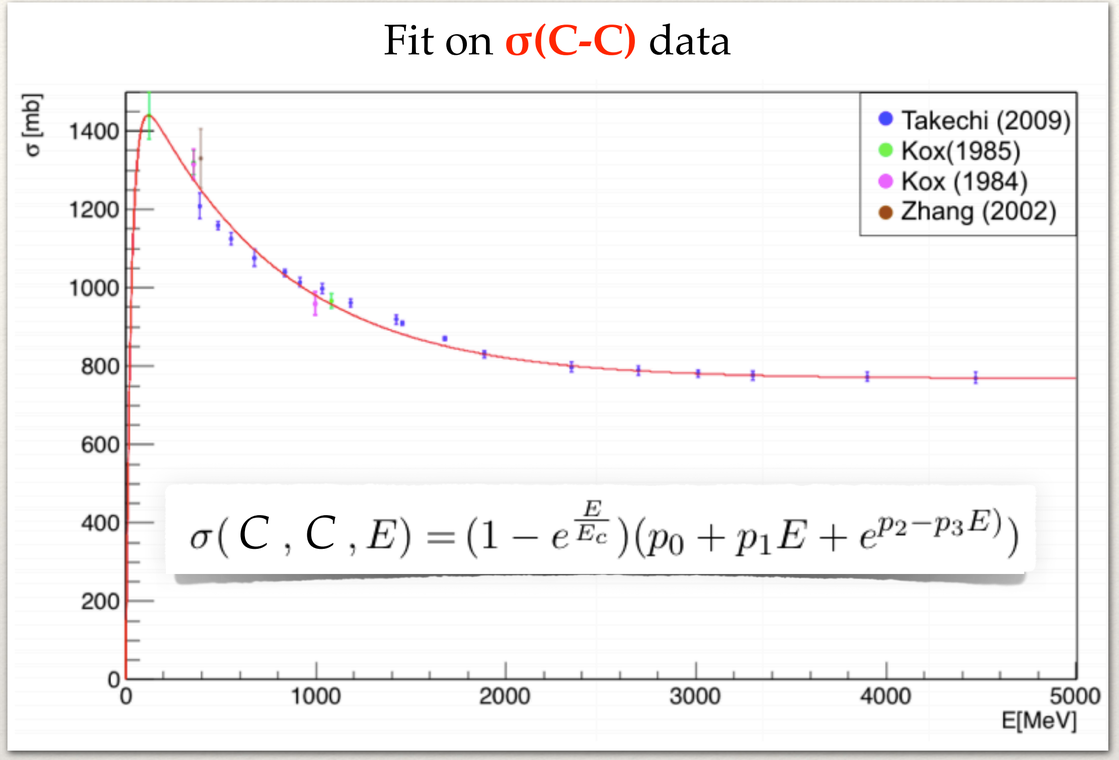

Fit on **σ(C-H)** data

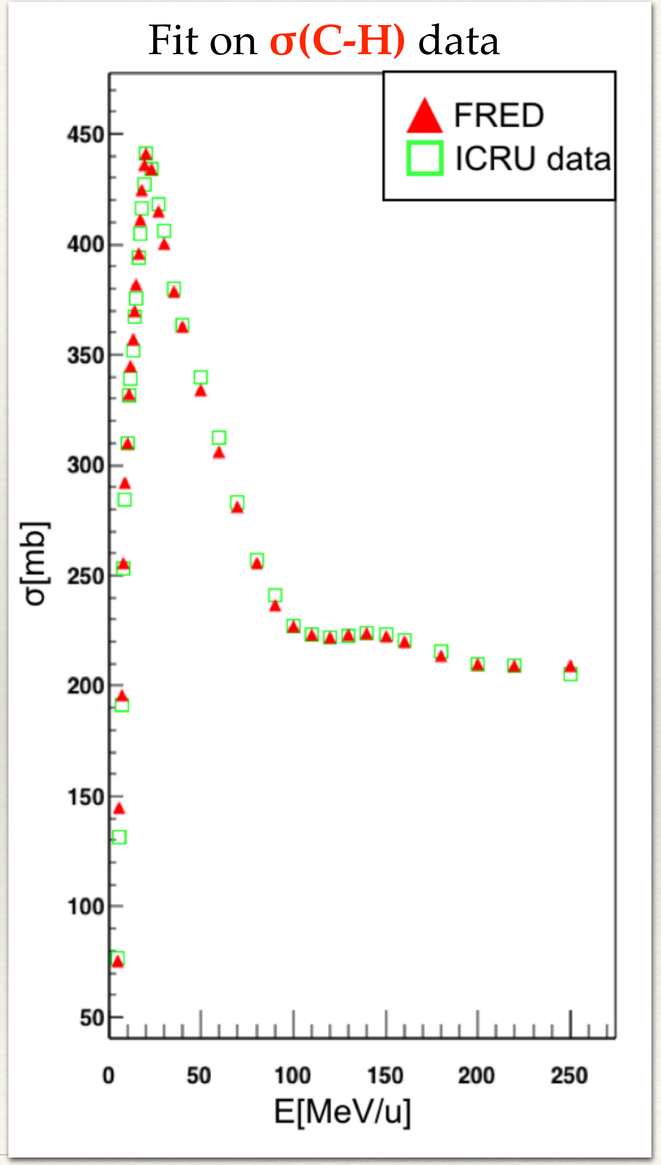

Non-elastic cross-section

$$\frac{\mu}{\rho} = \sum_i \frac{N_A w_i \sigma_i}{A_i}$$

Non-elastic cross-section
σ(C-C) and **σ(C-H)** obtained from a fit on data;

σ(C-Ca) and **σ(C-O)** obtained starting from **σ(C-C)** and scaled with the *Kox* formula (σ_K).

Kox S. et al. Phys Rev C 35 (1987)

$$\sigma(C, C, E) = (1 - e^{\frac{E}{E_c}})(p_0 + p_1 E + e^{p_2 - p_3 E})$$

$$K(N_p, N_t, E_{cm}) = \frac{\sigma_K(N_p, N_t, E_{cm})}{\sigma_K(^{12}C, ^{12}C, E_{cm})}$$

$$\sigma(N_p, N_t, E) = K(N_p, N_t, E)(1 - e^{\frac{E}{E_c}})(p_0 + p_1 E + e^{p_2 - p_3 E})$$

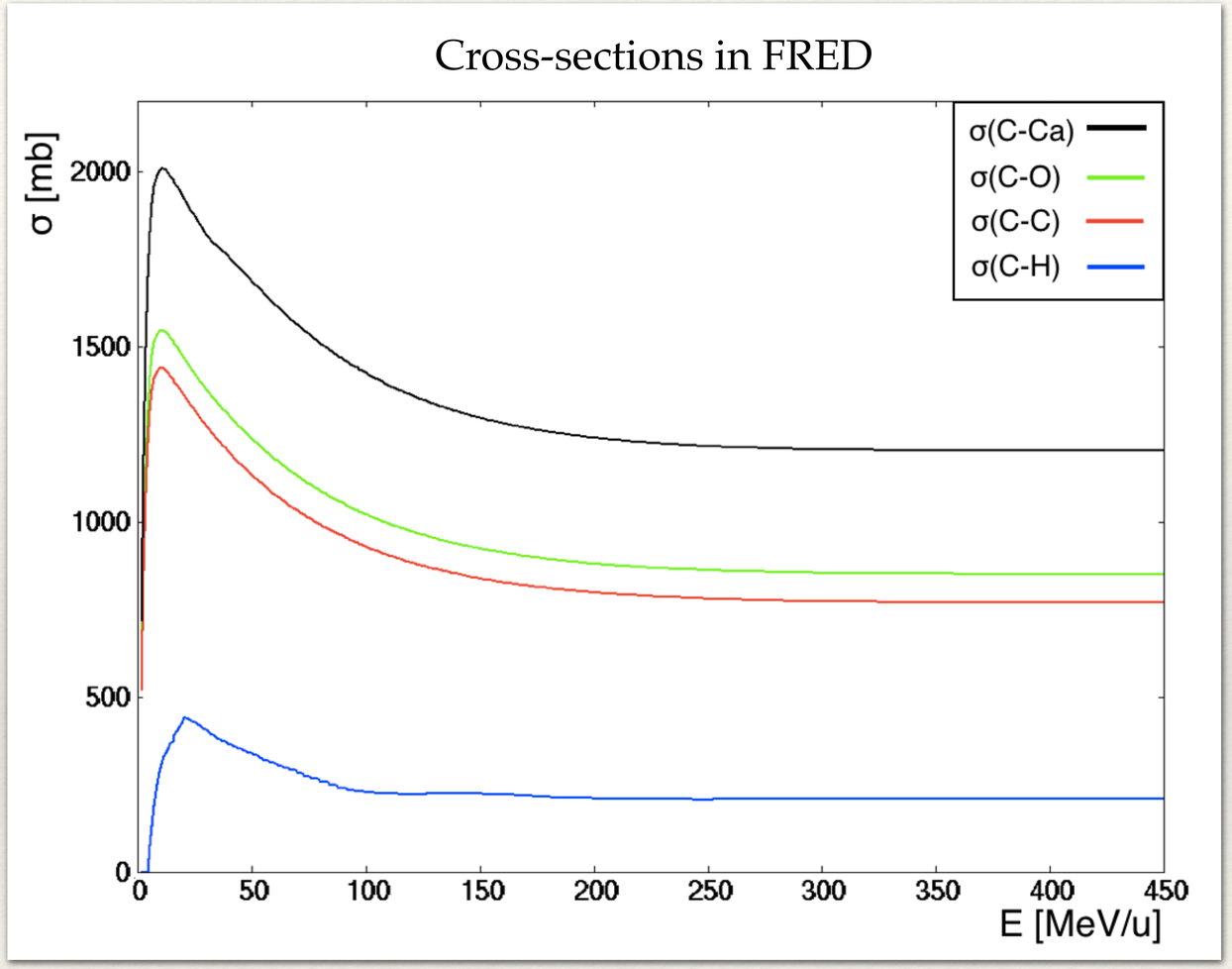

Generating a fragmentation event

simulated with FRED

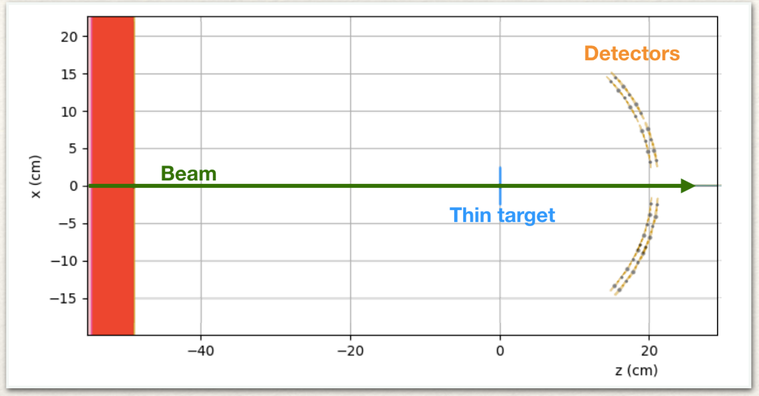

Dudouet. I. et al. Phys Rev C 88 (2013)

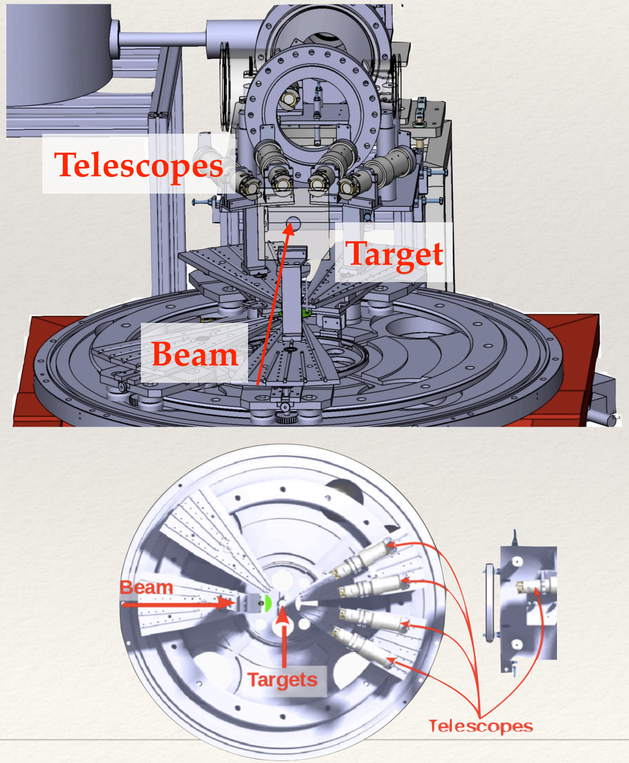

What do we have? **GANIL's probability of emission**

Fragmentation experiment of ^{12}C beam @95MeV/u on different thin targets (C, CH_2, Al, Al_2O_3, Ti, and PMMA). The only experiment which provides double differential cross-section at the energy of interest of PT.

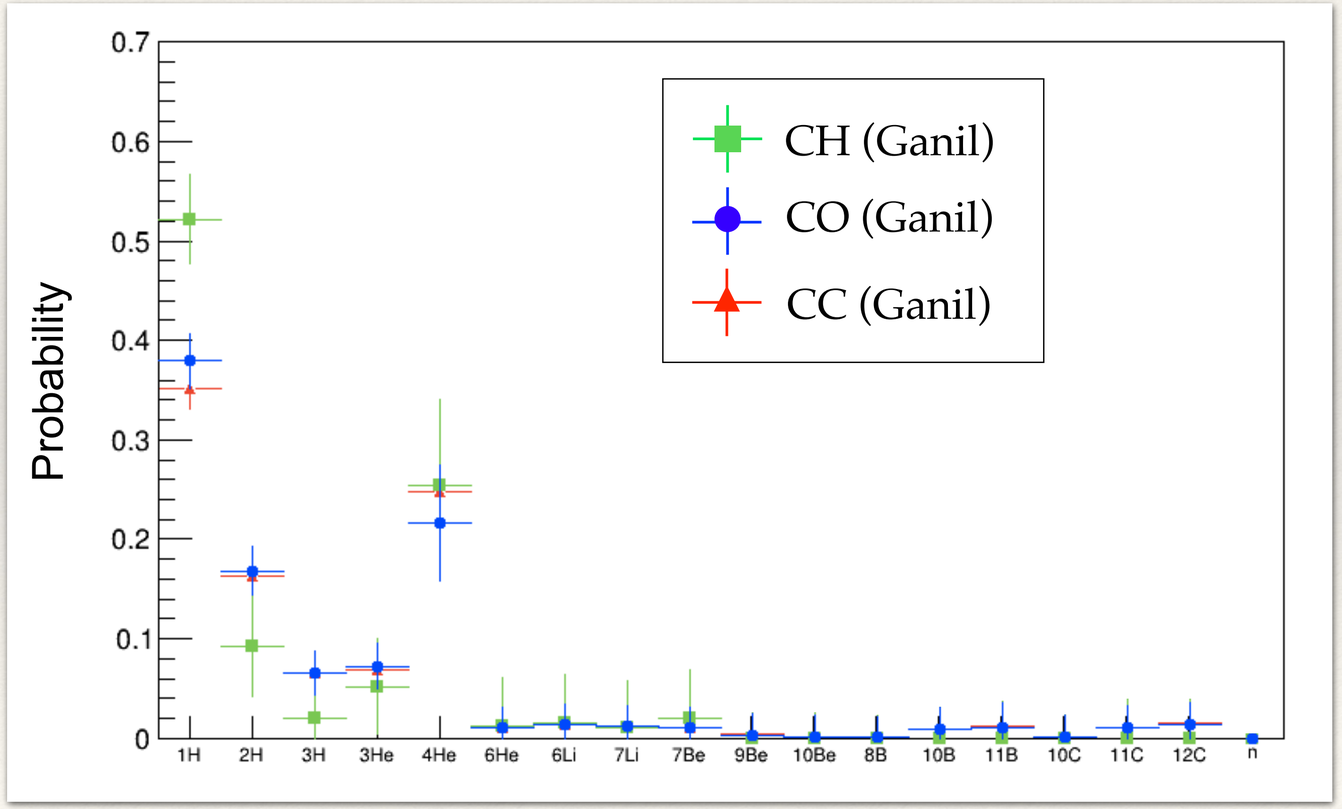

Generating a fragmentation event

In the Ganil experiment only 4 telescopes detected fragments simultaneously, doing different measurements changing their position. The probabilities obtained do not take into consideration the correlation between the set of fragment produced.

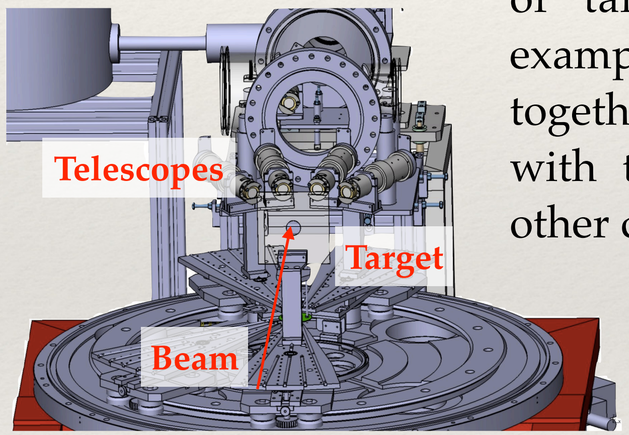

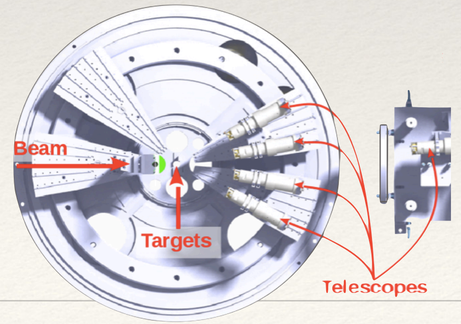

Dudouet. I. et al. Phys Rev C 88 (2013)

We do not know if it is a projectile or target fragment and if, for example, a ^{4}He has been produced together with other two ^{4}He or with two protons and a ^{6}He or other combinations.

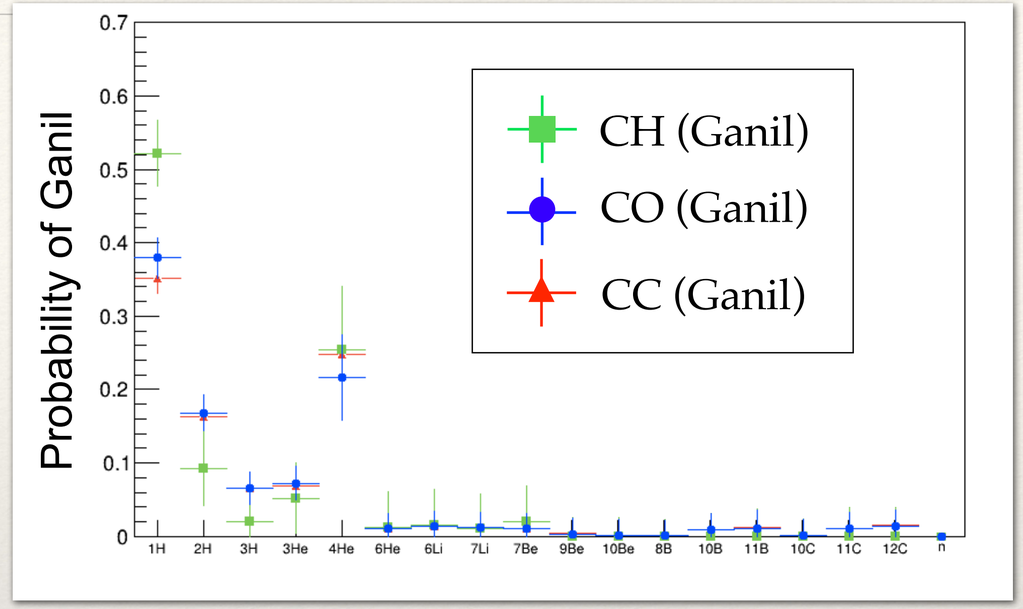

If Ganil probabilities would be used directly for the fragments sampling the final fragments' distribution would be different from that one measured by Ganil due to the sampling procedure.

FRED

Input = Ganil probabilities

↓

Extraction checking **mass and charge conservation**

↓

Output ≠ Ganil probabilities

Generating a fragmentation event

In the Ganil experiment only 4 telescopes detected fragments simultaneously, doing different measurements changing their position. The probabilities obtained do not take into consideration the correlation between the set of fragment produced.

Use of an **iterative formalism** to have the same generating probability of the Ganil experiment.

Minimization of the χ^2 to obtain the best set of probabilities in input:

$$\chi^2 = \sum_{k=1}^{k=N} \frac{(Y_k^{exp} - f_k(\alpha_i))^2}{\sigma_k^2}$$

Y_k^{exp} = experimental prob. Ganil

$f_k(\alpha_i)$ = generating prob. FRED

σ_k^2 = uncertainty relative to Y_k^{exp}

FRED

Input = **NEW probabilities**

↓

Extraction checking **mass and charge conservation**

↓

Output = Ganil probabilities

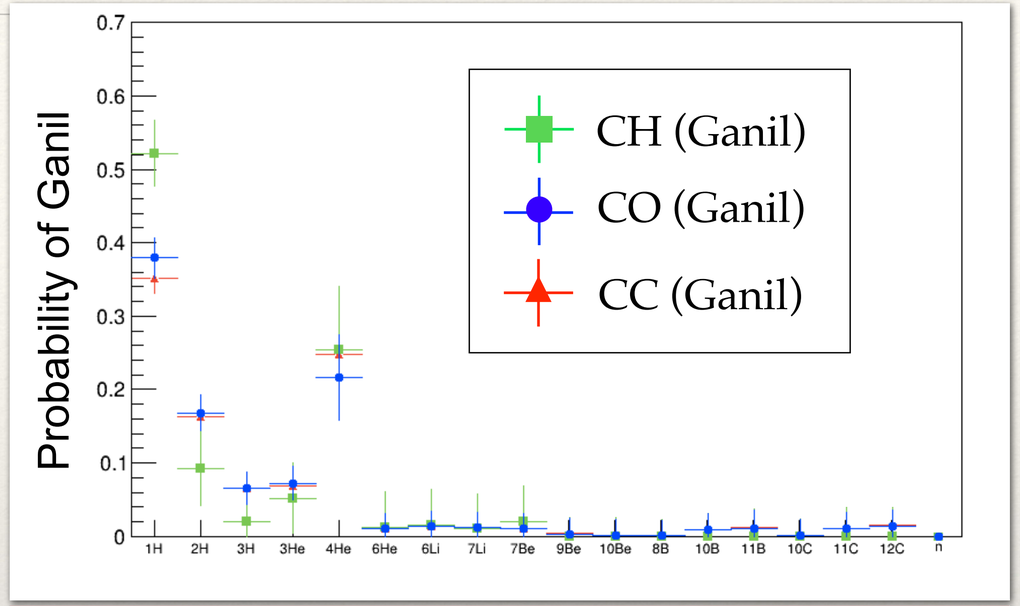

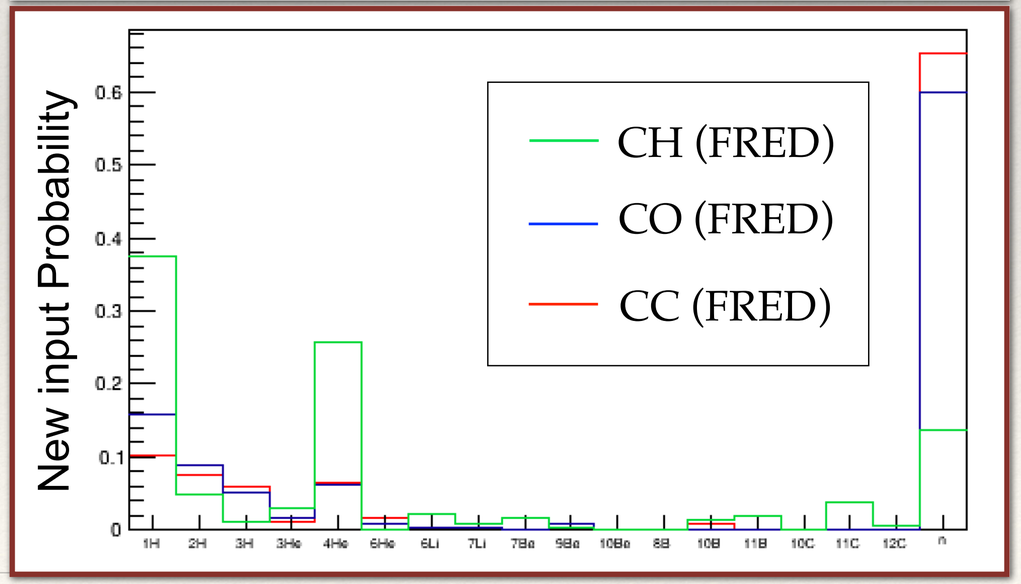

Sampling of energy and angular distribution

Bidimensional fits on GANIL data show that the distribution is composed of:

- a **gaussian** function (projectile fragmentation) ;
- an **exponential** function (target fragmentation).

$$f(E,\theta) = A_1 e^{-(\alpha_E E + \alpha_\theta \theta)} + A_2 e^{-\left(\frac{(E-<E>)^2}{2\sigma_E} + \frac{(\theta-<\theta>)^2}{2\sigma_\theta}\right)}$$

Oxygen target

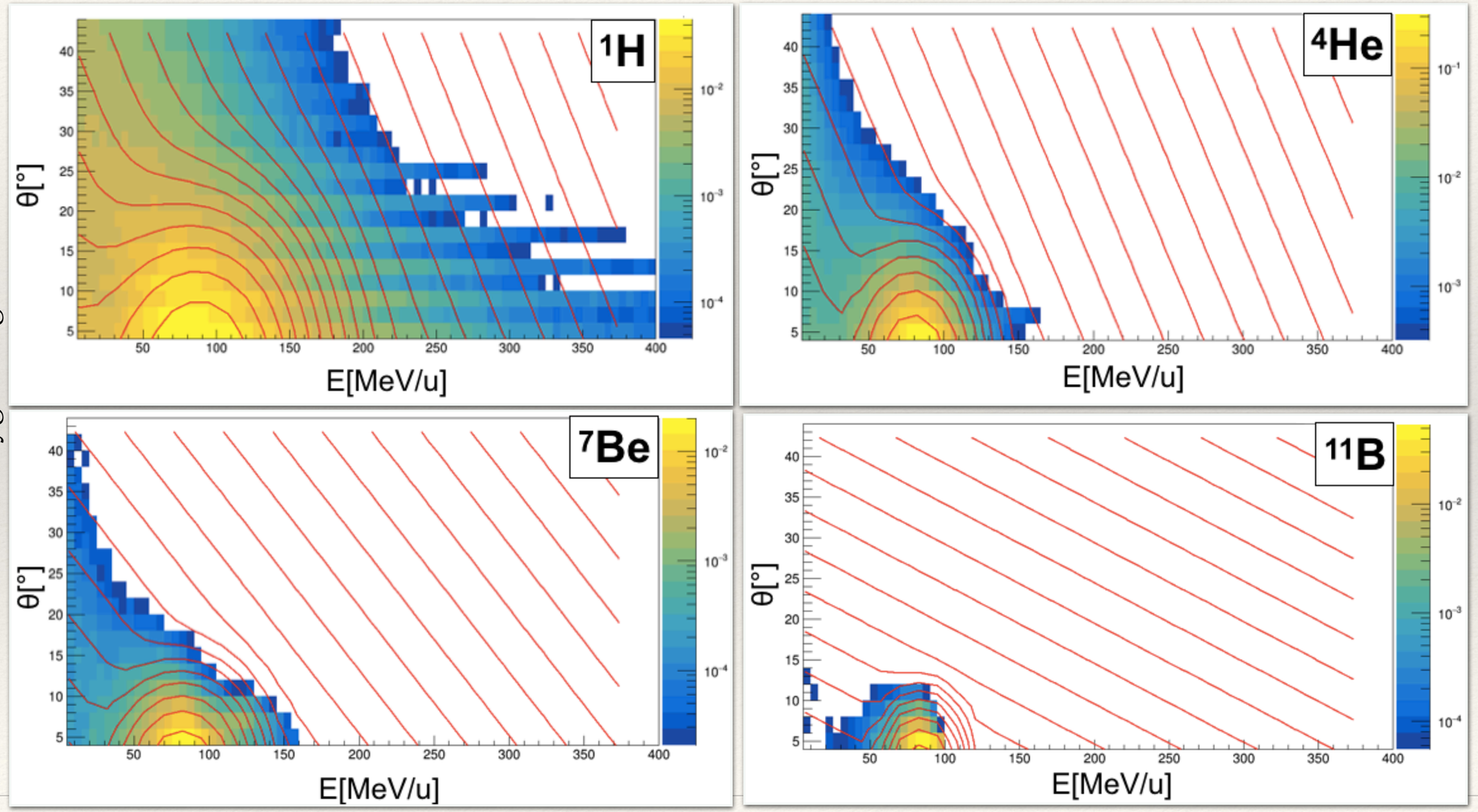

Sampling of energy and angular distribution

The projectile particles used in particle therapy proceed at relativistic velocities and, consequently, the interaction with the target takes place in the same relativistic condition. Using the inverse kinematics approach it is possible to switch from the laboratory reference system to the one of the projectile.

Taking the Gaussian component of the energy distribution and applying a **Lorentz transformation**, an exponential distribution is obtained.

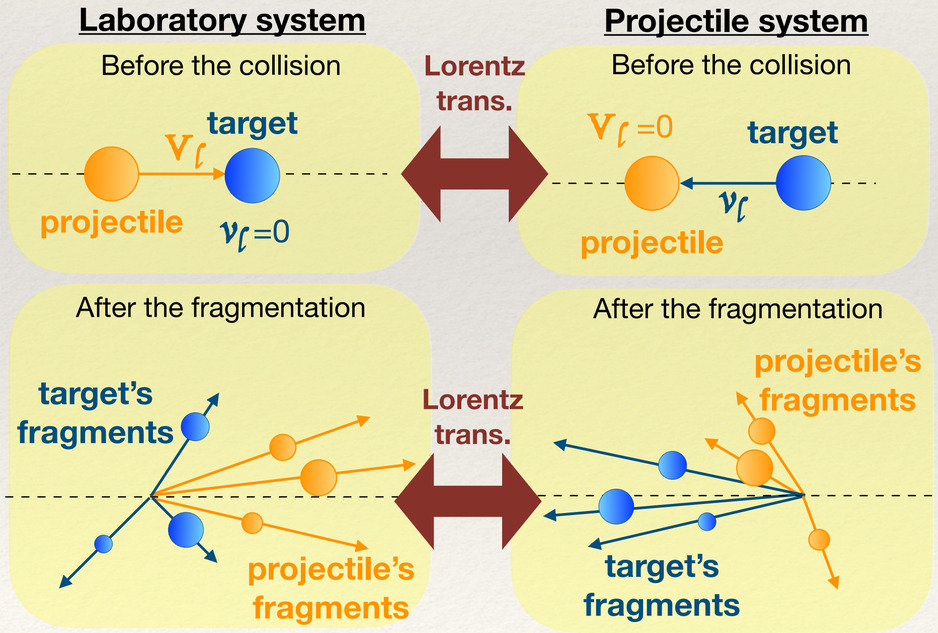

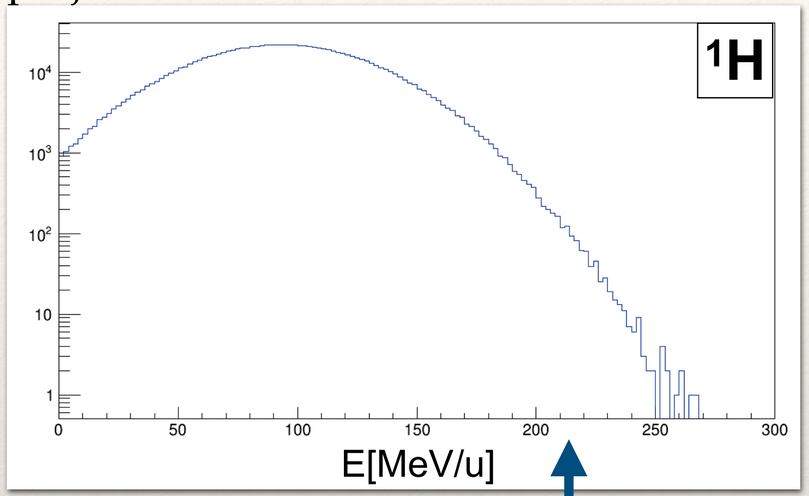

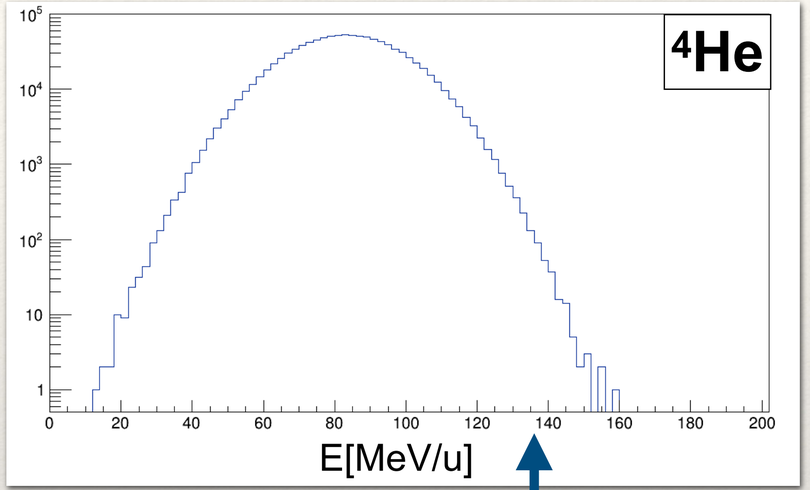

Lorentz Transformation

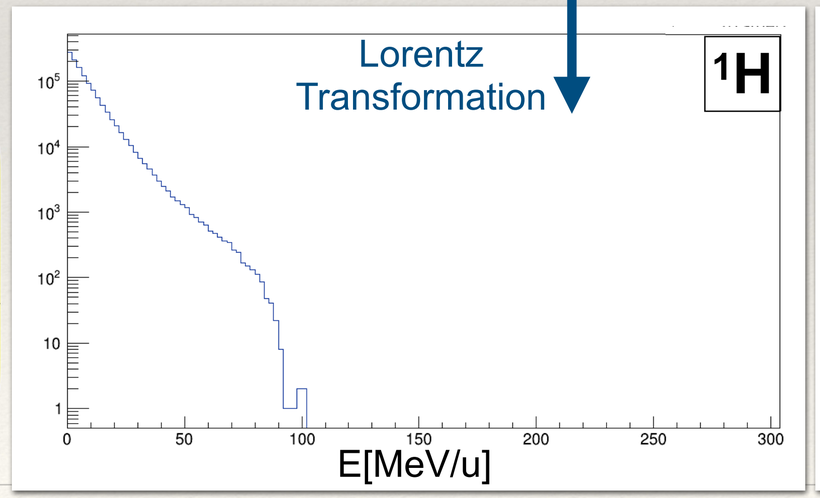

Lorentz Transformation

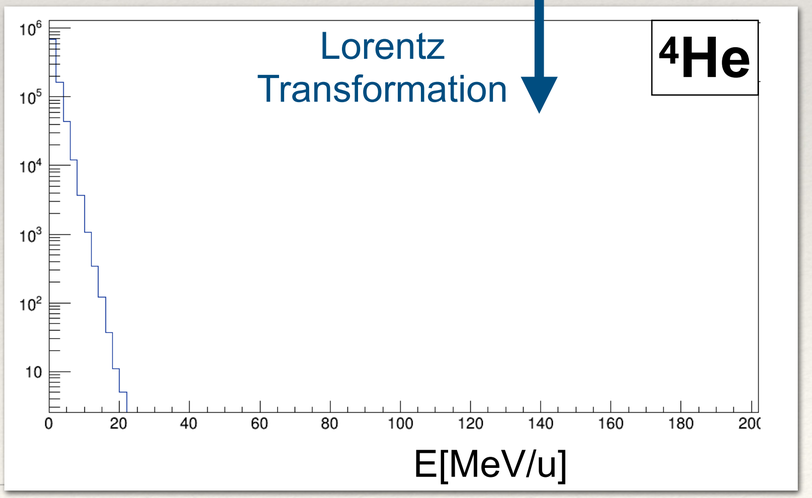

Sampling of energy and angular distribution

$$f(E,\theta) = A_1 e^{-(\alpha_E E + \alpha_\theta \theta)} + A_2 e^{-\left(\frac{(E-<E>)^2}{2\sigma_E} + \frac{(\theta-<\theta>)^2}{2\sigma_\theta}\right)}$$

Energy and angular distribution of GANIL correspond to a 95 MeV/u beam.
Extrapolation of new energy and angle:

$$\theta^i = \theta^i_{95\mathrm{MeV/u}} \sqrt{\frac{95}{E_{proj}[\mathrm{MeV/u}]}}.$$

$$E^i = E^i_{95\mathrm{MeV/u}} \frac{E_{proj}[\mathrm{MeV/u}]}{95}(1-k)$$

energy conservation

FRED SIMULATION (^{12}C-water)

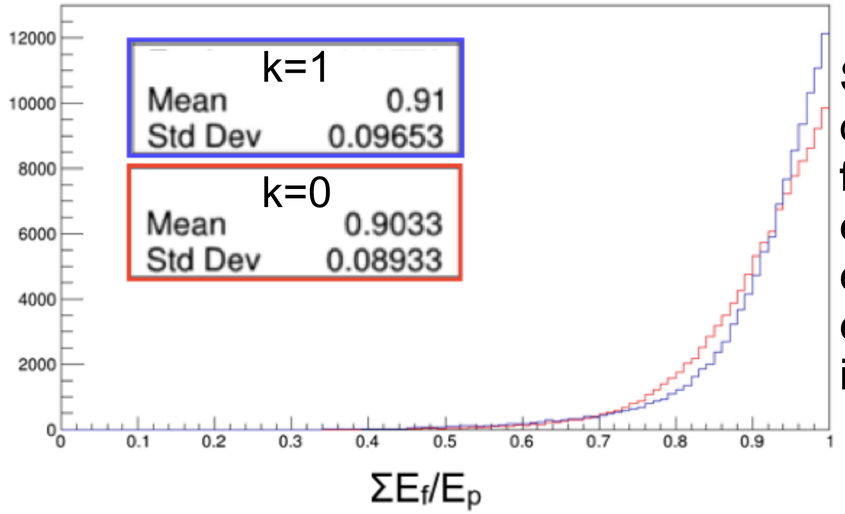

Sum of energy of **all fragments** emitted in an event over the energy of the incident particle

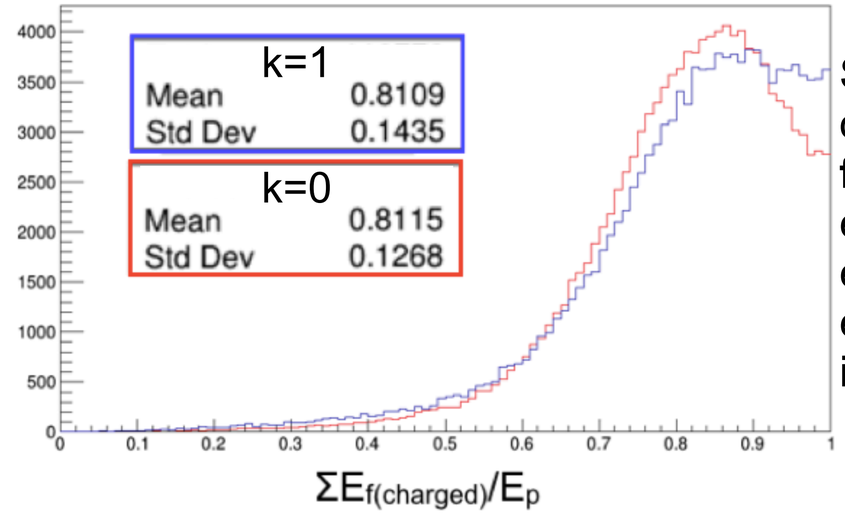

Sum of energy of **charged fragments** emitted in an event over the energy of the incident particle

Fragmentation

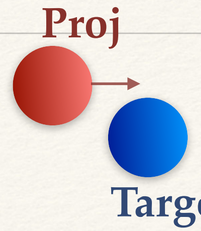

Sampling of the target

Using Kox's cross-section to build a cumulative distributions.

$$P^i = \frac{n^i \sigma_K^i}{\sigma^{tot}}$$

$$\sigma^{tot} = \sum_{j=0}^{j=N} n^j \sigma_K^j$$

Sampling of the fragments

The code reads probability tables built to have the same generating probability of the GANIL experiment

Fragments from the projectile

Fragments from the target

NO

Mass and charge conservation?

NO

Mass and charge conservation?

YES

YES

Based on GANIL data (next slide)

Sampling of energy and angle of new fragments

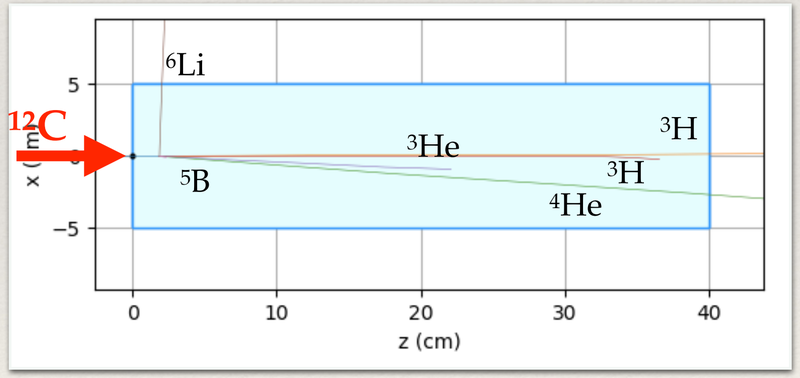

Extrapolation to different beam energy

NO

Energy conservation?

YES

Creating new particles and tracking them with FRED

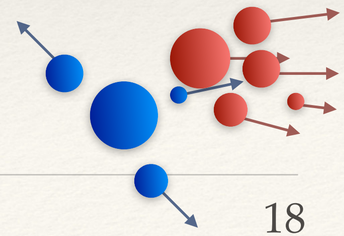

Result

Validation of the model

Where I started..

Depth Dose Distribution of single pencil beam of ^{12}C in water

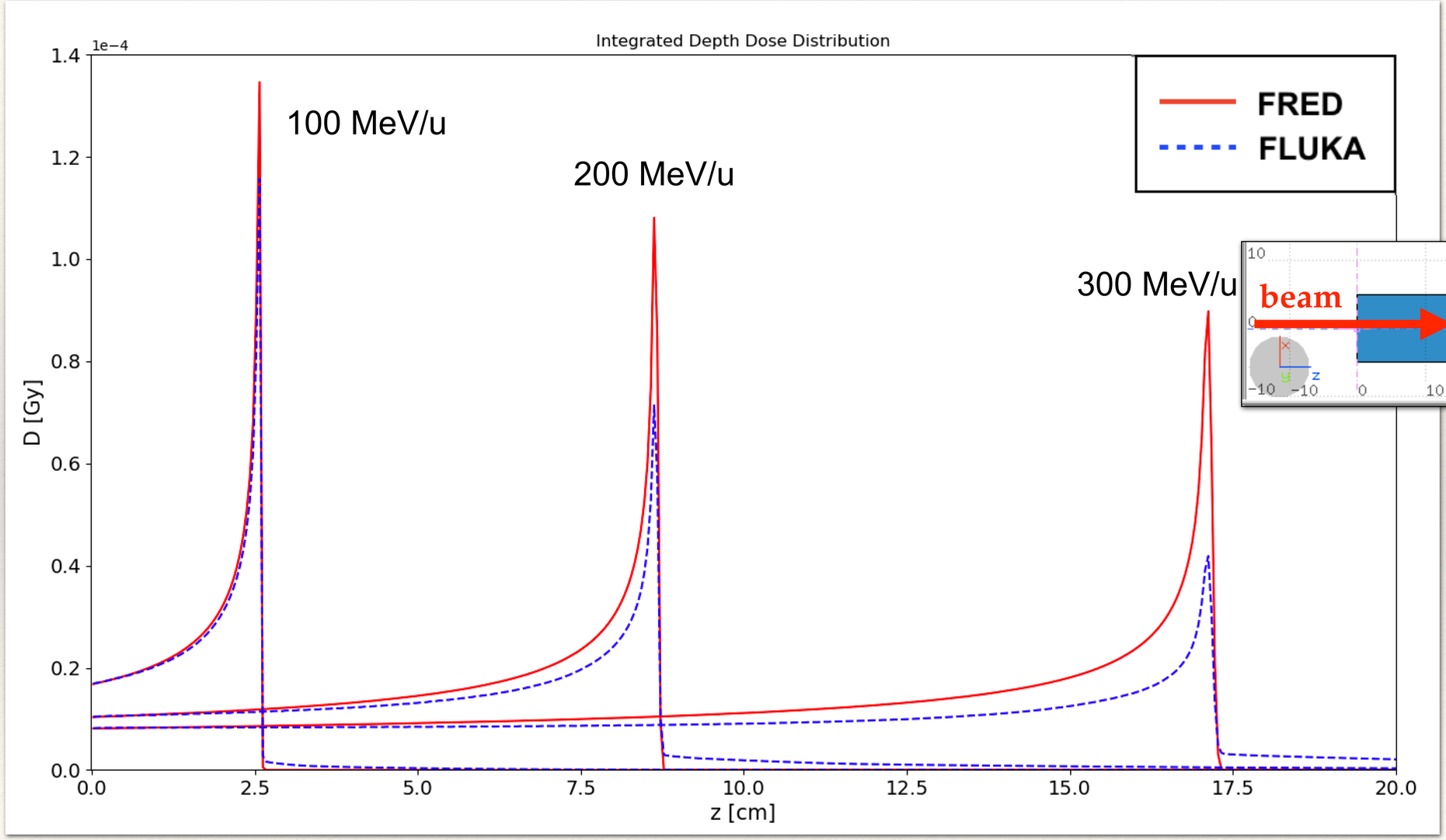

Without the nuclear model in FRED

Result

Validation of the model

.. where I arrived!

Depth Dose Distribution of single pencil beam of ^{12}C in water

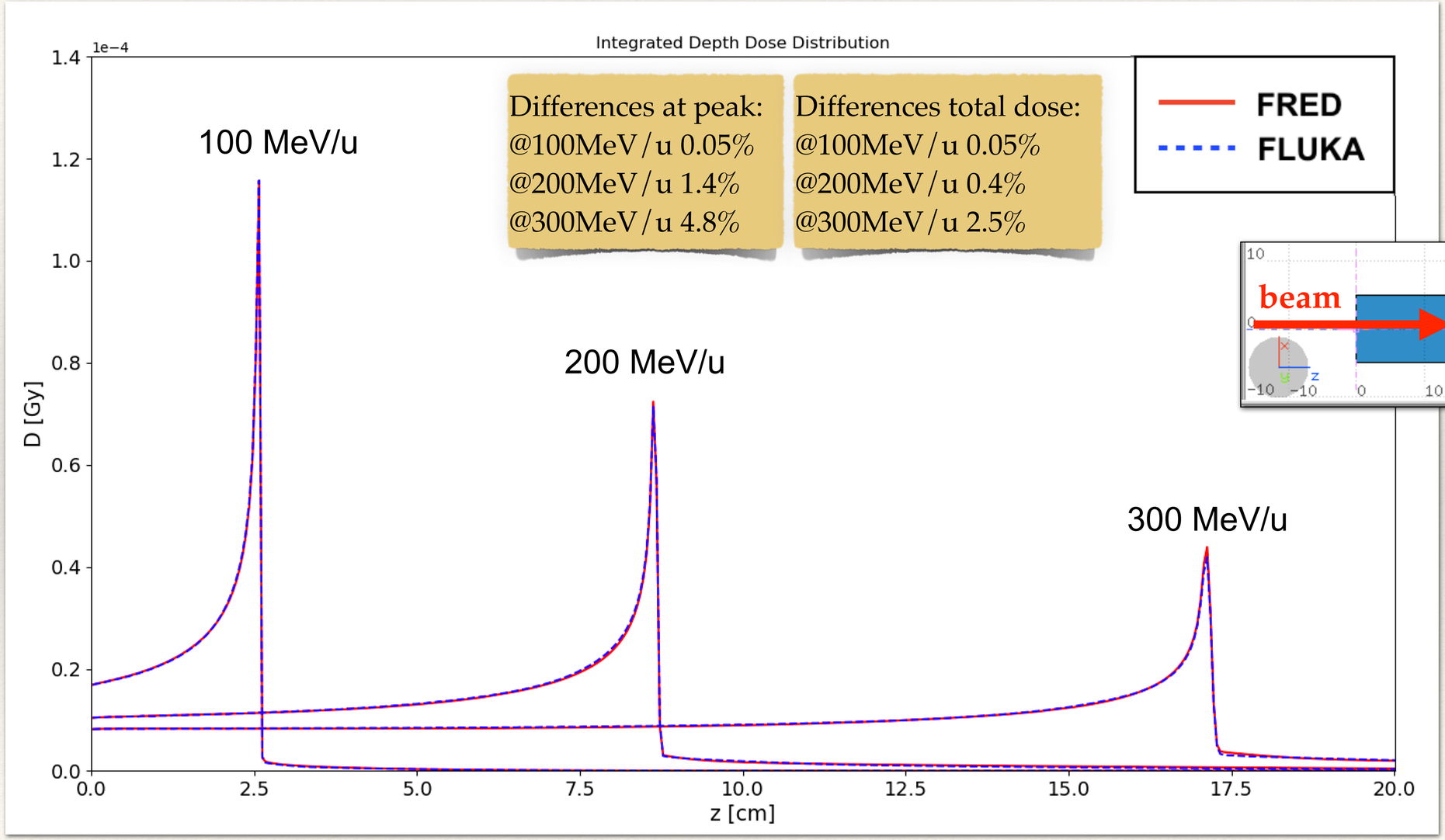

With the nuclear model in FRED

Result

Validation of the model

.. where I arrived!

Lateral distribution at Bragg Peak of single pencil beam of ^{12}C in water

With the nuclear model in FRED

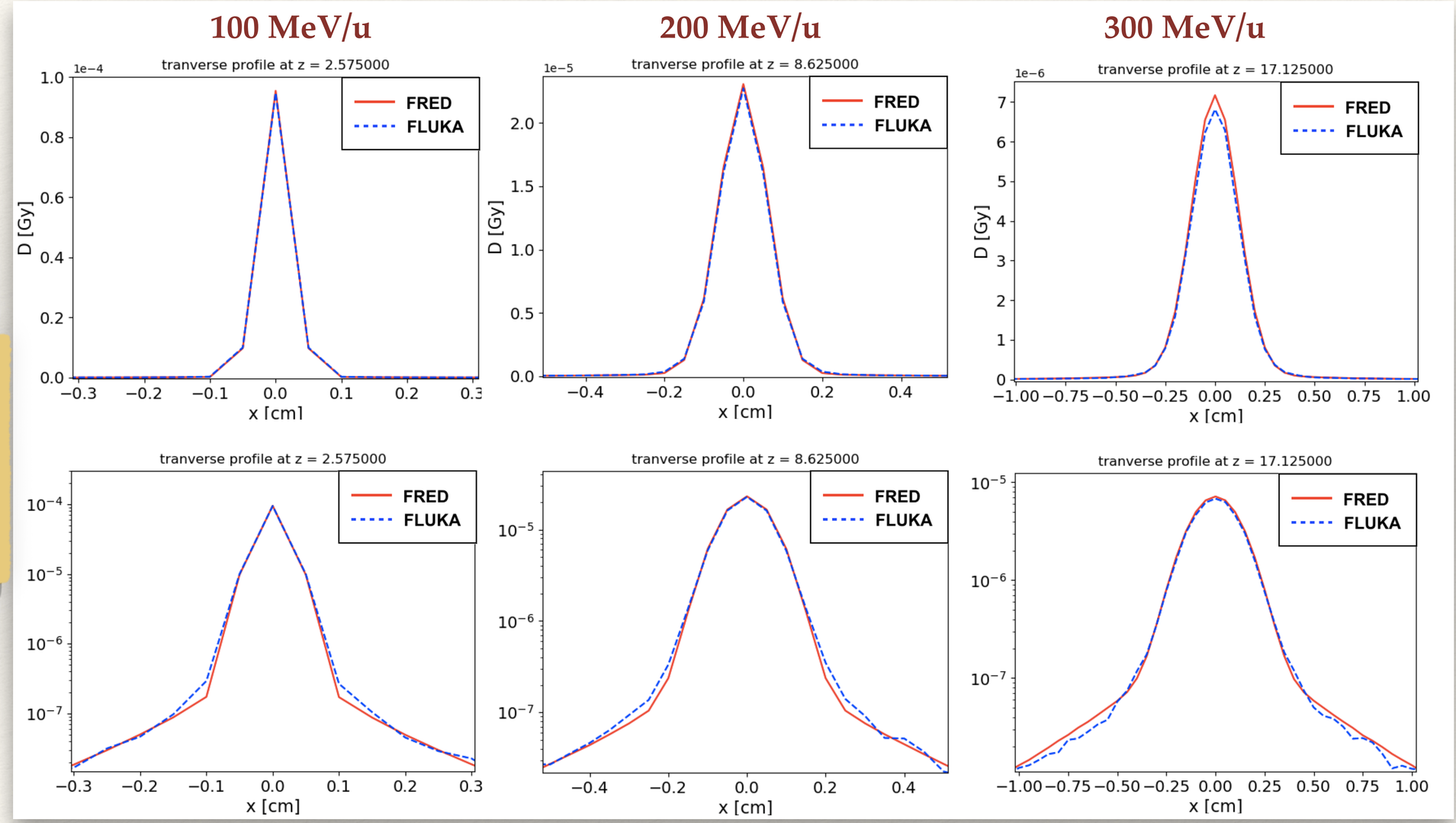

Result

Validation of the model

Study of the secondary fragmentation

Target = water
beams @200 MeV/u

With the nuclear model in FRED

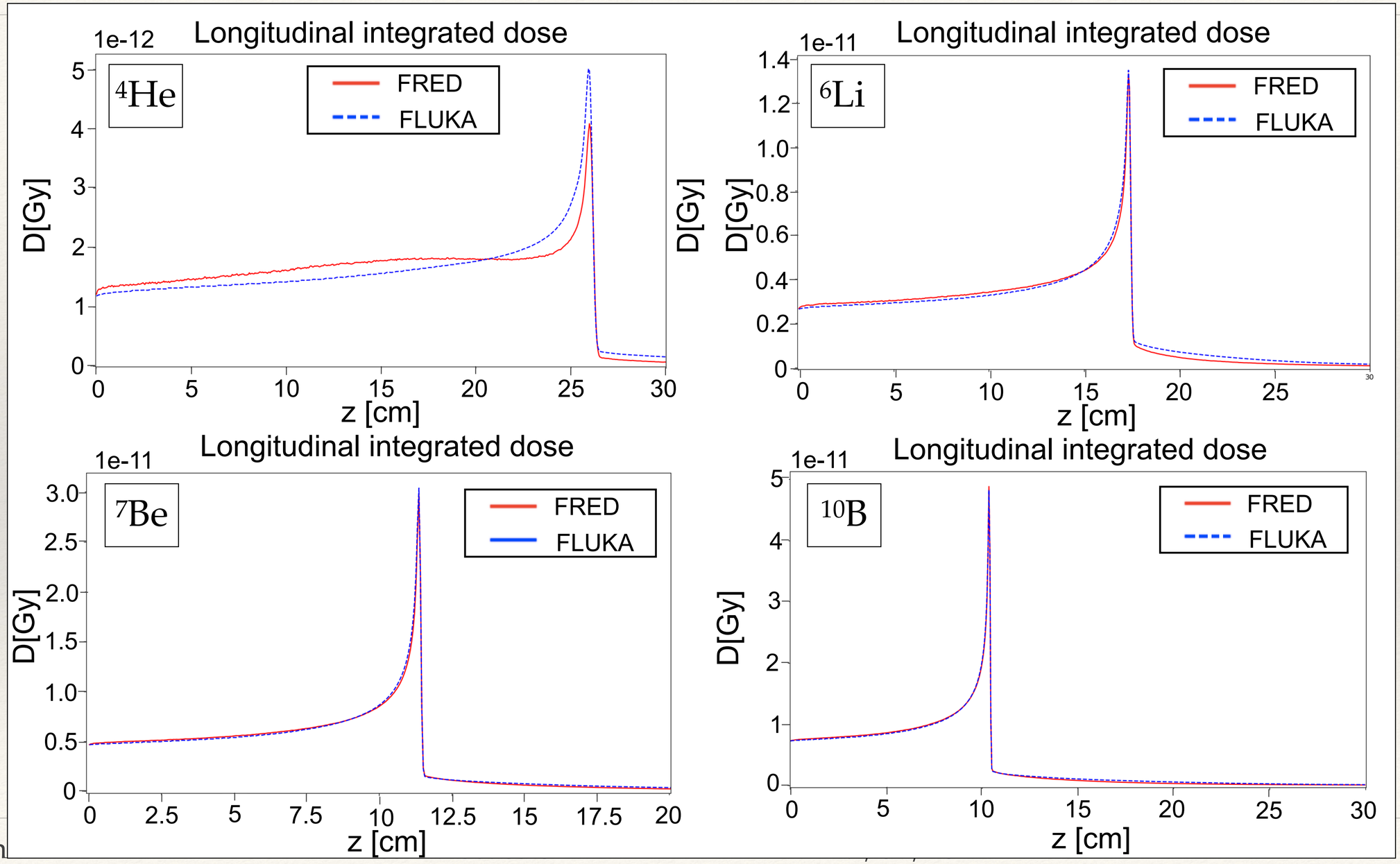

Result

Accelerator quality control

```
patient_id none
machine# 0
projectile 12C
charge 6
mass 12
bolus 0
ripplefilter 0
#submachines 14
#particles 21531.5 333787 2.03959E+08
submachine# 57 186.57 2 6.9
#particles 32280.4 32280.4 7.2631E+06
stepsize 2 2
#points 225
14 14 32280.4
12 14 32280.4
10 14 32280.4
8 14 32280.4
6 14 32280.4
4 14 32280.4
2 14 32280.4
0 14 32280.4
-2 14 32280.4
-4 14 32280.4
-6 14 32280.4
-8 14 32280.4
-10 14 32280.4
-12 14 32280.4
-14 14 32280.4
-14 12 32280.4
-12 12 32280.4
-10 12 32280.4
-8 12 32280.4
-6 12 32280.4
-4 12 32280.4
-2 12 32280.4
0 12 32280.4
2 12 32280.4
4 12 32280.4
6 12 32280.4
```

SOBP from CNAO raster file
3 cm side Cube at a depth of 7 cm

Combination of:
Beams at 14 different energies from 186.57 to 223.56 MeV/u,
for each energy 225 beams in different positions.
Spacing: 2 mm in x,y and z.

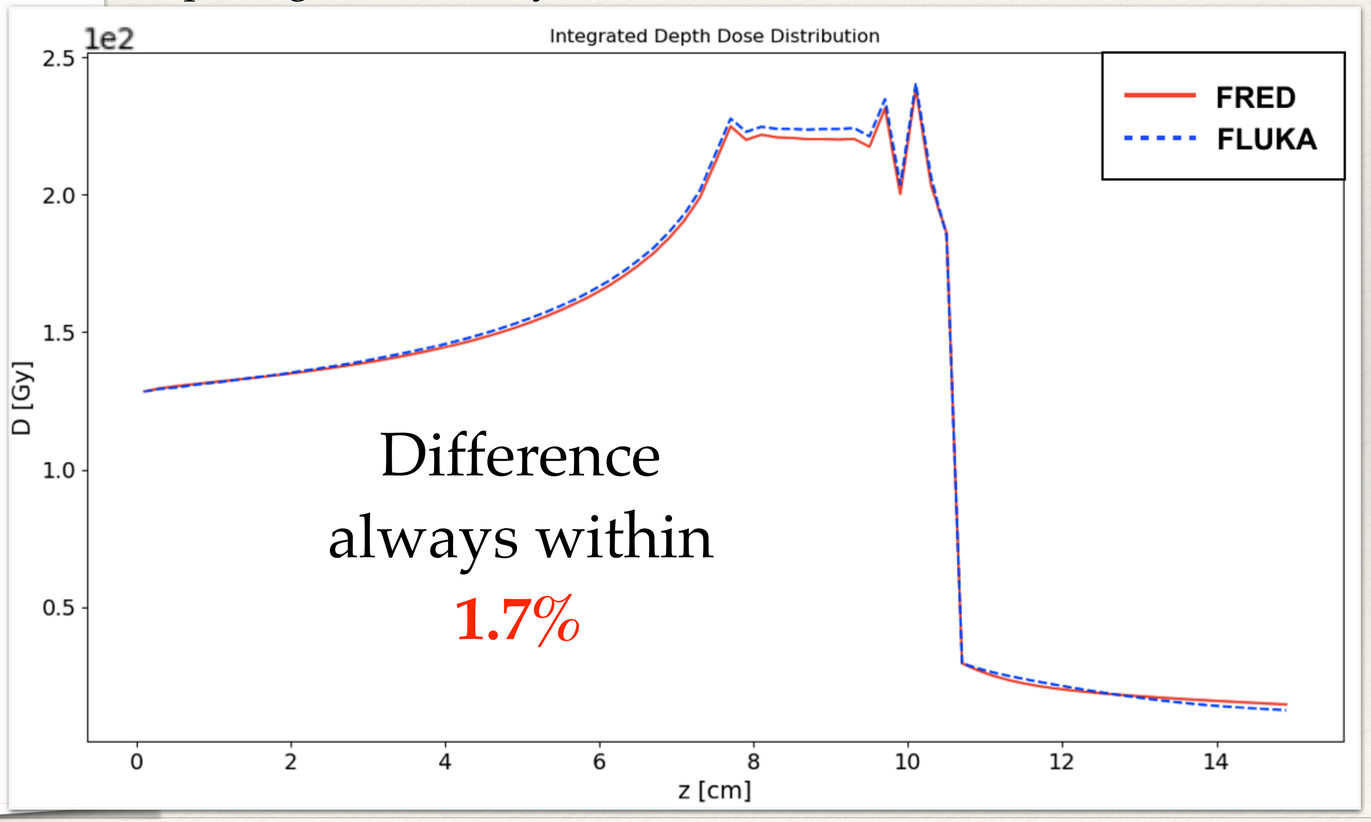

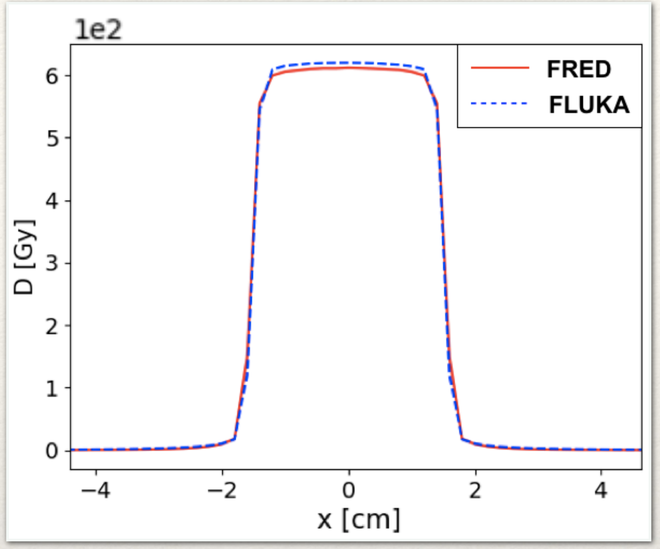

Result

Gamma-index

Reference Map (FLUKA)

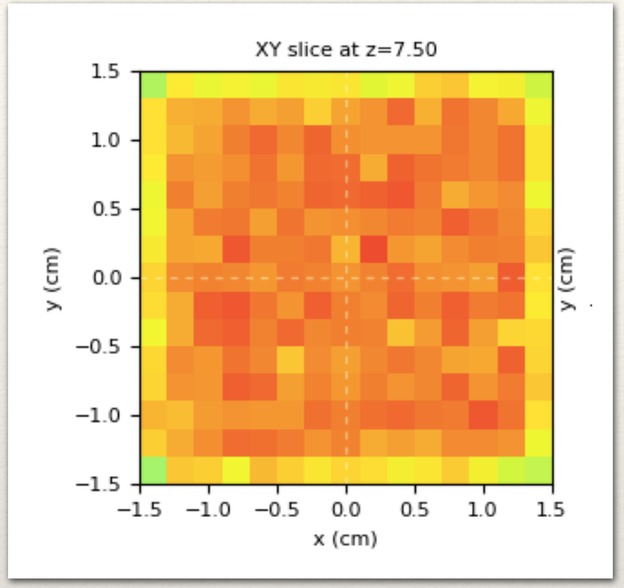

Evaluation Map (FRED)

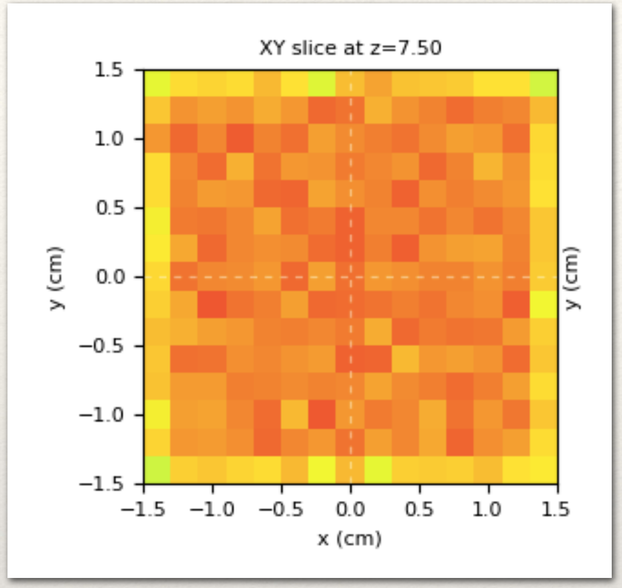

γ-index 2mm / 3%

Result

Gamma-index

Reference Map (FLUKA)

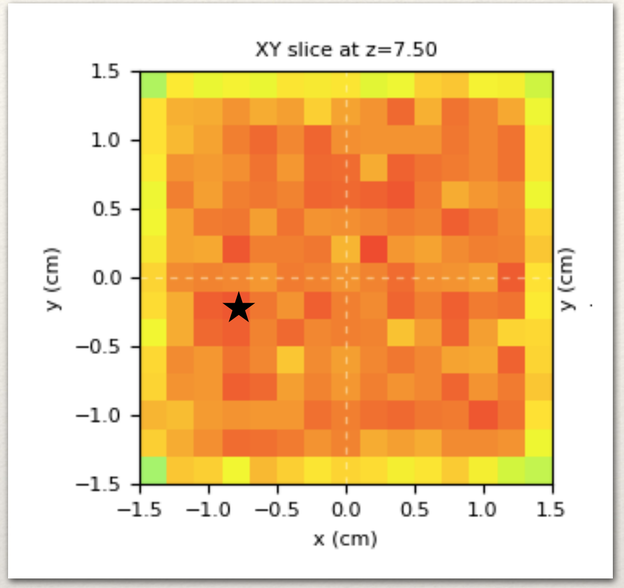

Evaluation Map (FRED)

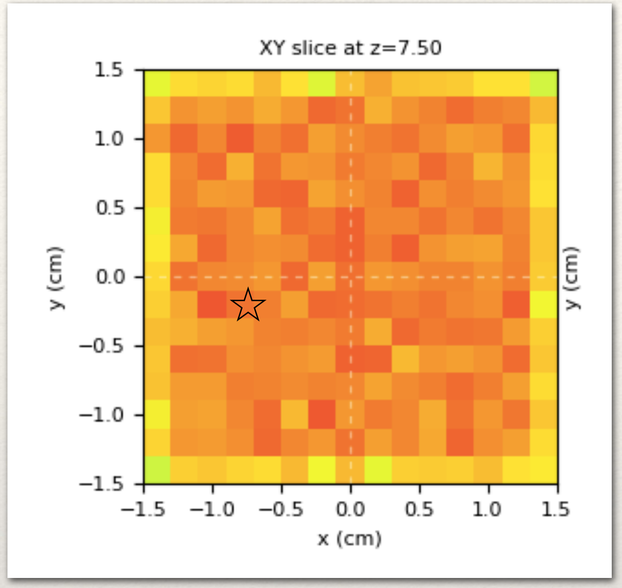

γ-index 2mm / 3%

Result

Gamma-index

Reference Map (FLUKA)

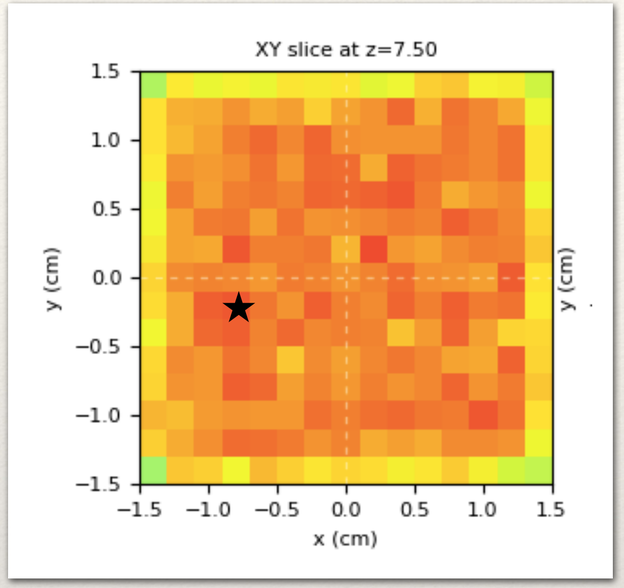

Evaluation Map (FRED)

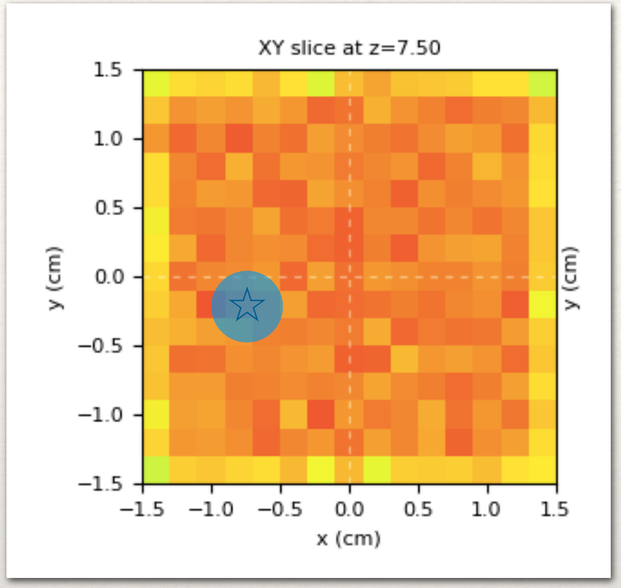

γ-index 2mm / 3%

Result

Gamma-index

Reference Map (FLUKA)

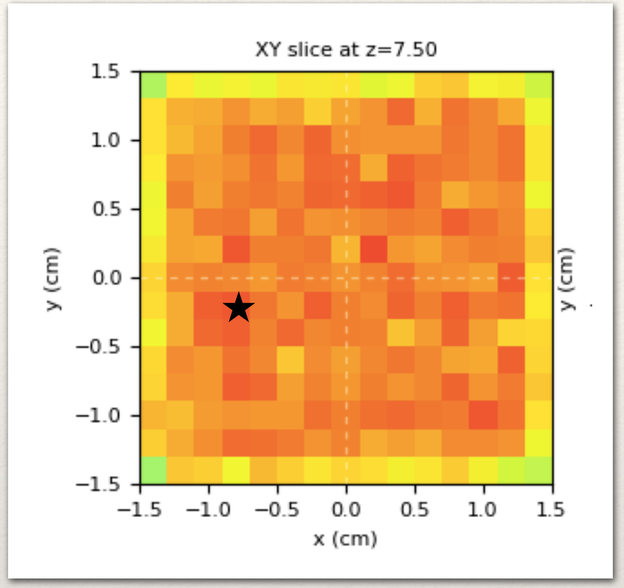

Evaluation Map (FRED)

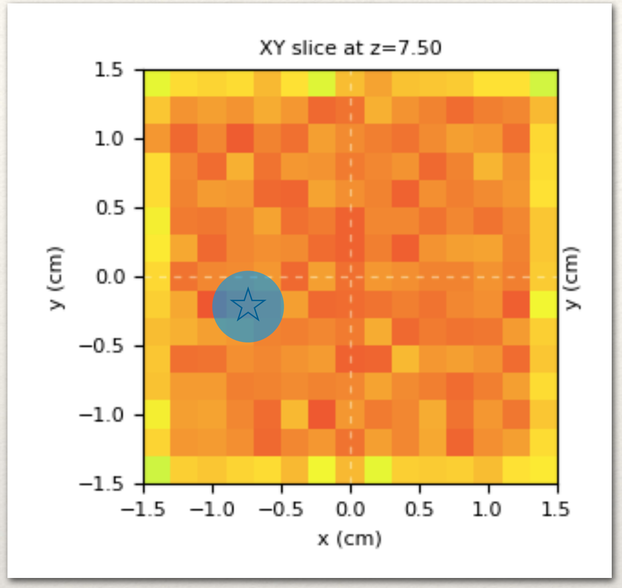

γ-index 2mm/3%

$$\Gamma(\vec{r_e}, \vec{r_r}) = \sqrt{\frac{|\vec{r_e} - \vec{r_r}|^2}{\Delta d^2} + \frac{[D_e(\vec{r_e}) - D_r(\vec{r_r})]^2}{\Delta D^2}}$$

D= dose (D_r of the reference map, D_e of the evaluation map)

r = position of the evaluated point (r_r of the reference map, r_e of the evaluation map)

Result

Gamma-index

Reference Map (FLUKA)

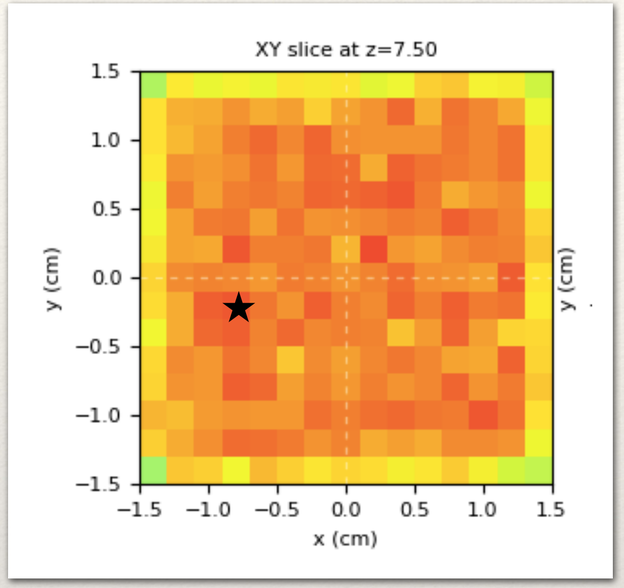

Evaluation Map (FRED)

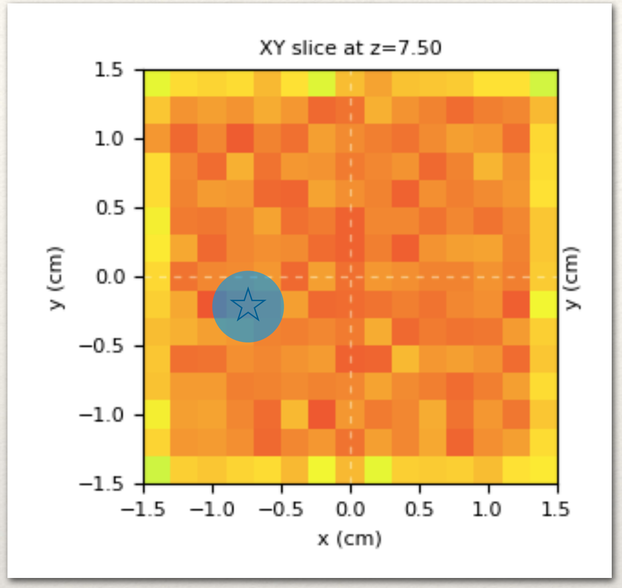

γ-index 2mm/3%

$$\Gamma(\vec{r_e}, \vec{r_r}) = \sqrt{\frac{|\vec{r_e} - \vec{r_r}|^2}{\Delta d^2} + \frac{[D_e(\vec{r_e}) - D_r(\vec{r_r})]^2}{\Delta D^2}}$$

D= dose (D_r of the reference map, D_e of the evaluation map)

r = position of the evaluated point (r_r of the reference map, r_e of the evaluation map)

$$\gamma(\vec{r_r}) = \min\{\Gamma(\vec{r_e}, \vec{r_r})\} \forall \{\vec{r_e}\}$$

$\gamma \leq 1$ = test passed

$\gamma > 1$ = test NOT passed

pass rate ≥ 92%
clinical acceptance

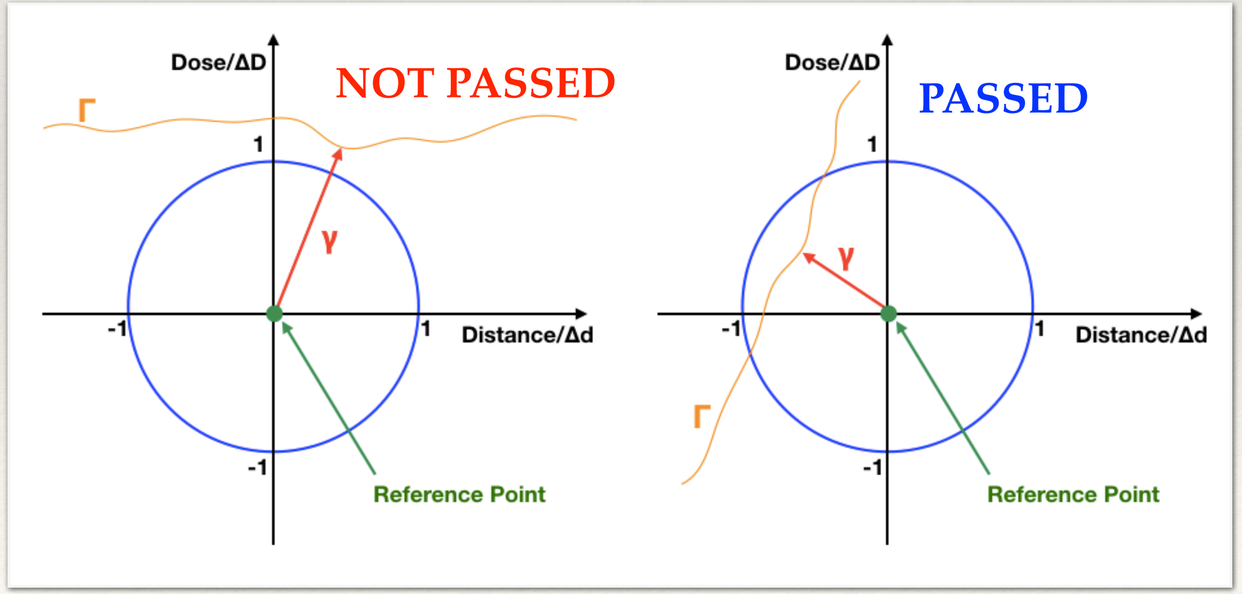

Result

SOBP from CNAO raster file

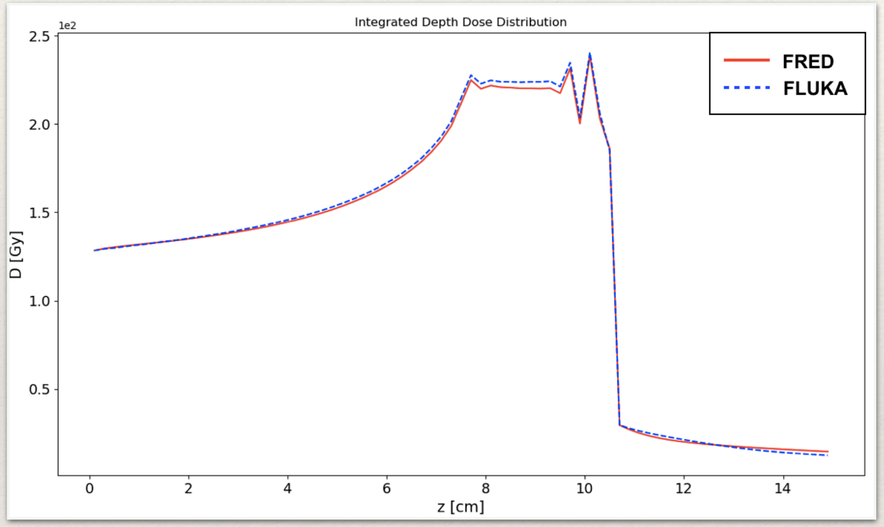

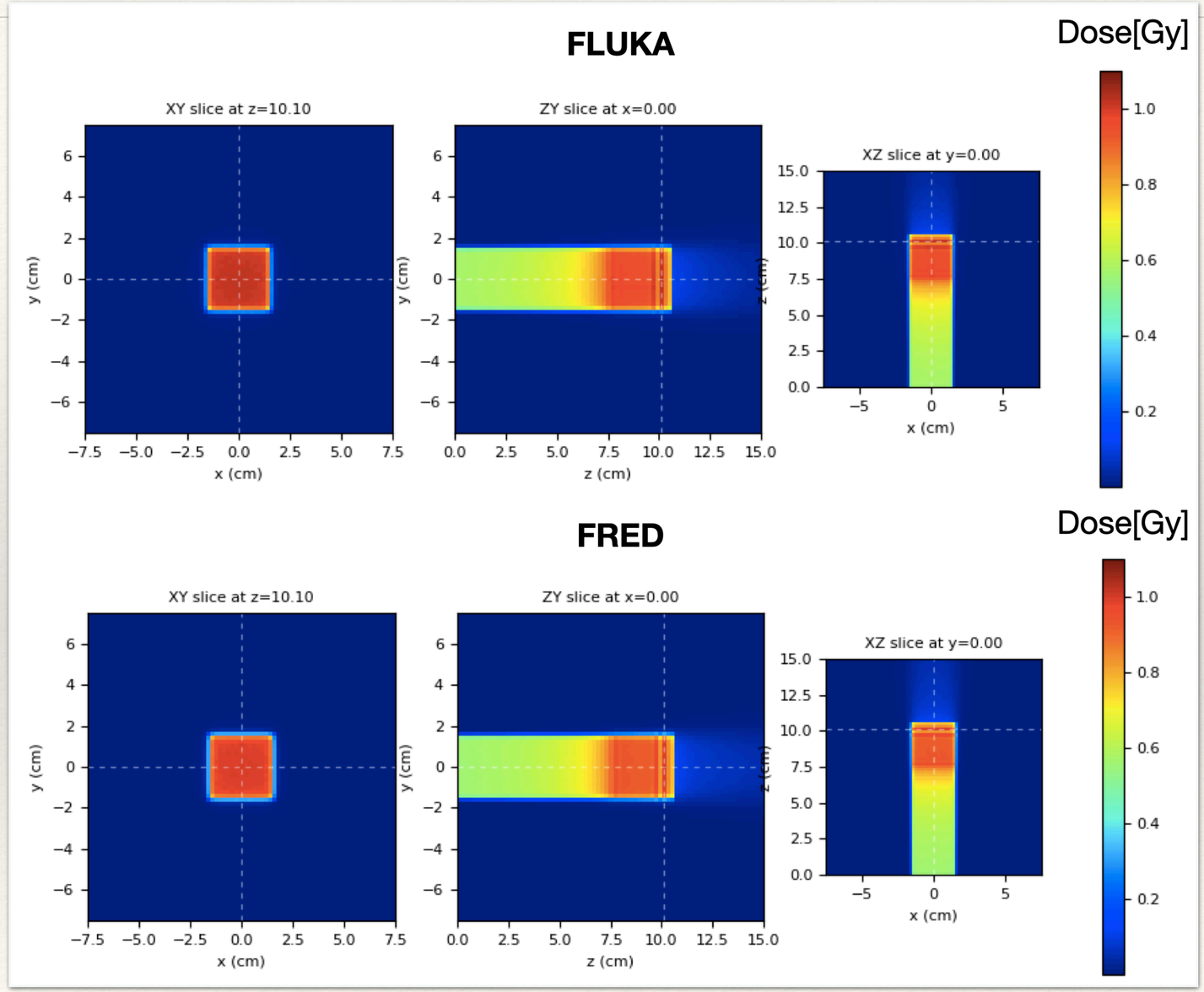

Result

SOBP from CNAO raster file

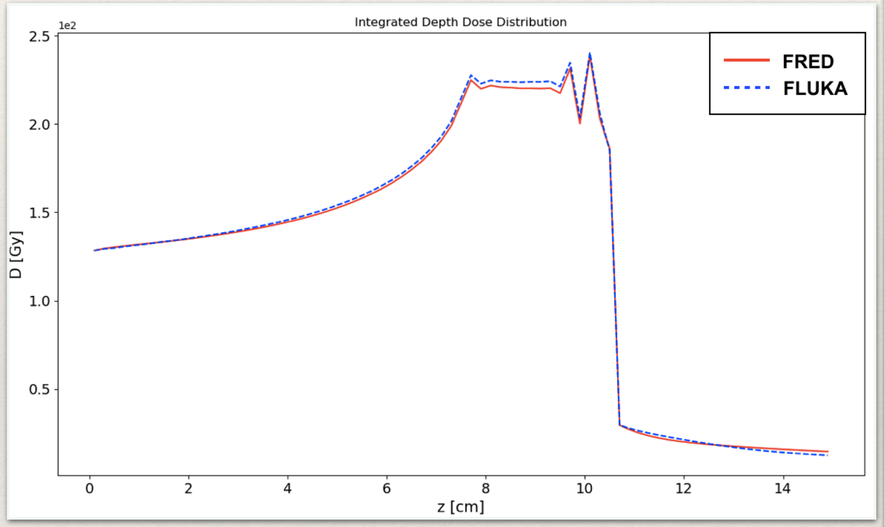

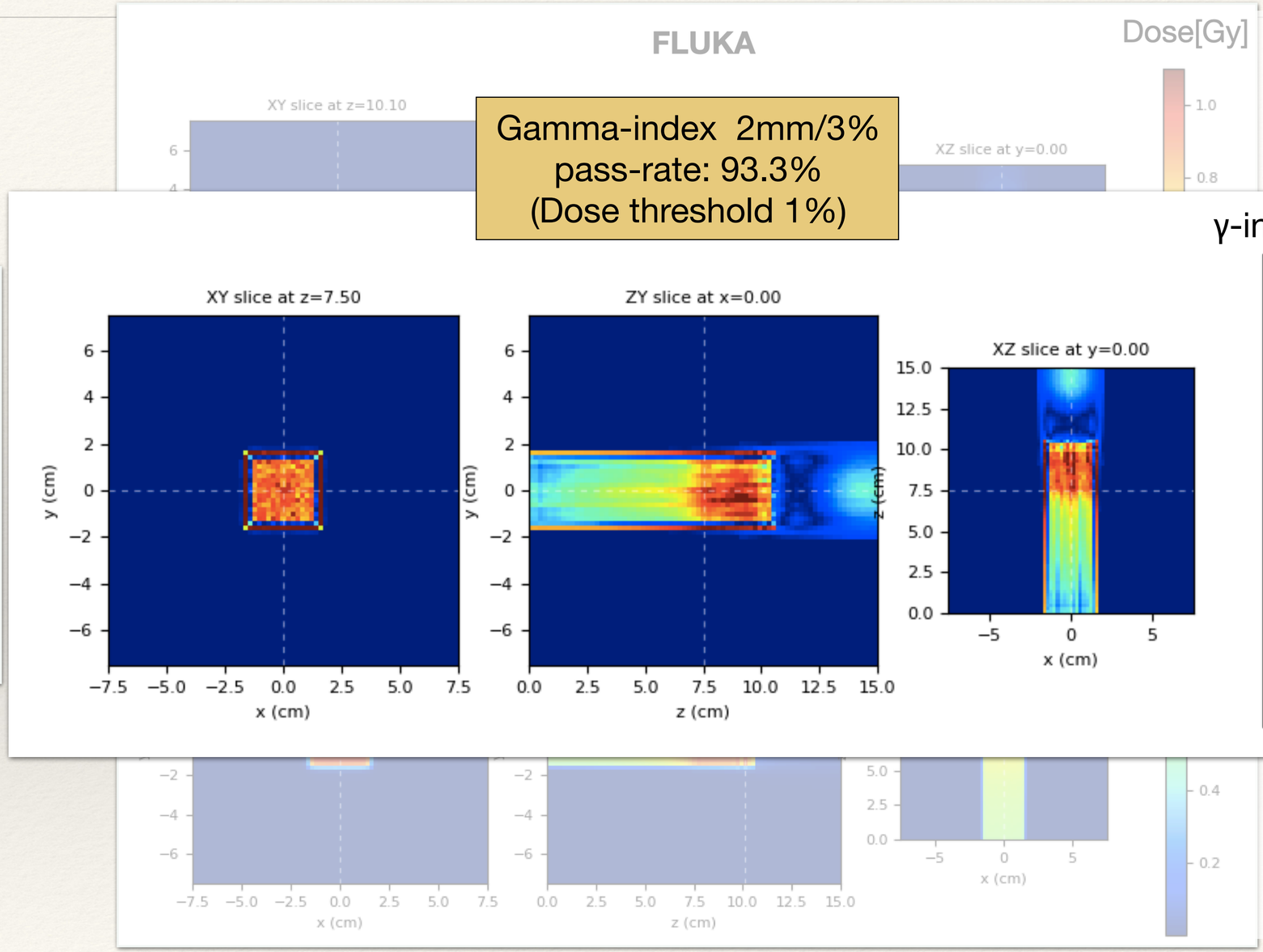

Biological Dose & Relative Biological Effectiveness

A given amounts of dose has effects on the cell that depends on the radiation.

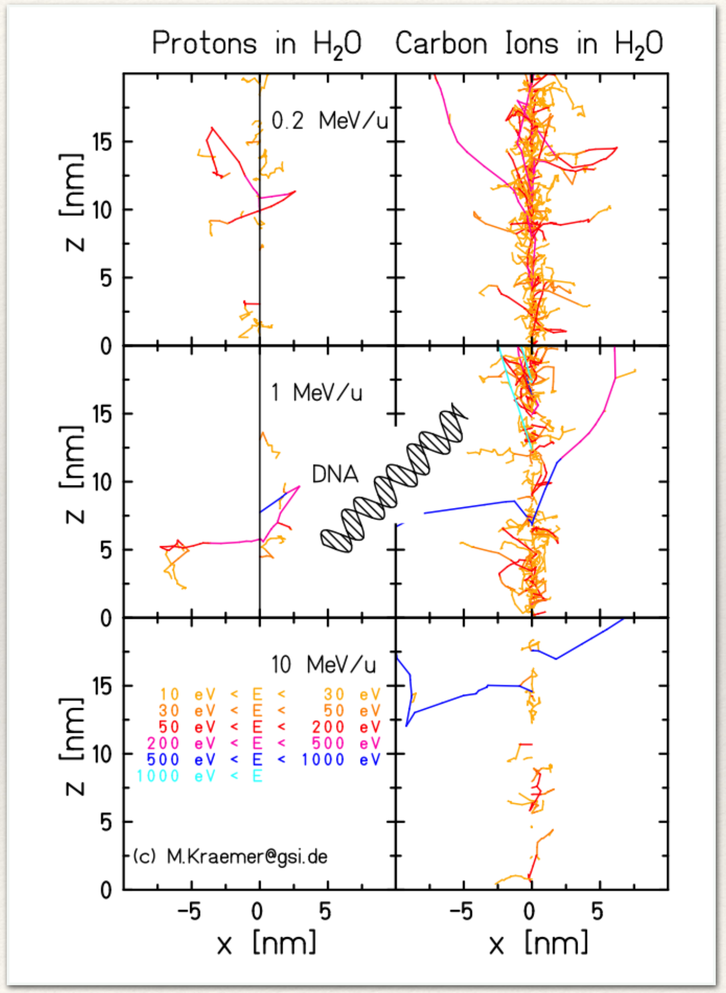

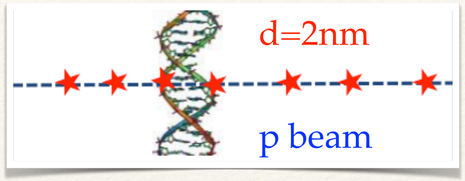

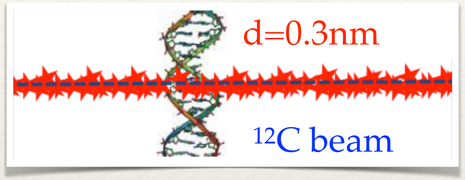

$$S(D) = \frac{N_{survival}}{N_{seed}} = e^{-(\alpha D + \beta D^2)}$$

Parameters α and β are strongly correlated to the type of radiation which release dose and its energy.

$$RBE = \left.\frac{D_x}{D_i}\right|_{Isoeffect}$$

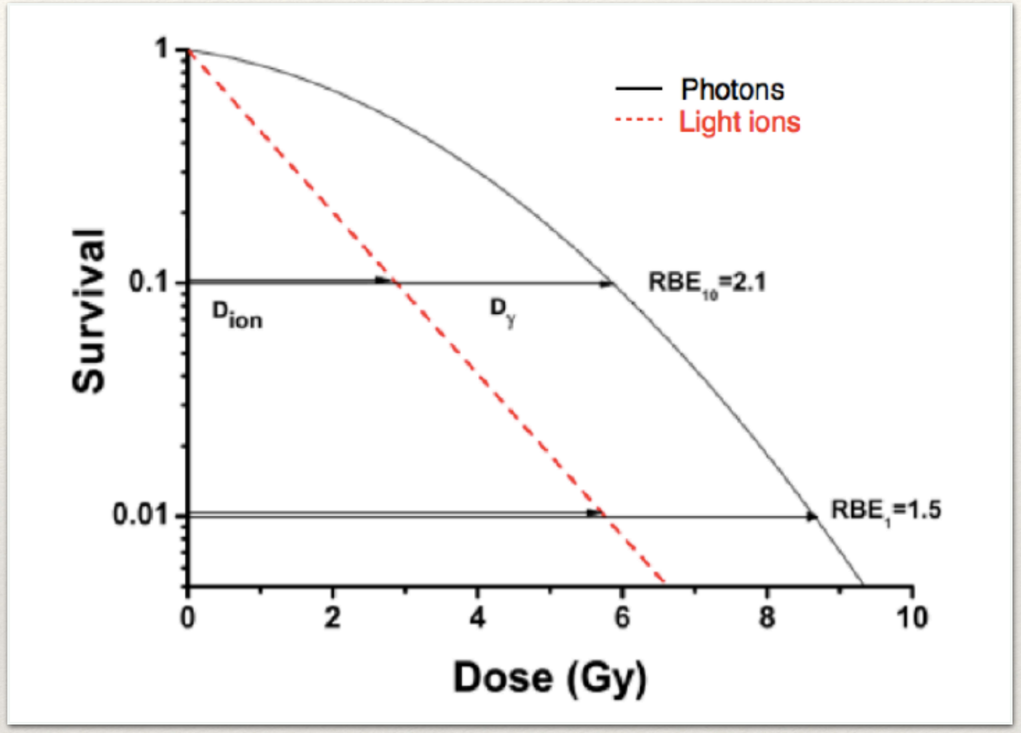

D_x = the dose of a photon radiation to cause the same damage of a ion radiation (D_i).

RBE depends on the fragments and on their energy spectrum.

LEM 1

The **LEM 1 (Local Effect Model)** has been implemented in FRED.

The principal assumption of the LEM 1 is that the total biological effect can be calculated using the scoring the local biological effect of all the particles that release dose.

During tracking

For each energy deposition, scoring of:

- D (dose)
- α•D
- $\sqrt{\beta}$•D

A wrong choice of the set of fragments emitted can lead to a wrong biological dose also if the dose distribution is correct.

At the end of the simulation

For each voxel, calculation of:

$$\bar{\alpha} = \frac{\sum_{i=1}^{n} \alpha_i D_i}{\sum_{i=1}^{n} D_i},$$

$$\bar{\beta} = \left(\frac{\sum_{i=1}^{n} \sqrt{\beta_i} D_i}{\sum_{i=1}^{n} D_i} \right)^2$$

For each voxel, calculation of:

$$-ln(S) = \begin{cases} (\bar{\beta} D_{abs} + \bar{\alpha}) D_{abs} & if\ D_{abs} \leq D_{cut} \\ (\bar{\beta} D_{cut} + \bar{\alpha}) D_{cut} + S_{max}(D_{abs} - D_{cut}) & if\ D_{cut} > D_{cut} \end{cases}$$

$$D_{RBE} = \begin{cases} \sqrt{\frac{-ln(S)}{\beta_x} + \left(\frac{\alpha_x}{2\beta_x}\right)^2} - \frac{\alpha_x}{2\beta_x} & if\ -ln(S) \leq -ln(S_{cut}) \\ \frac{-ln(S) + ln(S_{cut})}{S_{max}} + D_{cut} & if\ -ln(S) > -ln(S_{cut}) \end{cases}$$

For each voxel, calculation of:

$$RBE^i = \frac{D^i_{RBE}}{D^i}$$

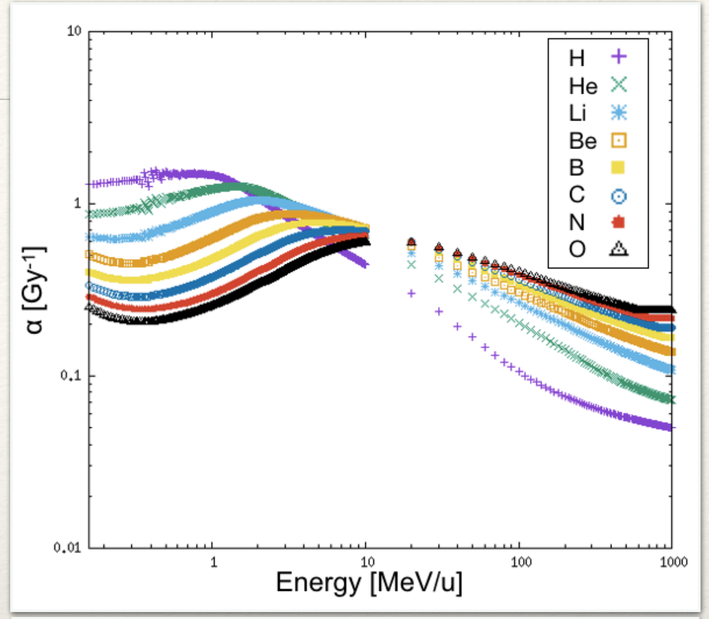

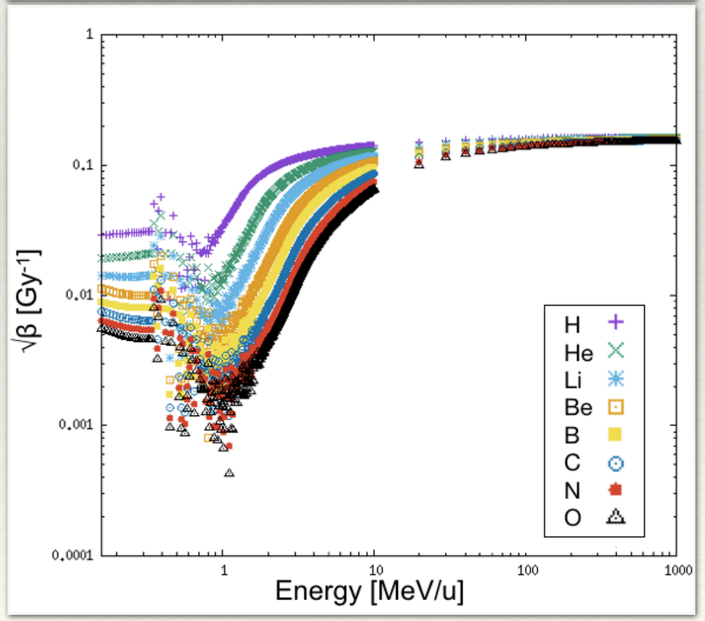

α and β from TOPAS database

Result

Biological Dose

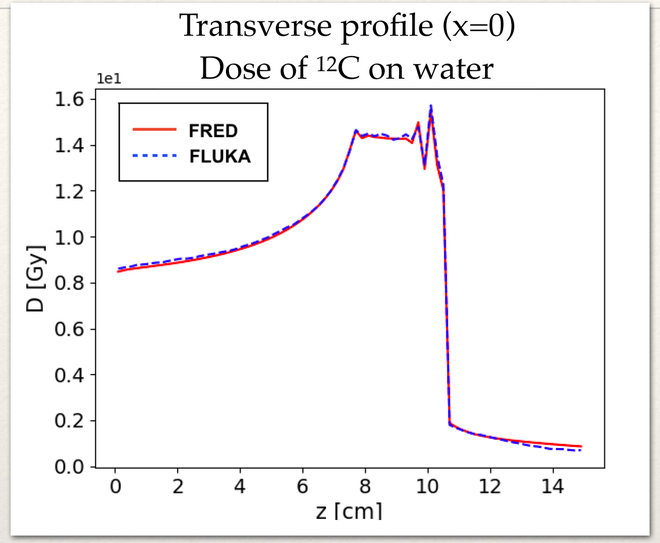

LEM 1

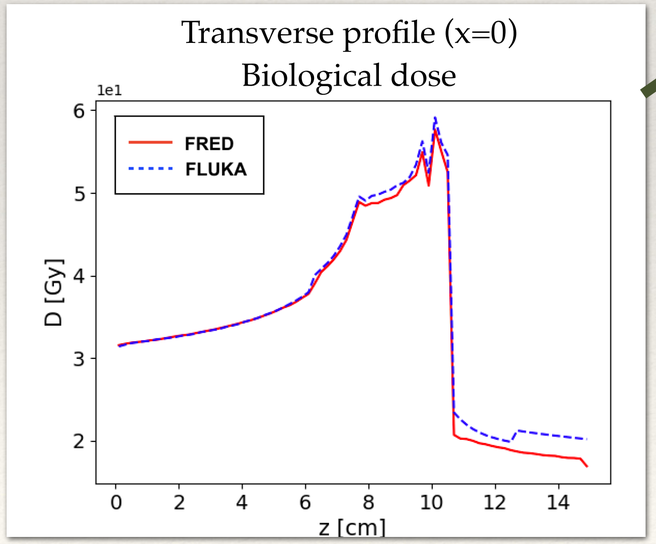

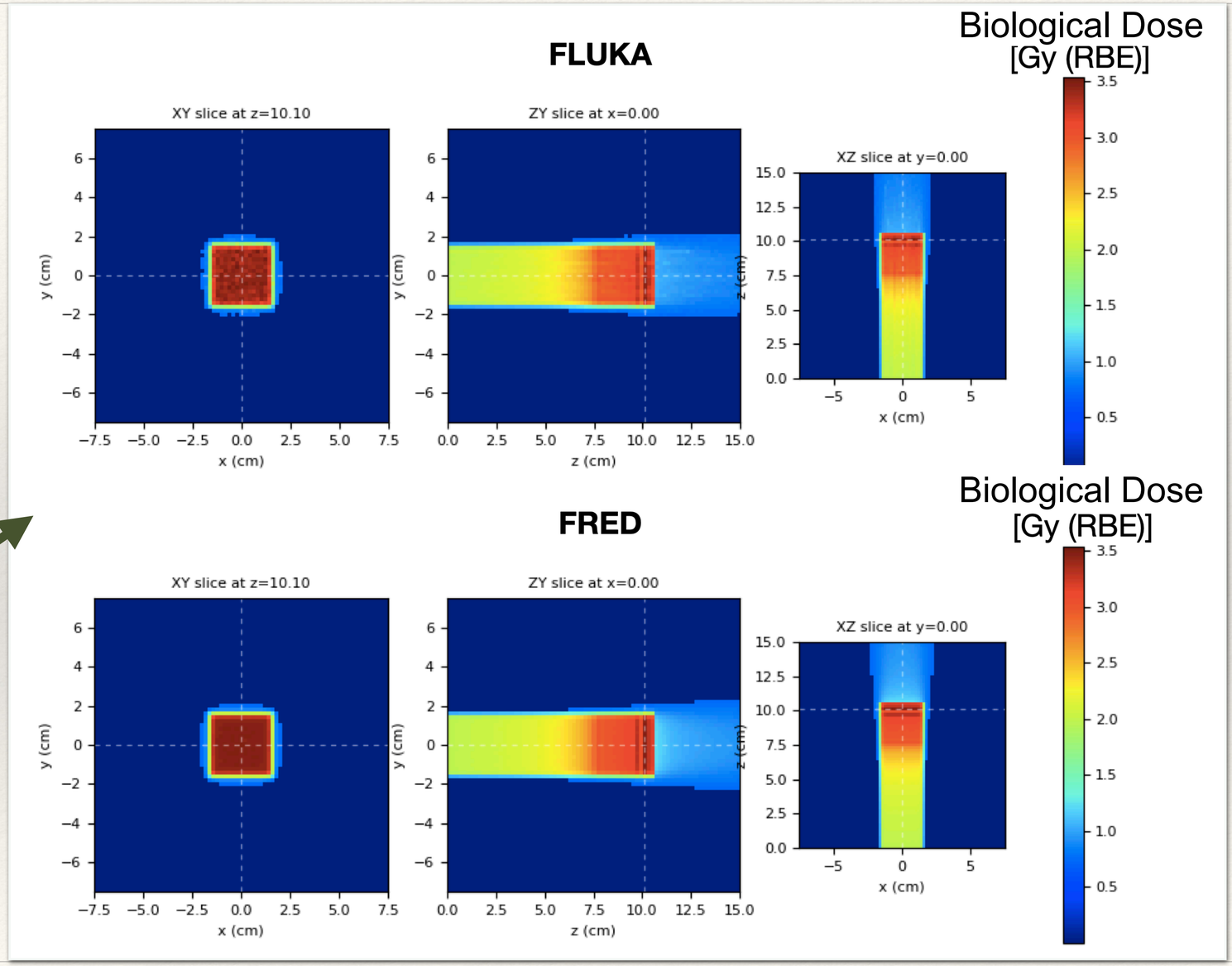

Result

Biological Dose

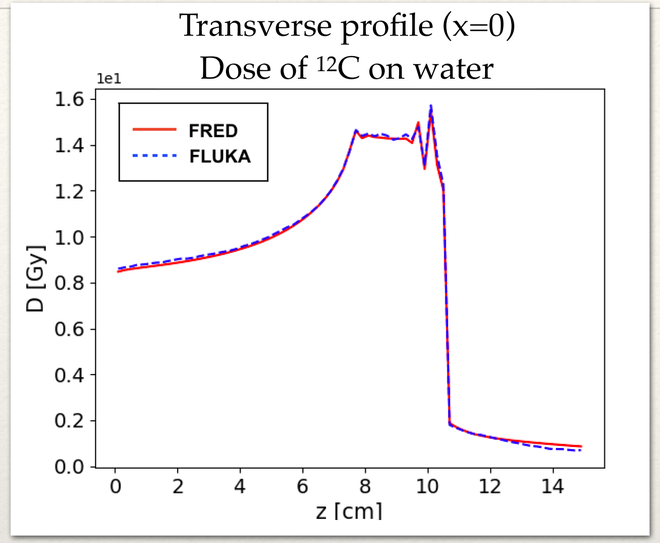

LEM 1

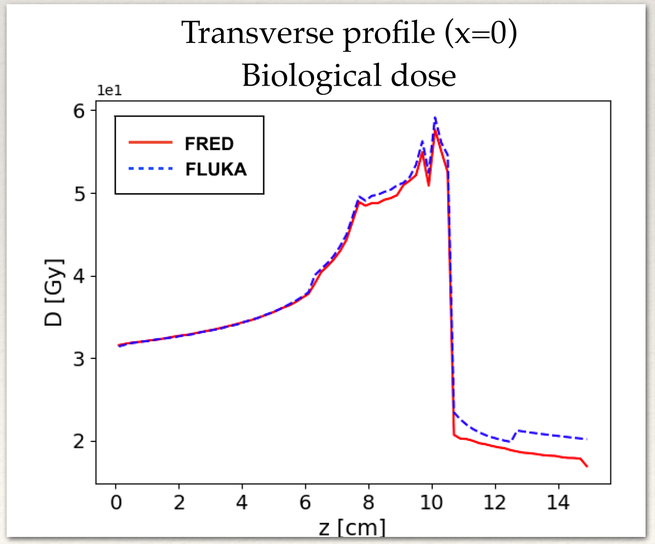

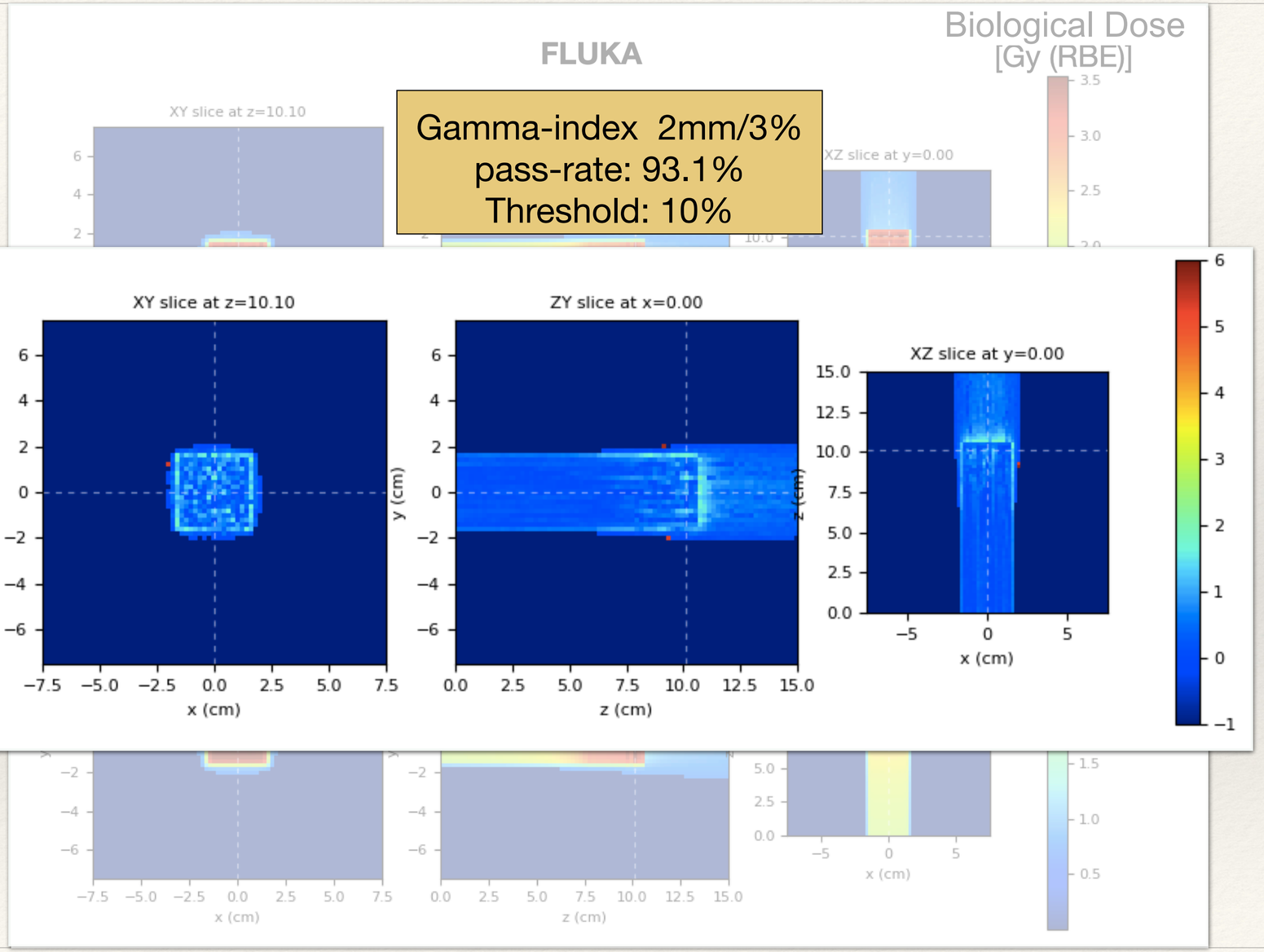

Result

Comparison with GANIL experiment

A simulation of a ^{12}C beam on a target of ^{12}C has been compared with data. The probabilities of emission of each fragment and the double differential cross-sections have been compared.

simulated with FRED

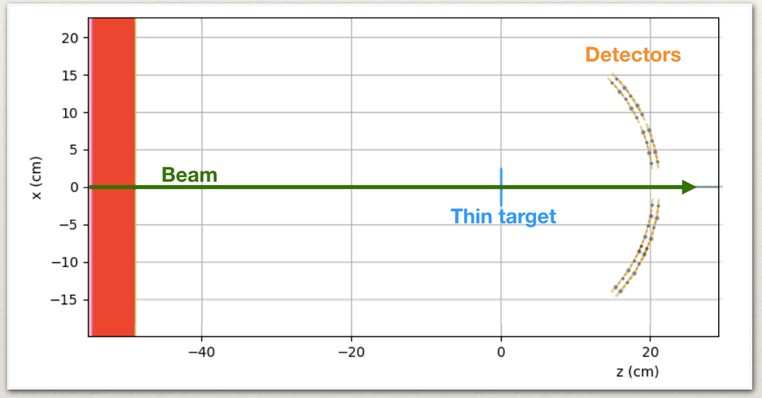

Neutrons are not shown because in the GANIL experiment only charged fragments were detected.

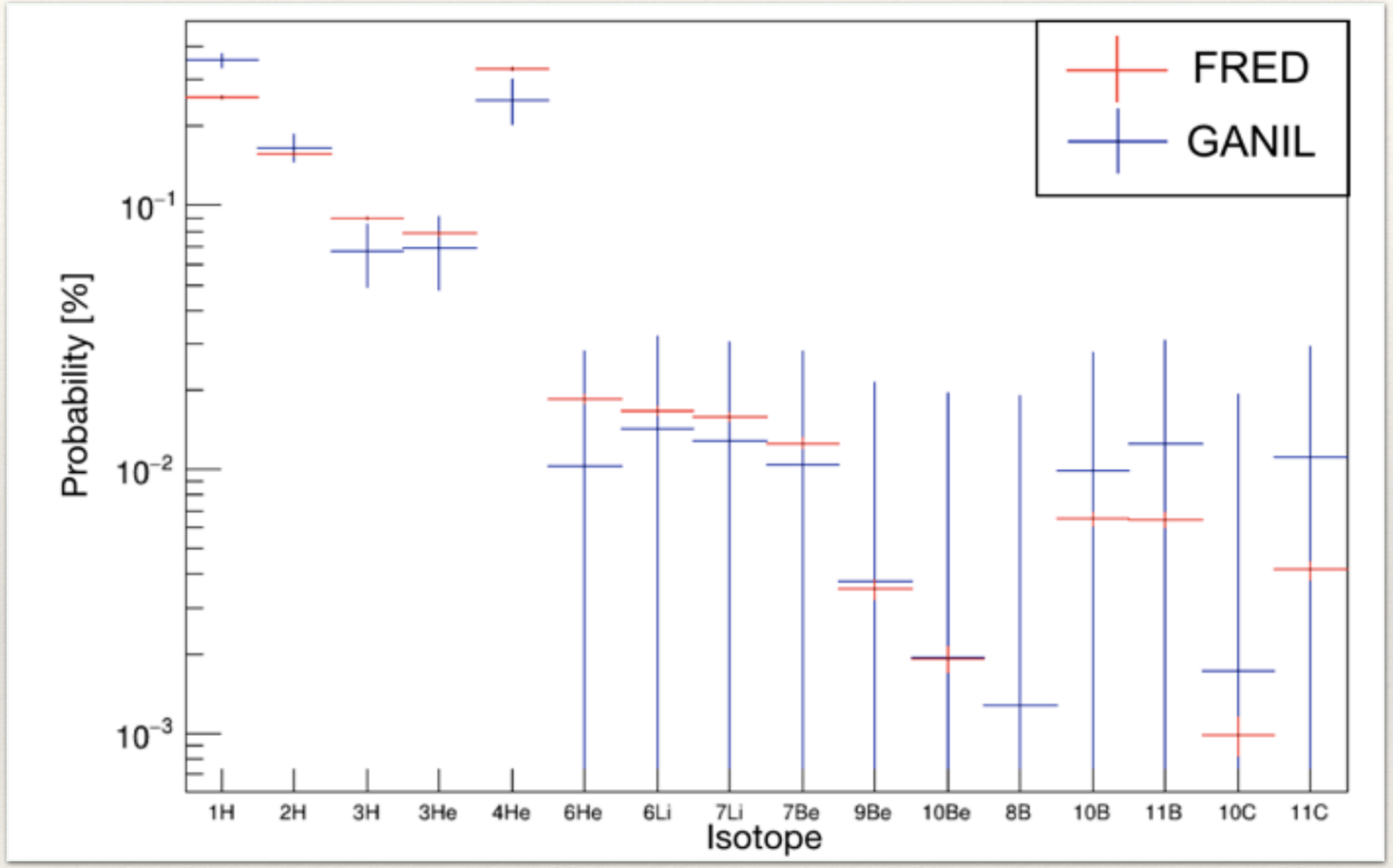

For what concern ^{12}C, even if in the experimental data the cross-section of production of this isotope is reported, physically it is not a production of fragmentation but a projectile scattering. For this reason, it is not shown in the figure.

Result

Comparison with GANIL experiment

Angular distributions for ^{12}C fragmentation on carbon target

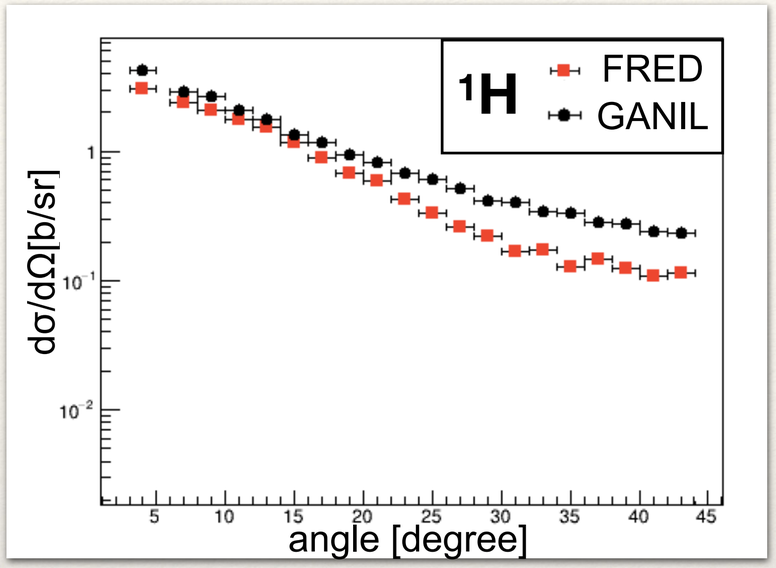

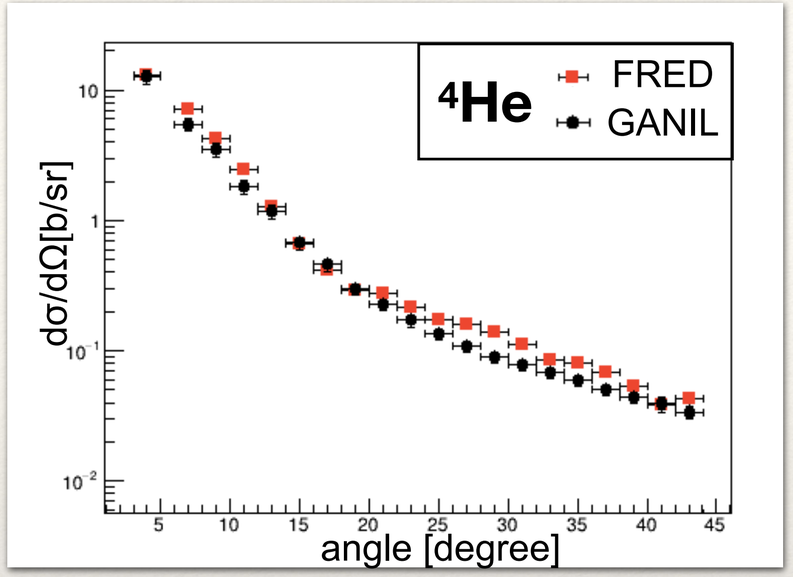

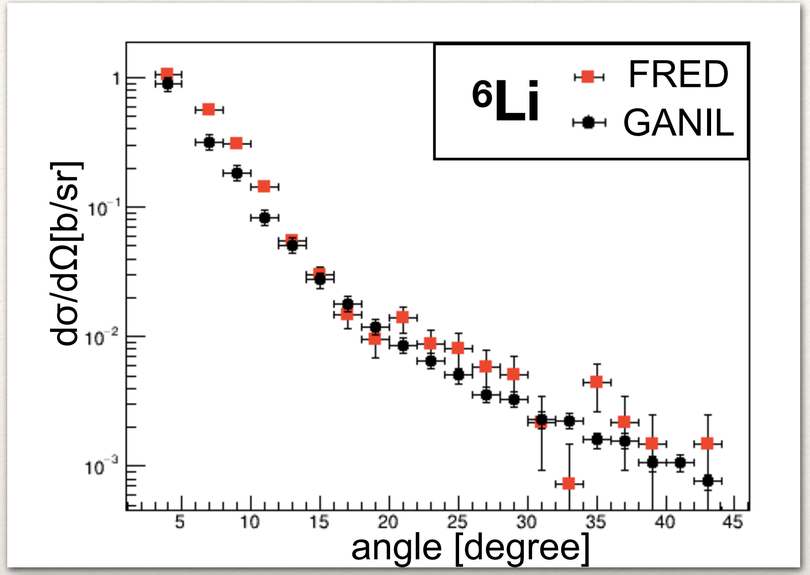

Energy distribution for a carbon target at different angles

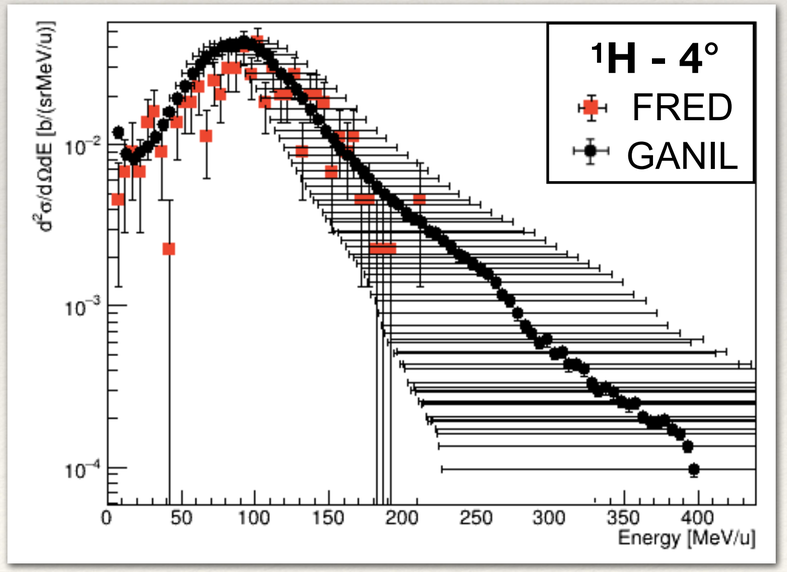

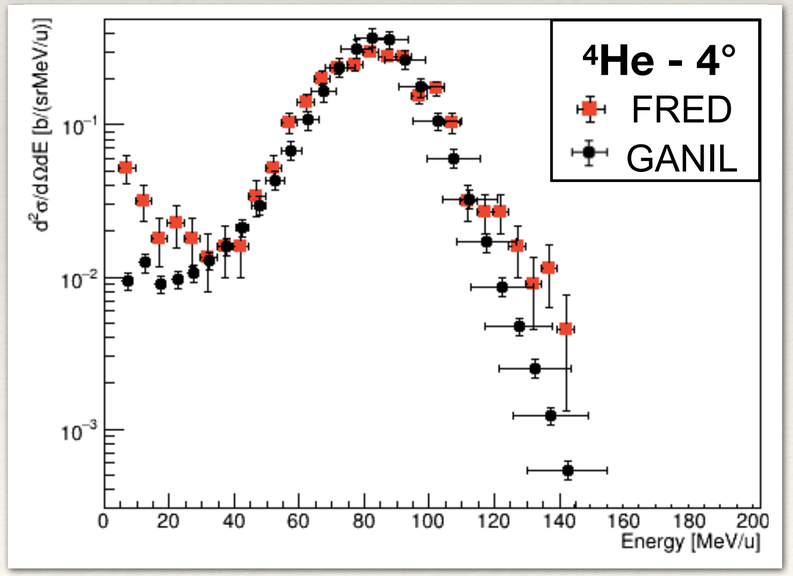

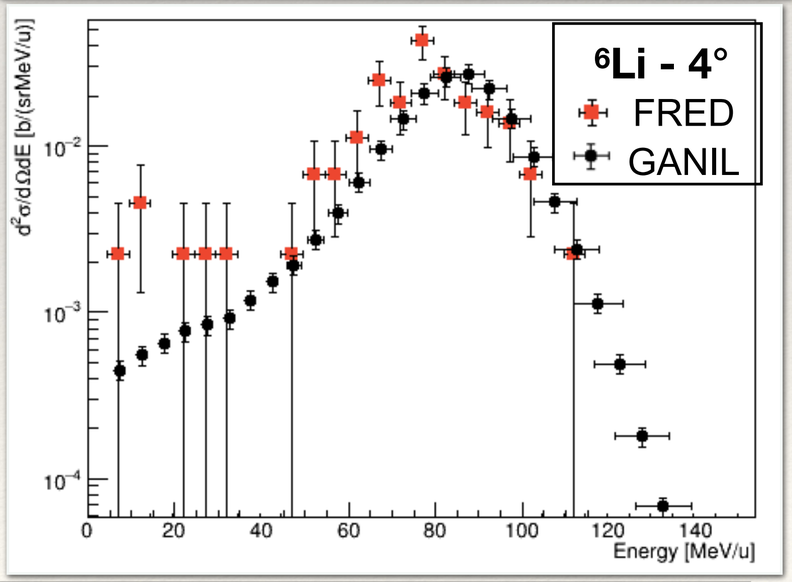

Conclusions

- ☑ Implementation of an entirely **new nuclear interaction model** of carbon on light target nuclei in the fast MC FRED. Thanks to it will be possible to run a complete TPS within minutes instead of days with the precision level of a full-MC.

- ☑ **Test** of the model against the full-MC code **FLUKA**: **excellent agreement**.
  - **Single PB**: always within **2.5%** of the total dose deposited in single pencil beams in the 100÷300 MeV/u energy range;
  - **SOBP**: agreement of the dose distribution within **1.7%** and the gamma-index 2mm/3% pass rate **93.3%**;
  - **Biological dose** and the **RBE** in **good agreement** with FLUKA.

- ☑ **Comparison** with experiments: **good agreement**.
  - **GANIL experiment;**
  - **Haettner experiment**.

- ☐ Next steps:
  - ☐ Port the model on **GPU:** A scaling from the proton version allows to estimate that the tracing kernel, running on GPU hardware, can achieve order of million primary per second on a single card.
  - ☐ Comparison of the accuracy of FRED dose recalculation with the CNAO TPS for carbon therapy to achieve **clinical validation**.

Publications

33 publications (+2 in PRESS)

h-index 5 in 3 years of research activity

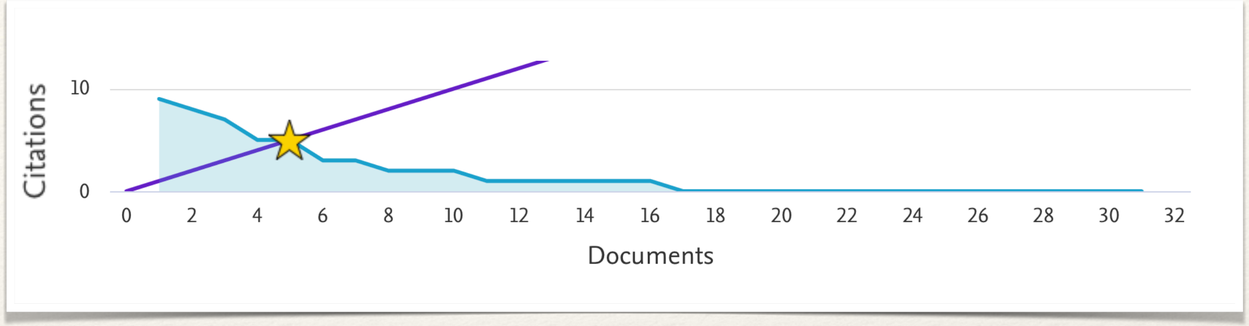

- Toppi M. et al. "PAPRICA: The Pair Production Imaging Chamber—Proof of Principle". In: *Frontiers in Physics* (2021). DOI: 10.3389/fphy.2021.568139
- Fiorina E. et al. "Detection of Interfractional Morphological Changes in Proton Therapy: A Simulation and In Vivo Study With the INSIDE In-Beam PET". In: *Frontiers in Physics* (2021). DOI: 0.3389/fphy.2020.578388
- Kraan, A.C. et al. "Charge identification of nuclear fragments with the FOOT Time-Of-Flight system" (2021)".In: *Nuclear Instruments and Methods in Physics Research, Section A: Accelerators, Spectrometers, Detectors and Associated Equipment*, DOI:10.1016/j.nima.2021.16520
- Battistoni G. et al. "Measuring the impact of Nuclear Interaction in Particle Therapy and in Radio Protection in Space: the FOOT experiment". In: *Frontiers in Physics* (2021): DOI: 10.3389/fphy.2020.568242.
- Toppi M. et al. "The MONDO Tracker: Characterisation and Study of Secondary Ultrafast Neutrons Production in Carbon Ion Radiotherapy". In: *Frontiers in Physics* (2020). DOI: 10.3389/fphy.2020.567990
- Fischetti M. et al. "Inter-fractional monitoring of ^{12}C ions treatments: results from a clinical trial at the CNAO facility". In: *Scientific Report, Nature* (2020). pp. 20735. DOI:10.1038/s41598-020-77843-z
- De Simoni M. et al. "FRED: A fast Monte Carlo code on GPU for quality control in Particle Therapy". In: *Journal of Physics: Conference Series* 1548 (2020), p. 012020. DOI: 10.1088/1742-6596/1548/1/012020
- Dong Y. et al. "The Drift Chamber detector of the FOOT experiment: Performance analysis and external calibration". In:*Nuclear Instruments and Methods in Physics Research, Section A: Accelerators, Spectrometers, Detectors and Associated Equipment* 986 (2020), DOI: 10.1016/j.nima.2020.164756
- Mattei I. et al. "Charged particles and neutron trackers: Applications to particle therapy". In: *Nuclear Instruments and Methods in Physics Research Section A: Accelerators, Spectrometers, Detectors and Associated Equipment* 954 (2020). p.161229 DOI: 10.1016/j.nima.2018.09.064
- Mattei I. et al. "Measurement of 12C Fragmentation Cross Sections on C, O, and H in the Energy Range of Interest for Particle Therapy Applications". In: *IEEE Transactions on Radiation and Plasma Medical Sciences* 4, pp 269-282 (2020), DOI: 10.1109/TRPMS.2020.2972197
- Traini G. et al. "Performance of the ToF detectors in the foot experiment". In: *Nuovo Cimento della Societa Italiana di Fisica C* 43 (2020), DOI: 10.1393/ncc/i2020-20016-5
- Morganti S. et al. "Tumor-non-tumor discrimination by a β^- detector for Radio Guided Surgery on ex-vivo neuroendocrine tumors samples", In: *Physica Medica* 72 (2020), pp. 96-102, DOI: 10.1016/j.ejmp.2020.03.021
- Collamati F. et al. "Radioguided surgery with β^- radiation in pancreatic Neuroendocrine Tumors: a feasibility study". In:*Scientific Reports* 10 (2020), p. 4015. DOI:10.1038/s41598-020-61075-2
- Collamati F. et al. "A DROP-IN beta probe for robot-assisted ^{68}Ga-PSMA radioguided surgery: first ex vivo technology evaluation using prostate cancer specimens". In: *EJNMMI Research* 10,92 (2020). DOI: https://doi.org/10.1186/s13550-020-00682-6
- Collamati F. et al. "Stability and efficiency of a CMOS sensor as detector of low energy β and γ particles". In: *Journal of Instrumentation* 15,11 (2020). DOI: https://10.1088/1748-0221/15/11/P11003
- Morrocchi M. et al "Performance Evaluation of the TOF-Wall Detector of the FOOT Experiment". In: IEEE Transactions on Nuclear Science (2020). DOI: 10.1109/TNS.2020.3041433
- Traini g. et al. "Review and performance of the Dose Profiler, a particle therapy treatments online monitor". In: *Physica Medica* 65 (2019). pp. 84-93. DOI:10.1016/j.ejmp.2019.07.010
- Rucinski A. et al. "Secondary radiation measurements for particle therapy applications: Charged secondaries produced by 16O ion beams in a PMMA target at large angles". In: *Physica Medica* 64 (2019). pp. 45-53. DOI: 10.1016/j.ejmp.2019.06.001
- Gioscio E. et al. "Development of a novel neutron tracker for the characterisation of secondary neutrons emitted in Particle Therapy". In: *Nuclear Instruments and Methods in Physics Research, Section A: Accelerators, Spectrometers, Detectors and Associated Equipment* 958 (2019). pp. 162862. DOI: 10.1016/j.nima.2019.162862
- Manuzzato E. et al. "A 16×18 Digital-SiPM Array with Distributed Trigger Generator for Low SNR Particle Tracking". In: *IEEE Solid-State Circuits Letters* (2019). pp. 75-78. DOI:10.1109/LSSC.2019.2934598
- Manuzzato, E. et al. "A 16 8 Digital-SiPM Array with Distributed Trigger Generator for Low SNR Particle Tracking" ESSCIRC 2019 - IEEE 45th European Solid State Circuits Conference (2019) DOI:10.1109/ESSCIRC.2019.8902571
- Montesi M. C. et al. "Ion charge separation with new generation of nuclear emulsion films". In: *Open Physics* 17 (2019). pp. 233-240. DOI: 10.1515/phys-2019-0024
- Morrocchi M. et al. "Development and characterization of a ΔE-TOF detector prototype for the FOOT experiment". In: *Nuclear Instruments and Methods in Physics Research, Section A: Accelerators, Spectrometers, Detectors and Associated Equipment* 916 (2019).pp. 116-124. DOI: 10.1016/j.nima.2018.09.086
- Collamati F. et al. "Characterisation of a β detector on positron emitters for medical applications", In: *Physica Medica* 67 (2019). pp. 85-90, DOI: 10.1016/j.ejmp.2019.10.025
- De Simoni M. et al. "In-room test results at CNAO of an innovative PT treatments online monitor (Dose Profiler)". In: *IL NUOVO CIMENTO 41 C* 209 (2018). DOI: 10.1393/ncc/i2018-18209-2
- Fischetti M. et al. "Characterisation of the secondary-neutron production in particle therapy treatments with the MONDO tracking detector". In: *IL NUOVO CIMENTO 41 C* 206 (2018). DOI: 10.1393/ncc/i2018-18206-5
- Collamati F. et al. "Radioguided surgery with β radiation: a novel application with Ga^{68}". In. *Scientific Report* 8 (2018). p. 16171. DOI:10.1038/s41598-018-34626-x
- Giacometti V. et al. "Characterisation of the MONDO detector response to neutrons by means of a FLUKA Monte Carlo simulation". In: *Radiation Measurements* 119 (2018). pp. 144-149. DOI: 10.1016/j.radmeas.2018.10.006
- Valle S. M. et al. "The FOOT (FragmentatiOn Of Target) experiment". In: *IL NUOVO CIMENTO 41 C* 41 (2018). p. 169. DOI: 10.1393/ncc/i2018-18169-5
- Mattei I. et al. "Scintillating fiber devices for particle therapy applications". In: *IEEE Transactions on Nuclear Science* 65 (2018). pp. 2054-2060. DOI: 10.1109/TNS.2018.2843179
- Morganti S. et al. "Position sensitive β^- Detector based on p-terphenyl scintillator for medical applications". In: *Journal of Instrumentation* 13 (2018). p. 07001. DOI: 10.1088/1748-0221/13/07/P07001
- Mirabelli R. et al. "In-room performance evaluation of a novel online charged secondary particles monitor of light ions PT treatments". In: *2018 IEEE Nuclear Science Symposium and Medical Imaging Conference Proceedings* (2018). pp. 1-3. DOI: 10.1109/NSSMIC.2018.8824552
- Andrey A. et al. "The foot fragmentation of target experiment"In: *Proceedings of the 15th International Conference on Nuclear Reaction Mechanisms, NRM 2018* (2018), pp. 305-311
- Toppi M. et al. "Monitoring carbon ion beams transverse position detecting charged secondary fragments: results from patient treatment performed at CNAO". In: *Frontiers in Oncology* IN PRESS
- A. Sarti et al., Feasibility study of a prostate cancer FLASH therapy treatment with electrons of high energy (2021), Frontiers in Physics. IN PRESS

Conferences

9 presentations at international conferences
(5 oral presentations and 4 poster presentations)

Oral Presentations

- **Nov. 2020,** *IEEE Nuclear Science Symposium and Medical Imaging Conference* - Online/Virtual, “In vivo verification of carbon ion therapy treatments at CNAO by means of charged fragments detection”
- **Sept. 2019,** *International Conference on Medical Accelerators and Particle Therapy* - Seville (Spain), ”A data-driven nuclear fragmentation model for a fast Monte-Carlo code, FRED, in Particle Therapy with Carbon beams”
- **Jun. 2019,** *10th Young Researcher Meeting* - Rome (Italy), "FRED: a fast Monte Carlo code on GPU for quality control in Particle Therapy”
- **Jan. 2019**, *57th International Winter Meeting on Nuclear Physics* - Bormio (Italy), "The Dose Profiler tracker: an online Particle Therapy monitor”
- **Sept. 2018**, *Società italiana per le ricerche sulle radiazioni* - Roma (Italy), "In-room characterization, using an anthropomorphic phantom, of a novel detector for on-line dose monitoring in light ions cancer therapy")

Posters Presentations

- **Nov. 2020,** *IEEE Nuclear Science Symposium and Medical Imaging Conference* - Online/Virtual, “Fragmentation model for Treatment Planning System of carbon ions implemented in a fast MC code (FRED)”
- **Nov. 2020,** *IEEE Nuclear Science Symposium and Medical Imaging Conference* - Online/Virtual, “Study of secondary neutron production in PT treatments using MONDO, an innovative ultra-fast neutrons tracker”
- **Sept. 2018,** *Società italiana per le ricerche sulle radiazioni* - Roma (Italy), “Applications in Particle Therapy of FRED, a fast Monte Carlo code on GPUs for energy deposition of proton beams in matter"
- **Sept. 2019,** *International Conference on Medical Accelerators and Particle Therapy* - Seville (Spain), ”Spectrum and flux measurements of secondary ultra-fast neutrons produced in Particle Therapy treatments using the innovative MONDO tracker”

Thank you for your attention

Any questions?

Backup

Dose

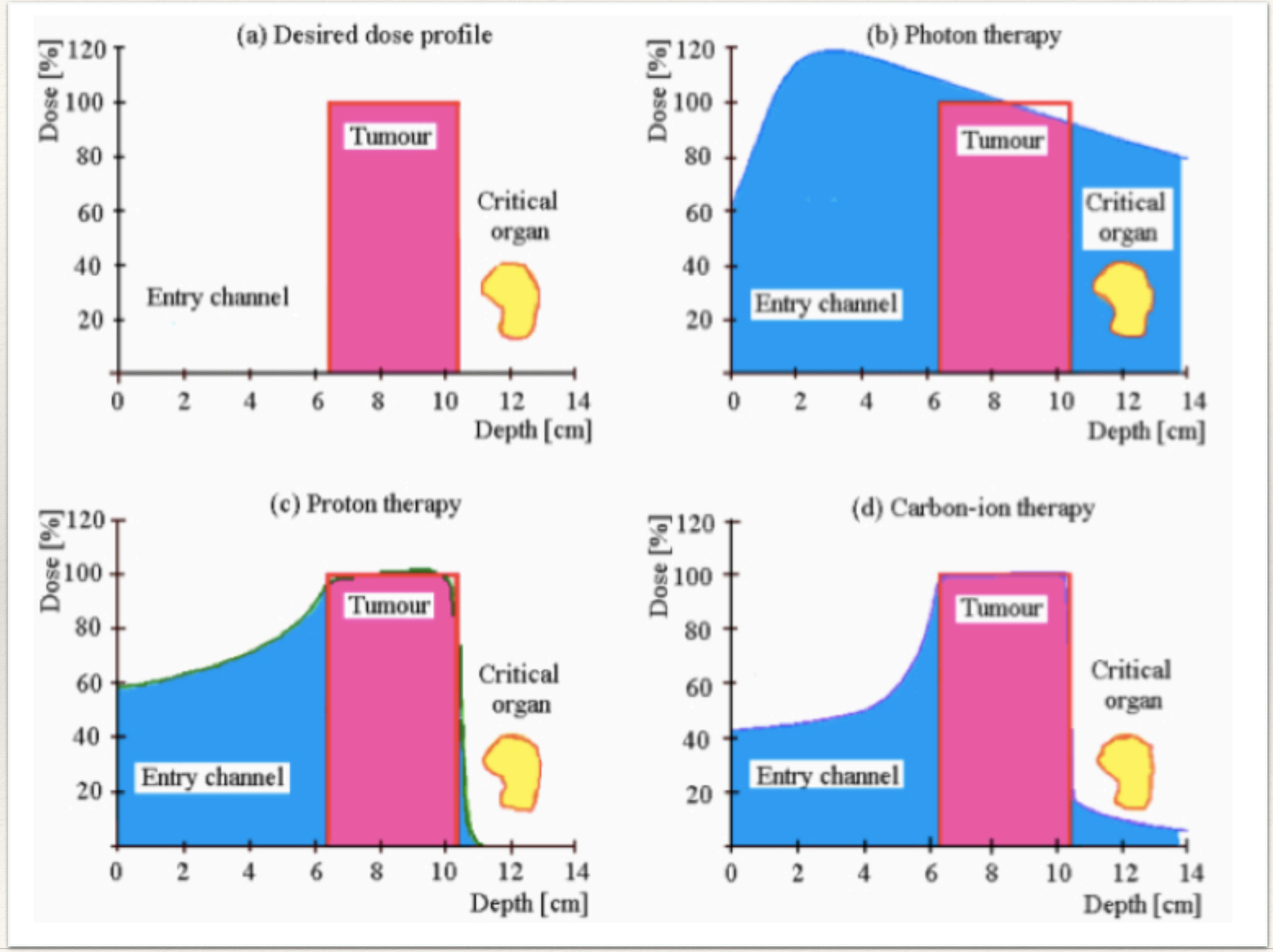
(a) Desired dose profile
Dose [%]
120
100
80
60
40
20
Tumour
Critical organ
Entry channel
0 2 4 6 8 10 12 14
Depth [cm]
(b) Photon therapy
Dose [%]
120
100
80
60
40
20
Tumour
Critical organ
Entry channel
0 2 4 6 8 10 12 14
Depth [cm]
(c) Proton therapy
Dose [%]
120
100
80
60
40
20
Tumour
Critical organ
Entry channel
0 2 4 6 8 10 12 14
Depth [cm]
(d) Carbon-ion therapy
Dose [%]
120
100
80
60
40
20
Tumour
Critical organ
Entry channel
0 2 4 6 8 10 12 14
Depth [cm]

Linear Energy Transfer

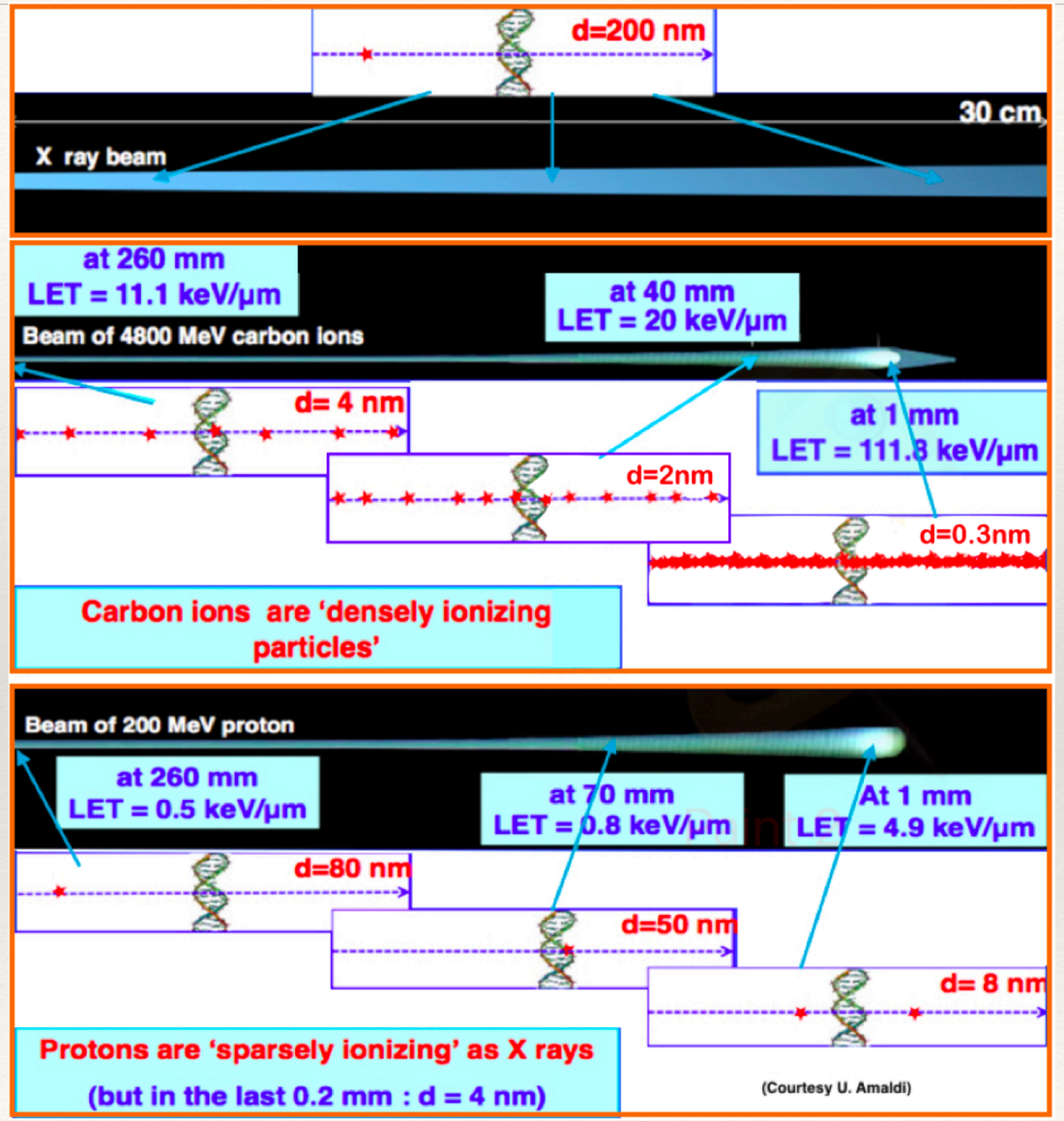

Requirements for particle therapy

Typical clinical requirements for particle therapy using carbon ions or protons

Parameter	**Value**
Extraction energy (**proton**) (min,max)	60,240 MeV
Extraction energy (**carbon**) (min,max)	110, 450 MeV/u
Energy step (**proton**) (at min, at max)	5, 1 MeV
Energy step (**carbon**)(at min, at max)	15, 6 MeV/u
Energy resolution (at min, at max)ΔE/E	3.5%,1.8%
Voxel size (min, max)	$4 \times 4 \times 4, 10 \times 10 \times 10$ mm^3
Smallest field of view (min, max)	$100 \times 100, 250 \times 250$ mm^2
Clinical dose rate (min, max)	2, $>$ 10 Gy/min
Cycle rate (min, max)	0.5, 2 kHz
Bunch charge (**proton**) (min, max)	1.6, 16 fC
Bunch charge (**carbon**) (min, max)	300, 3000 fC
Bunch charge stability and bunch charge measurement accuracy	$<$10%

Performance of FRED tracking protons

	Hardware	Primary / s	µs / primary
FLUKA/ GEANT4	single CPU core	0.75 k	1340
FRED	single CPU core	15 k	68
FRED	single GPU card (NVIDIA GTX 980)	5000 k	0.2

[1]*De Simoni M. et al. Journal of Physics: Conference Series 1548 (2020)*

Primary / s ∝ #GPUs

Multiple Coulomb Scattering

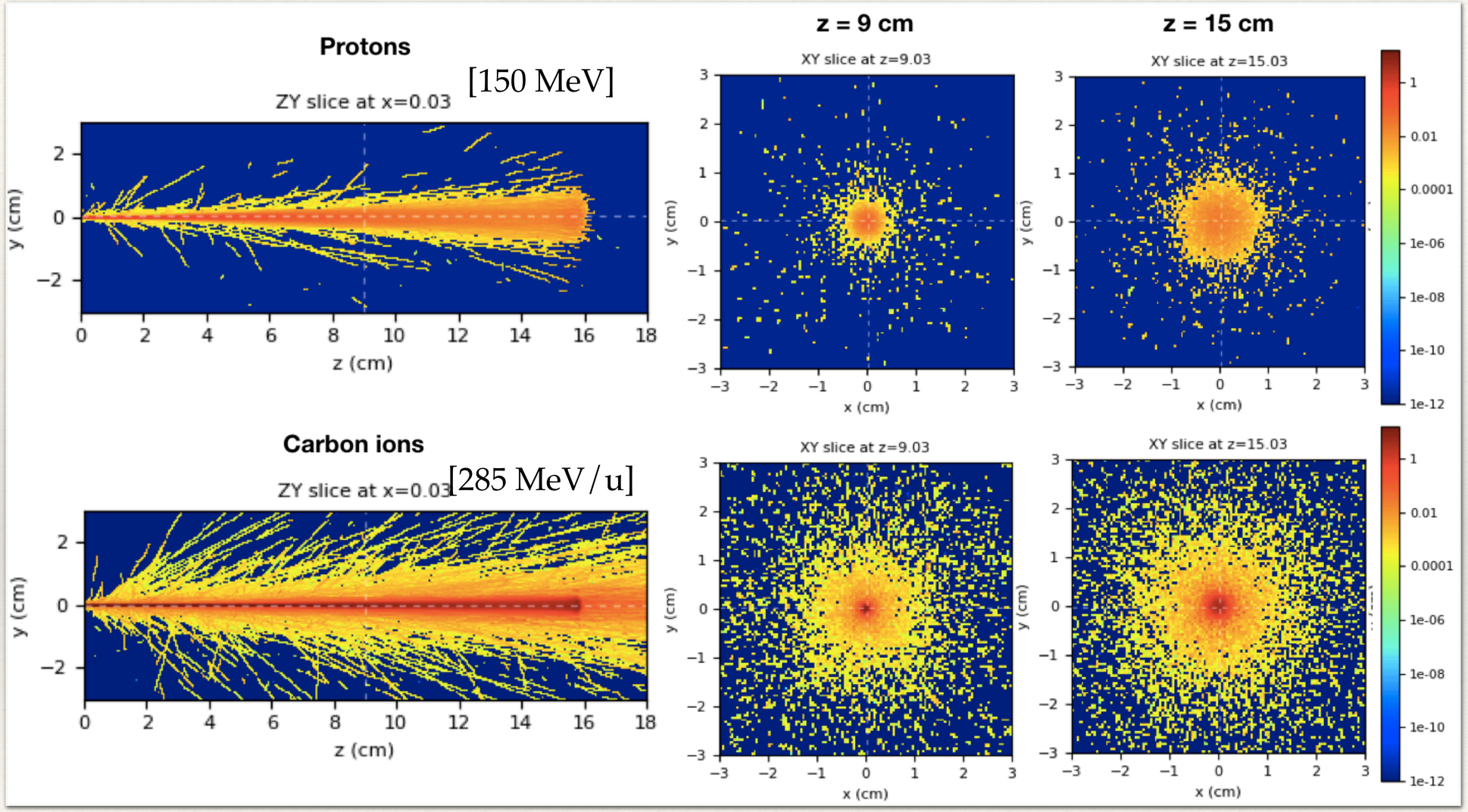

carbon beam shows a lateral spread smaller than protons

Multiple Coulomb Scattering

Moliére theory with some assumptions:

- the target crossed by the particle beam is made of a single element;
- the material is thin enough that the energy of the particle can be considered constant;
- the scattering angle with respect to the initial direction of the beam is small, to approximate sinθ with θ .

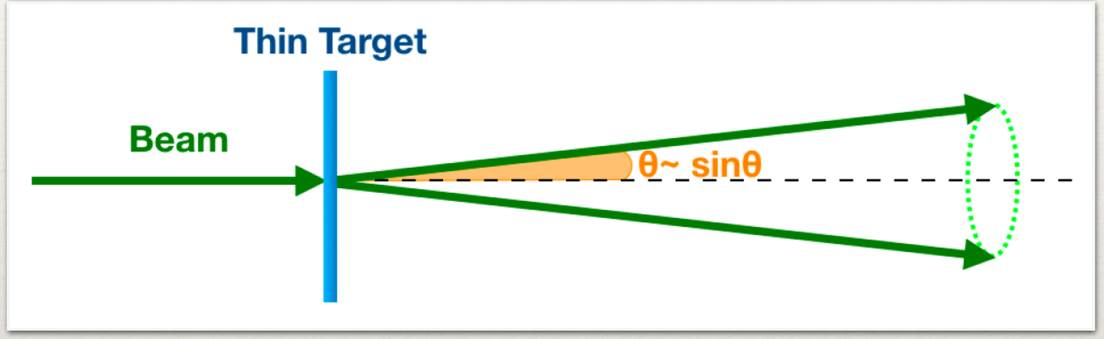

Single Gaussian approximation

$$f_G(\theta) = \frac{1}{\sqrt{2\pi}\theta_0} exp\left[-\frac{1}{2}\frac{\theta^2}{\theta_0^2}\right]$$

$$\theta_0 = \frac{14.1\text{MeV}}{pv} z\sqrt{\frac{L}{L_R}}\left[1 + \frac{1}{9}log\left(\frac{L}{L_R}\right)\right]\text{rad}$$

The standard deviation θ was multiplied by a scaling factor f_{mcs}.This factor was obtained by comparing FRED and FLUKA simulations of a single pencil beam in water in the mid of the therapeutic energy range and with nuclear interactions switched off.

Multiple Coulomb Scattering

To find the best value for the SRF, the error between σ_{FRED} and σ_{FLUKA} at 90% of Range is minimized

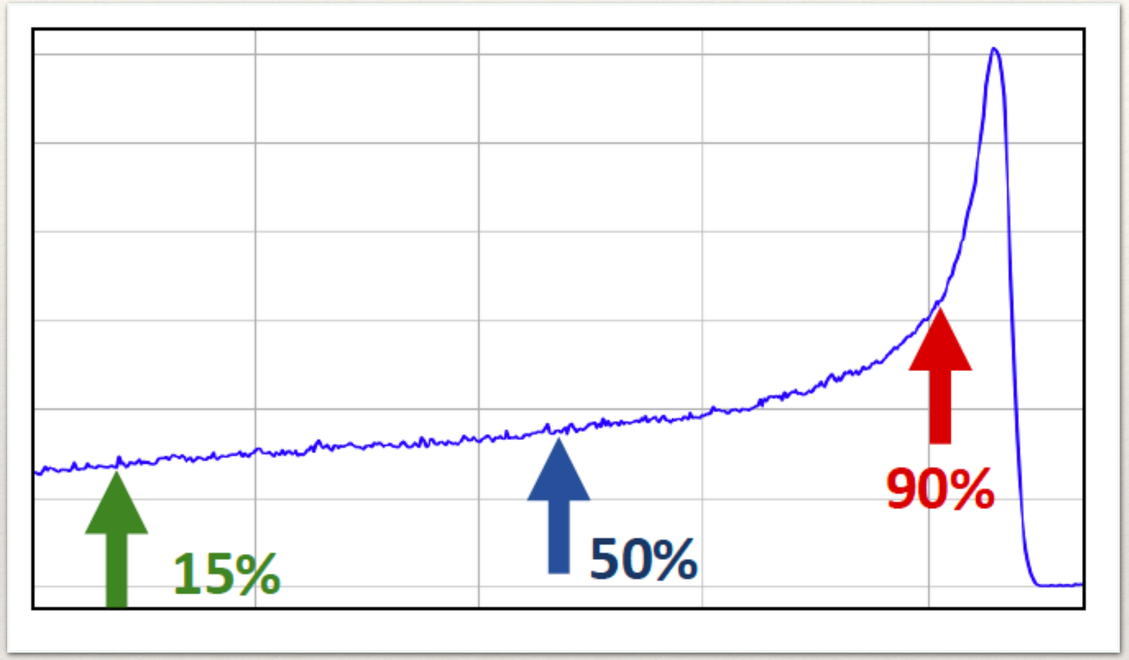

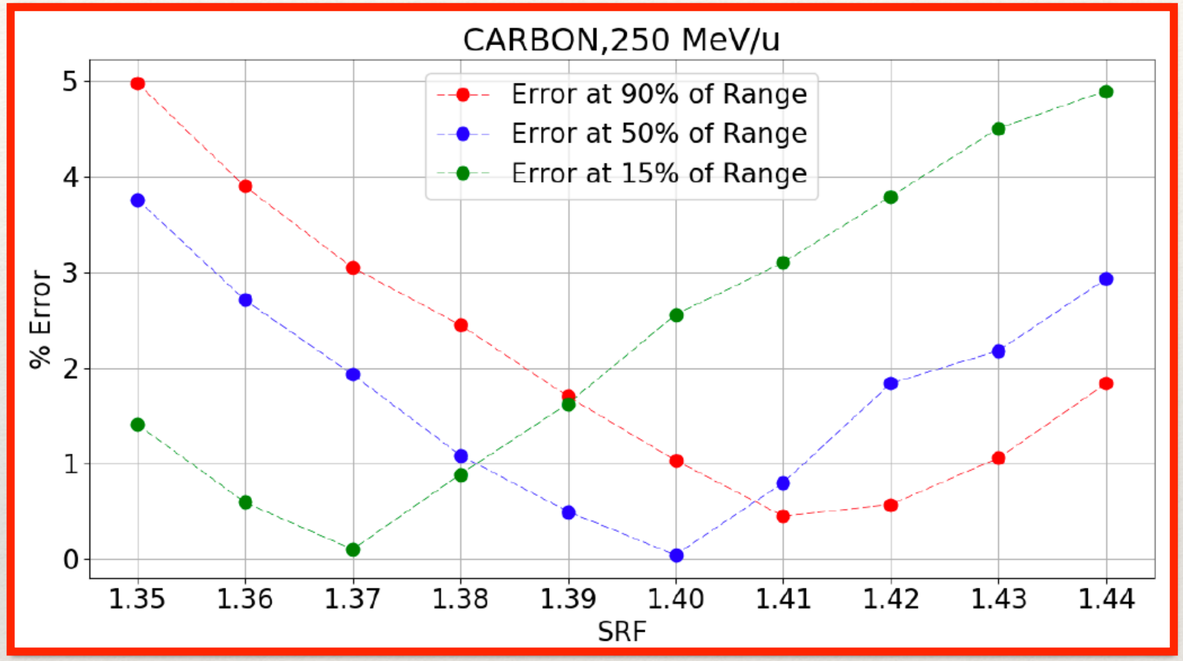

Particle	Atomic number Z	Best SRF value
Alpha	2	1.36
Lithium 7	3	1.39
Beryllium 9	4	1.40
Boron 10	5	1.41
Carbon 12	6	1.41
Oxygen 16	8	1.42

Multiple Coulomb Scattering

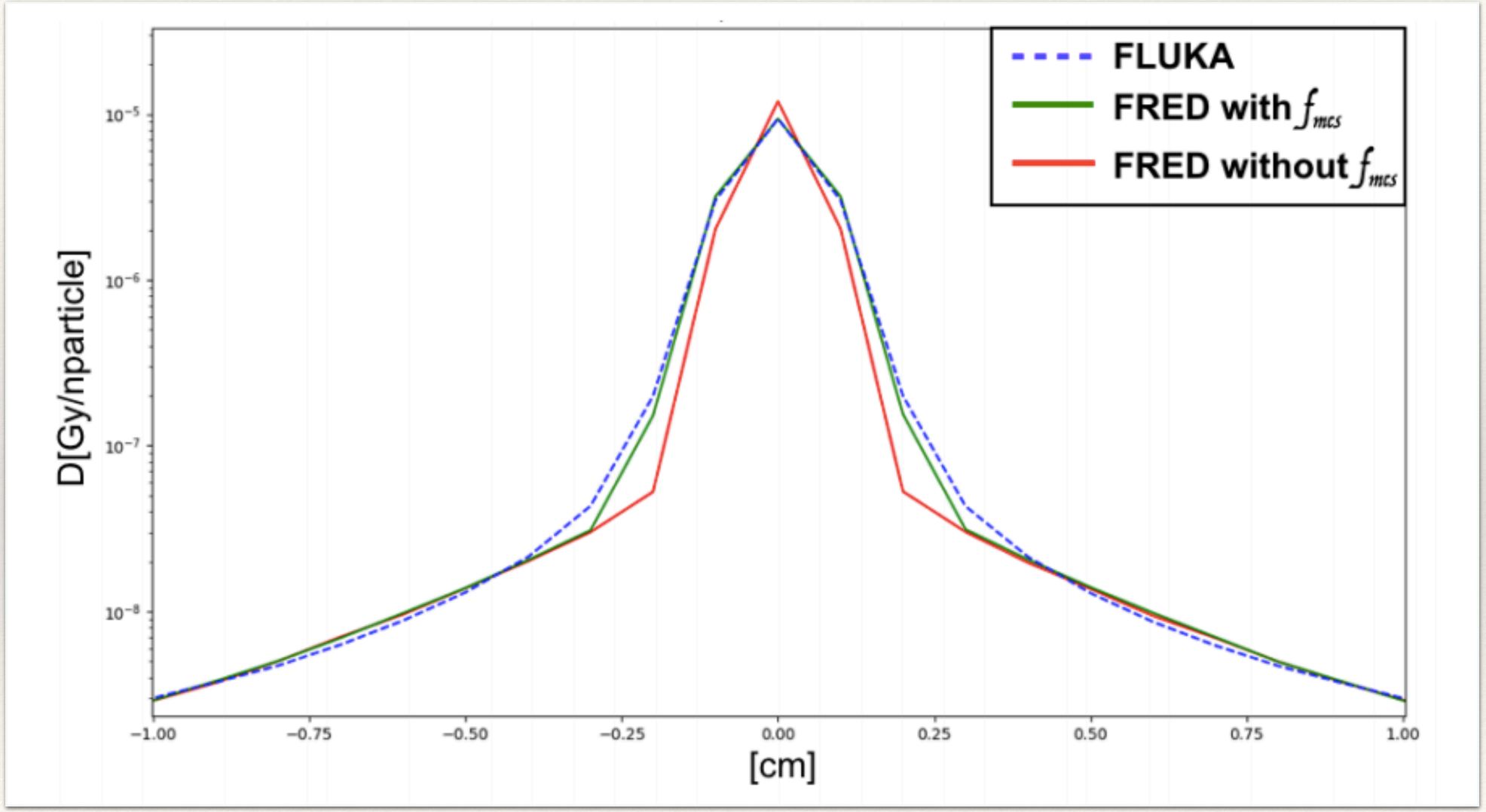

Elastic cross-section

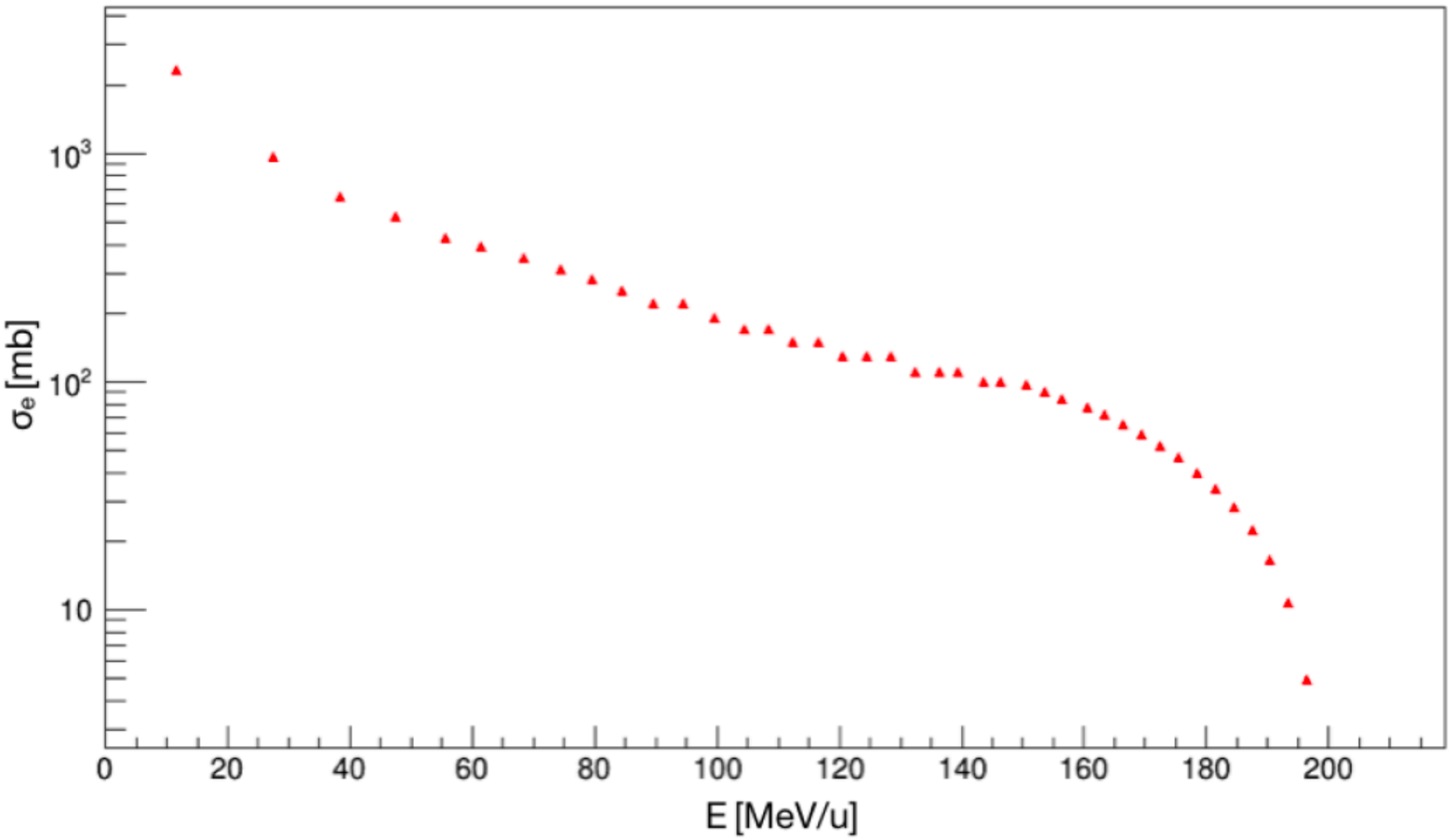

Elastic cross-sections of a beam of carbon ion on hydrogen targets obtained with FRED interpolating data of incident-proton on carbon target

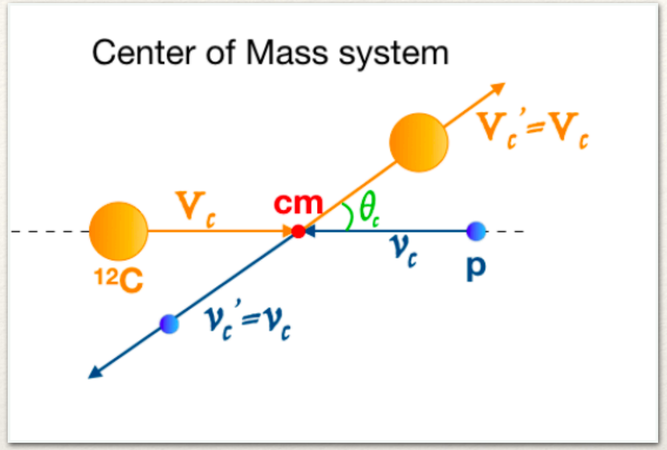

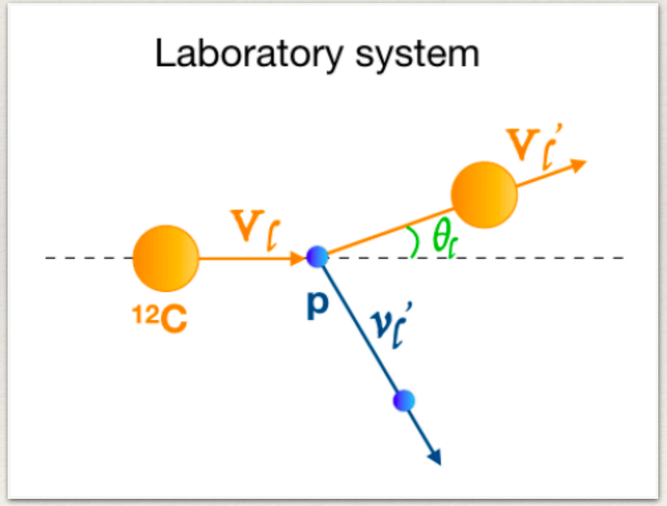

ENDF/B-VII Incident-Proton Data

Elastic cross-section

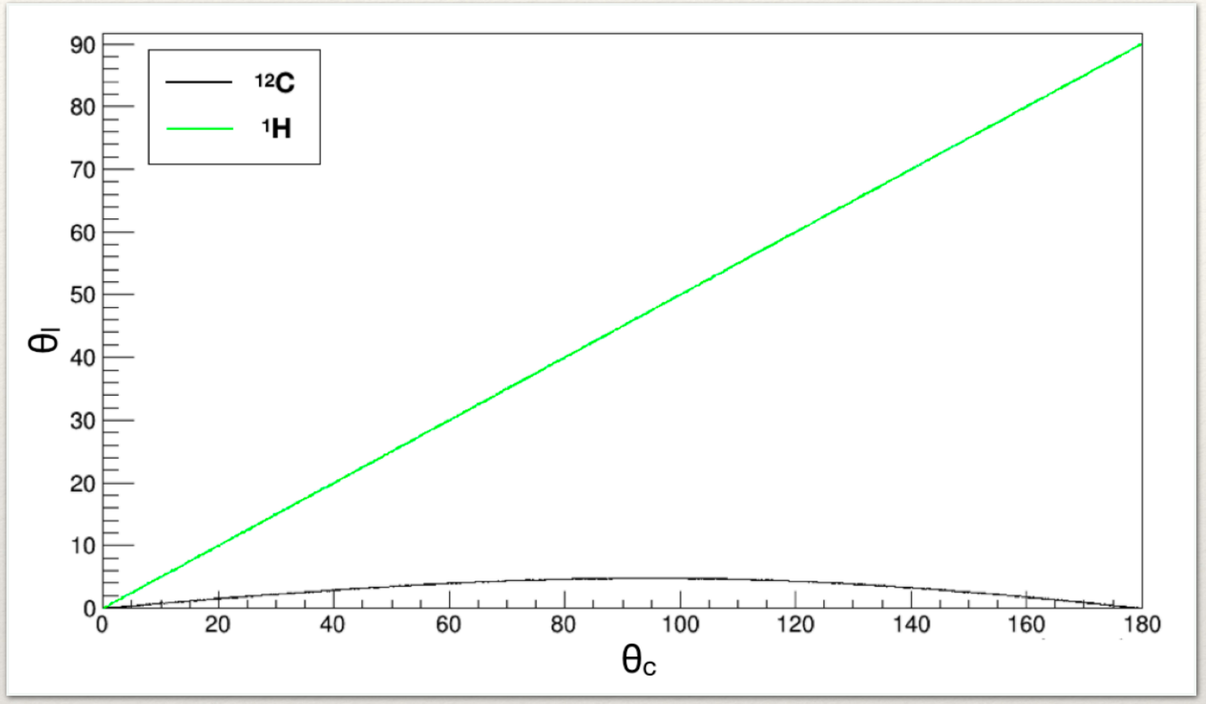

Distribution of the angle of scattering, θ_l , of the proton and of the carbon int he laboratory system versus the angle in the center of mass, θ_c.

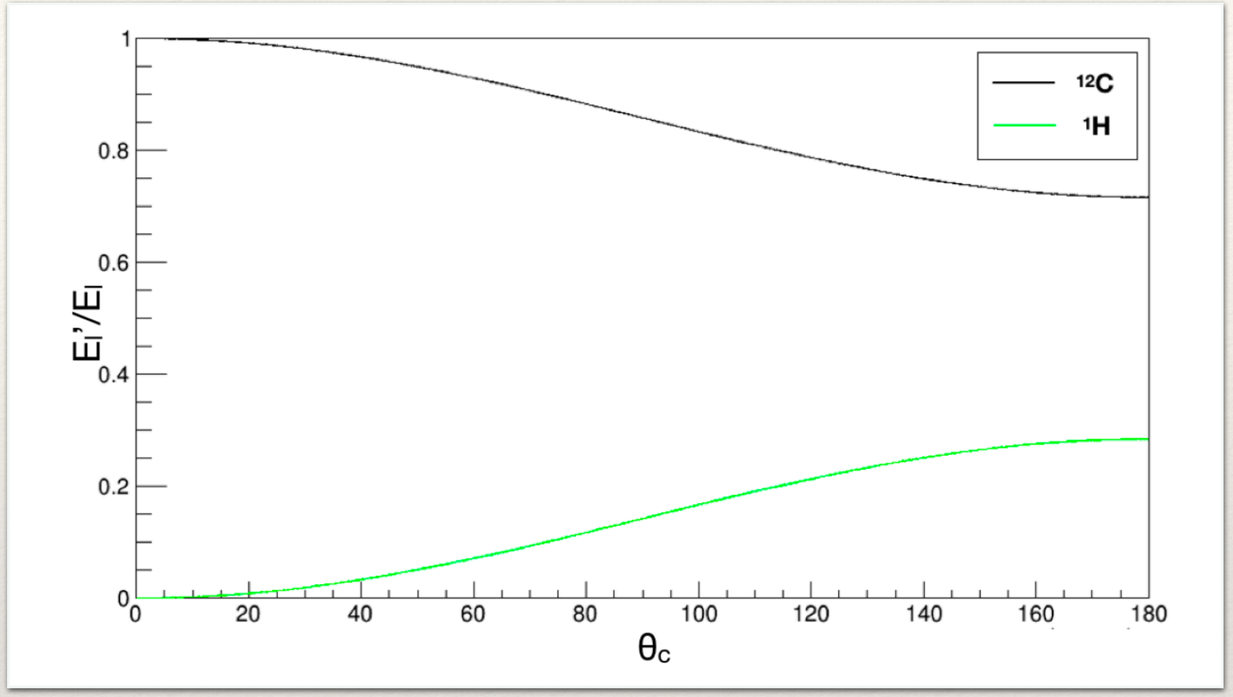

Distribution of the fraction of energy lost and gain after the elastic event, respectively by the carbon ion and by the proton in the laboratory system versus the angle in the center of mass, θ_c.

Elastic cross-section

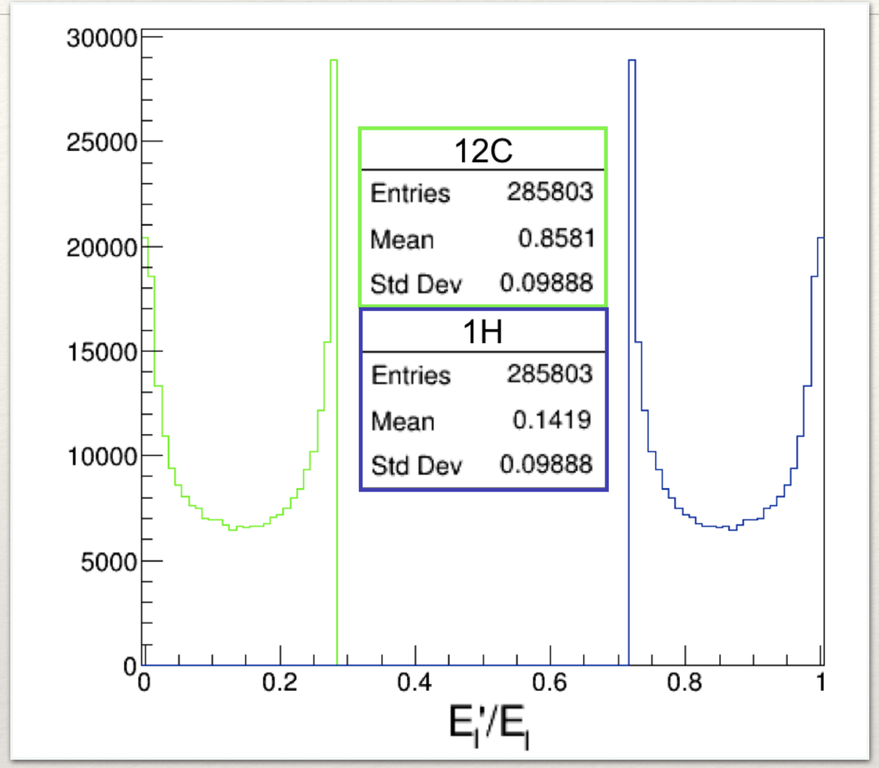

Fraction of energy loss and gain by the proton (green) and the carbon ion (blue) respectively. The result has been obtained by observing particles escaping from a thin target of hydrogen crossed by a carbon ion beam in a FRED simulation with the non-elastic event switched off. Primary carbon ions which were not affected by the elastic event have not been represented in the plot.

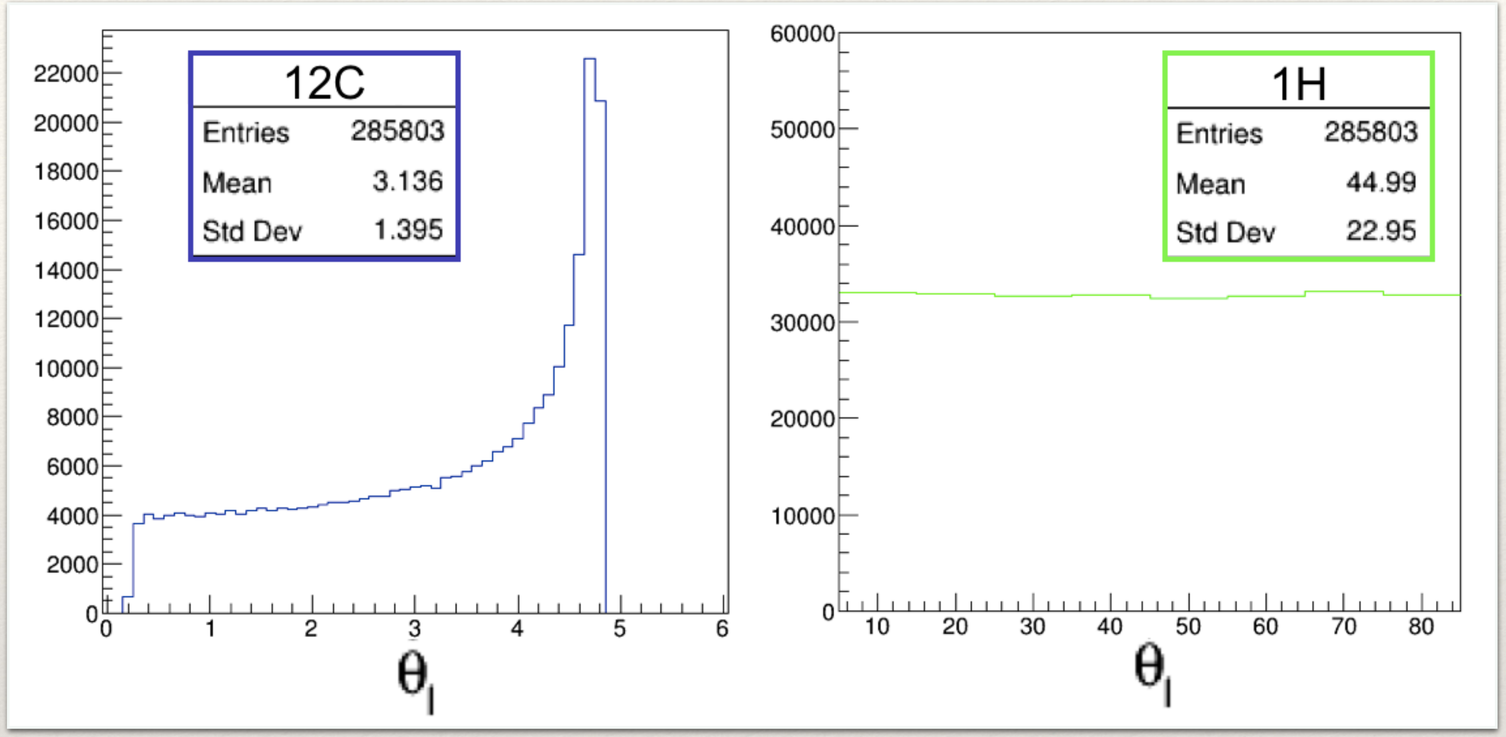

Scattering angle due to an elastic event for the proton (right) and the carbon ion (left) respectively. The result has been obtained by observing particles escaping from a thin target of hydrogen crossed by a carbon ion beam in a FRED simulation with the non-elastic event switched off. Primary carbon ions which were not affected by the elastic event have not been represented in the plot.

Kox

The Kox formula is based on the strong absorption model and it expresses the total reaction cross-section in terms of the interaction radius R_{int}, the nucleus-nucleus interaction barrier B_c and the center-of-mass energy of the colliding system E_{cm}:

$$\sigma_K(N_p, N_t, E_{cm}) = \pi R_{int}^2 \left[1 - \frac{B_c}{E_{cm}}\right],$$

where the Coulomb barrier B_c of the projectile-target system is given by:

$$B_c = \frac{Z_t Z_p e^2}{r_c(A_t^{1/3} + A_p^{1/3})},$$

where $r_c = 1.3$ fm, e is the electron charge and A_t, A_p, Z_t and Z_p are the mass and atomic numbers of the target and of the projectile nuclei.

The interaction radius R_{int} is divided in a volume and a surface terms:

$$R_{int} = R_{vol} + R_{surf},$$

$$R_{vol} = r_0(A_t^{1/3} + A_p^{1/3}),$$

$$R_{surf} = r_0 \left[a \frac{A_t^{1/3} A_p^{1/3}}{A_t^{1/3} + A_p^{1/3}} - c\right] + D.$$

$r_0 = 1.1$ fm and $a = 1.85$. The energy dependent term c is calculated using the analytical function:

$$c = -\frac{10}{x^5} + 2.0, \quad \text{if} \quad x \geq 1.5;$$

$$c = (-\frac{10}{x^5} + 2.0) \times \left(\frac{x}{1.5}\right)^3, \quad \text{if} \quad x < 1.5;$$

$$x = \log_{10}(E_k),$$

where E_k is the projectile kinetic energy in MeV/u in the laboratory system.

The neutron-excess D is given by the formula:

$$D = \frac{5(A_t - 2Z_t)Z_p}{A_p A_t}.$$

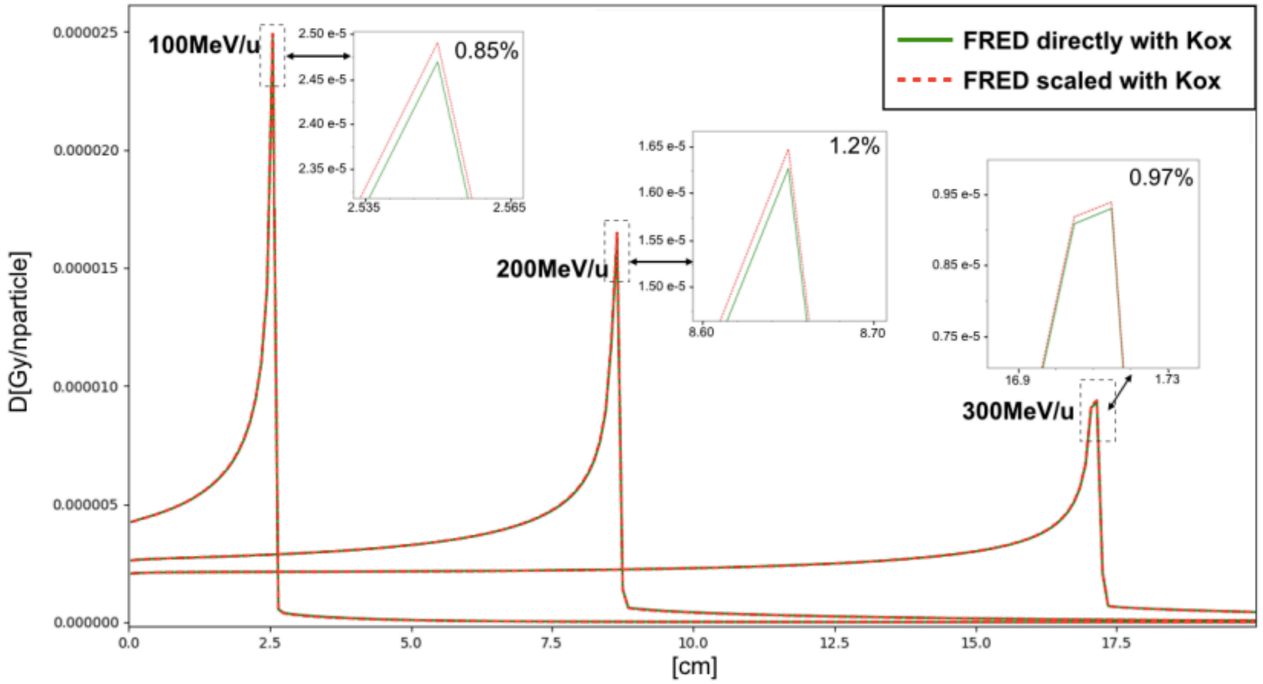

Longitudinal integrated dose for carbon ion beams in water at different energies. The dose is relative to one primary particle but the simulation has been run with a statistics of about 10^6 histories . Comparison between using directly Kox formula (green) and using it just to correct the mass attenuation of C-C (red), with the same scoring grid, and the same statistics is presented. The inserts show the peak details and the value of the difference in percent.

Sampling of fragments' energy and angles

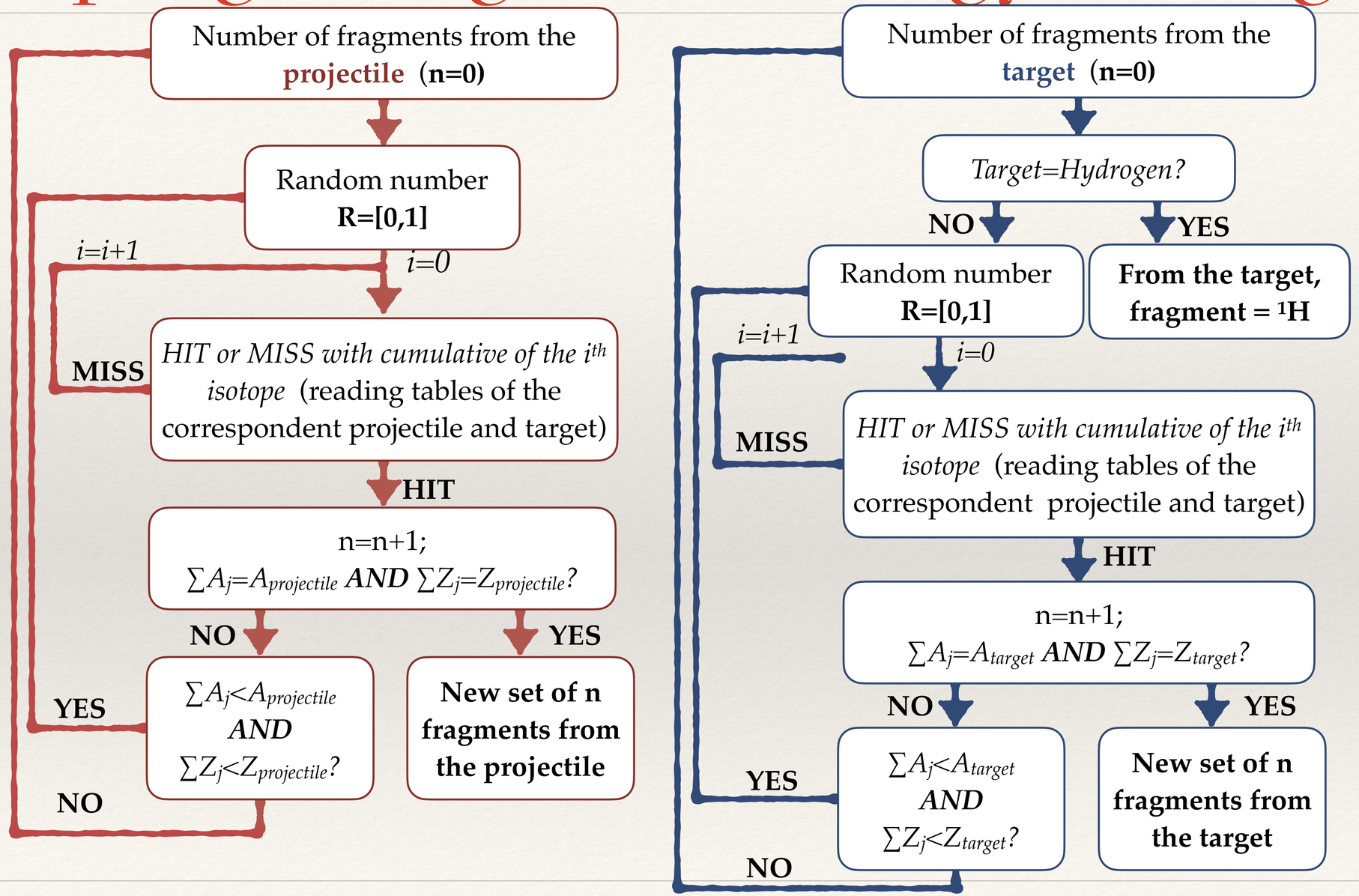

Scaling

ENERGY

The energy of emission of an i-th fragment is scaled in the following way:

$$E^i = E^i_{95\text{MeV/u}} \frac{E_{proj}[\text{MeV/u}]}{95}(1-k), \quad 1$$

where $E^i_{95\text{MeV/u}}$ is the energy extracted from the Gaussian distribution of the Ganil experiment. This formula respects the properties that the fragment's energy per nucleon is on average the same as the projectile E_p, so it increases linearly with it. To take into account that the energy of fragments from the same event is correlated and that the total energy of all fragments from the same event must not exceed the energy of the projectile, a correlation factor, c, has been added in the following way:

$$k = c(1-R),$$

where R, for each i-th fragments, depends on the energy of the previous i-1 fragments:

$$R = \frac{E^i_{nucl}}{E_p},$$

$$E^i_{nucl} = \frac{\sum_{j=0}^{j=i} E_j A_j}{\sum_{j=0}^{j=i} A_j},$$

where E_j and A_j are the energy and the atomic number of the previously generated fragments in the current event.
The conservation of energy is preserved and the computational time is reduced since the code does not discard combinations of possible fragments due to their energy. Energies are extracted from a range in agreement with the conservation of the energy.

ANGLE

The scaling factor for an angle of emission of an i-th fragment, θ^i, can be deduce starting from te relation:

$$|\vec{p}|sin\theta = p_\perp,$$

where $|\vec{p}|$ and $p_\perp$ are the magnitude of momentum and the transverse momentum of the fragment and θ is the angle described by $\vec{p}$ with respect to the beam trajectory. Considering that the angles of emission are small, it is possible to write:

$$\theta \sim sin\theta = \frac{p_\perp}{|\vec{p}|}. \quad 2$$

The transverse momentum does not depend on the projectile energy, whom momentum is parallel to the direction of the beam. As a consequence, the dependence of the angle on the beam energy is due only to the denominator of Eq. 2

$$\frac{\theta}{\theta_{95\text{MeV/u}}} = \frac{|\vec{p}_{95\text{MeV/u}}|}{|\vec{p}|},$$

where $\theta_{95\text{MeV/u}}$ is the angle extracted from the Gaussian distribution of the Ganil experiment and $|\vec{p}_{95\text{MeV/u}}|$ the correspondent momentum.
Making explicit $|\vec{p}|$ in function of the kinetic energy of the fragment, the equation becomes:

$$\frac{\theta}{\theta_{95\text{MeV/u}}} = \frac{\sqrt{E_{95\text{MeV/u}}}}{\sqrt{E}},$$

where $E_{95\text{MeV/u}}$ and E are the kinetic energy of the fragments of the Ganil experiment and of the one of the fragment emitted from a generic energy of the beam. Knowing the scaling factor of the energy of the fragment (Eq. 1), the relation between an angle of emission θ^i produced by a beam of energy E_{proj} and the angle of Ganil data, $\theta^i_{95MeV/u}$, is:

$$\theta^i = \theta^i_{95\text{MeV/u}} \sqrt{\frac{95}{E_{proj}[\text{MeV/u}]}}.$$

It is possible to observe that, as physically expected, the angle decreases with the energy of the beam.

Iterative formalisme

Considering N possible fragments that could be produced in the fragmentation, the probability of sampling a fragment, S_i, has been expressed as C^{α} with the constraint:

$$\sum_{i=0}^{N-1} S_i = \sum_{i=0}^{N-1} C^{\alpha_i} = 1,$$

$$\vec{\alpha} = log\vec{S}.$$

The same notation for the probability of sampling obtained in the Ganil experiment, P^{exp}, is:

$$\vec{Y}^{exp} = log\vec{P}^{exp}.$$

The sampling process has been considered as a function which, starting from the sampling probability S_i, produces generation probabilities Y_i at the end of the procedure:

$$\vec{Y} = f(\vec{\alpha}).$$

Of course the sampling procedure is statistical in nature. The Eq. 4.32 is related to the probabilities obtained after averaging on a sufficient number of the sampling procedure. The $\vec{Y}$ obtained should be equal to $\vec{Y}^{exp}$. It is possible to require that the equality between $\vec{Y}$ and $\vec{Y}^{exp}$ satisfied "as closely as possible" by minimizing the χ^2 statistic:

$$\chi^2 = \sum_{k=1}^{k=N} \frac{(Y_k^{exp} - Y_k)^2}{\sigma_k^2} = \sum_{k=1}^{k=N} \frac{(Y_k^{exp} - f_k(\alpha))^2}{\sigma_k^2},$$

where N is the number of fragments. The values of α_i must be chosen so as to minimize χ^2.
It is possible to obtain σ_k, which is the uncertainty relative to Y_k^{exp}, looking Eq. 4.31 from which:

$$\sigma_k = \frac{\partial Y_k^{exp}}{\partial P_k^{exp}} \sigma_k^{exp},$$

where σ_k^{exp} are the experimental uncertainties associated to the probability of producing a fragment k measured by the Ganil experiment. Knowing that $\partial Y_k^{exp}/P_k^{exp} = 1/P_k^{exp}$, Eq. 4.34 can be express also as:

$$\sigma_k = \frac{\sigma_k^{exp}}{P_k^{exp}}.$$

The requirement that the χ^2 function be at a minimum is usually guaranteed by:

$$\frac{\partial \chi^2}{\alpha_i} = 0.$$

Unfortunately, no general method exists for solving these equations since $f_k(\alpha)$ and its first derivatives can, in general, be highly nonlinear functions of the parameters α_i. So, to minimize χ^2, it is necessary to define two matrices and expand to first order the function $f(\alpha)$. The first matrix is the matrix of coefficients:

$$A_{ij} = \frac{\partial Y_i}{\partial \alpha_j},$$

which describes as the logarithm of the generation probability changes with the logarithm of the sampling probability. The matrix A_{ij} has been calculated by a MC code, increasing by $\partial\alpha$ the parameters $\vec{\alpha}$ and evaluating the variation of $\vec{dY}$ observing values of $\vec{Y}$. A critical part in computing this derivative matrix with MC evaluation is chosen an adequate statistic. We took care that the minimization results remain stable with respect to the statistic used to compute the A derivative matrix.

The second matrix is the inverse of the measurement covariance matrix, called weight matrix:

$$V_{ij}^{-1} = \frac{1}{\sigma_{ij}^2}.$$

The functions $\vec{Y} = f(\vec{\alpha})$ vary slowly enough so that one can expand to first order about an approximate solution:

$$\vec{Y}_{i+1} = \vec{Y}_i + \vec{A}\vec{\eta}_i,$$

where $\eta_i = \alpha_i - \alpha_{iA}$. Under this approximation, the χ^2 function can be written as:

$$\chi^2 = (\Delta\vec{Y} - \vec{A}\vec{\eta})^T \vec{V}_y^{-1} (\Delta\vec{Y} - \vec{A}\vec{\eta}).$$

It can be proved that the parameters η_i obtained by minimizing χ^2 function are unbiased and have minimum variance σ_i^2.
Taking the partial derivative with respect to the parameters η one obtains the equations:

$$\vec{A}^T \vec{V}_y^{-1} (\Delta\vec{Y} - \vec{A}\vec{\eta}) = 0,$$

which can be written as:

$$\vec{A}^T \vec{V}_y^{-1} \vec{A}\vec{\eta} = \vec{A}^T \vec{V}_y^{-1} \Delta\vec{Y}.$$

Defining $\vec{V}_A = (\vec{A}^T \vec{V}_y^{-1} \vec{A})^{-1}$, it is possible to express the $\vec{\eta}$ equations as:

$$\vec{\eta} = \vec{V}_A \vec{A}^T \vec{V}_y^{-1} \Delta\vec{Y}.$$

The parameters α, used for built the input cumulative for the code, have been determined from the equation $\alpha = \alpha_A + \eta$.

4He->H2O @200MeV/u

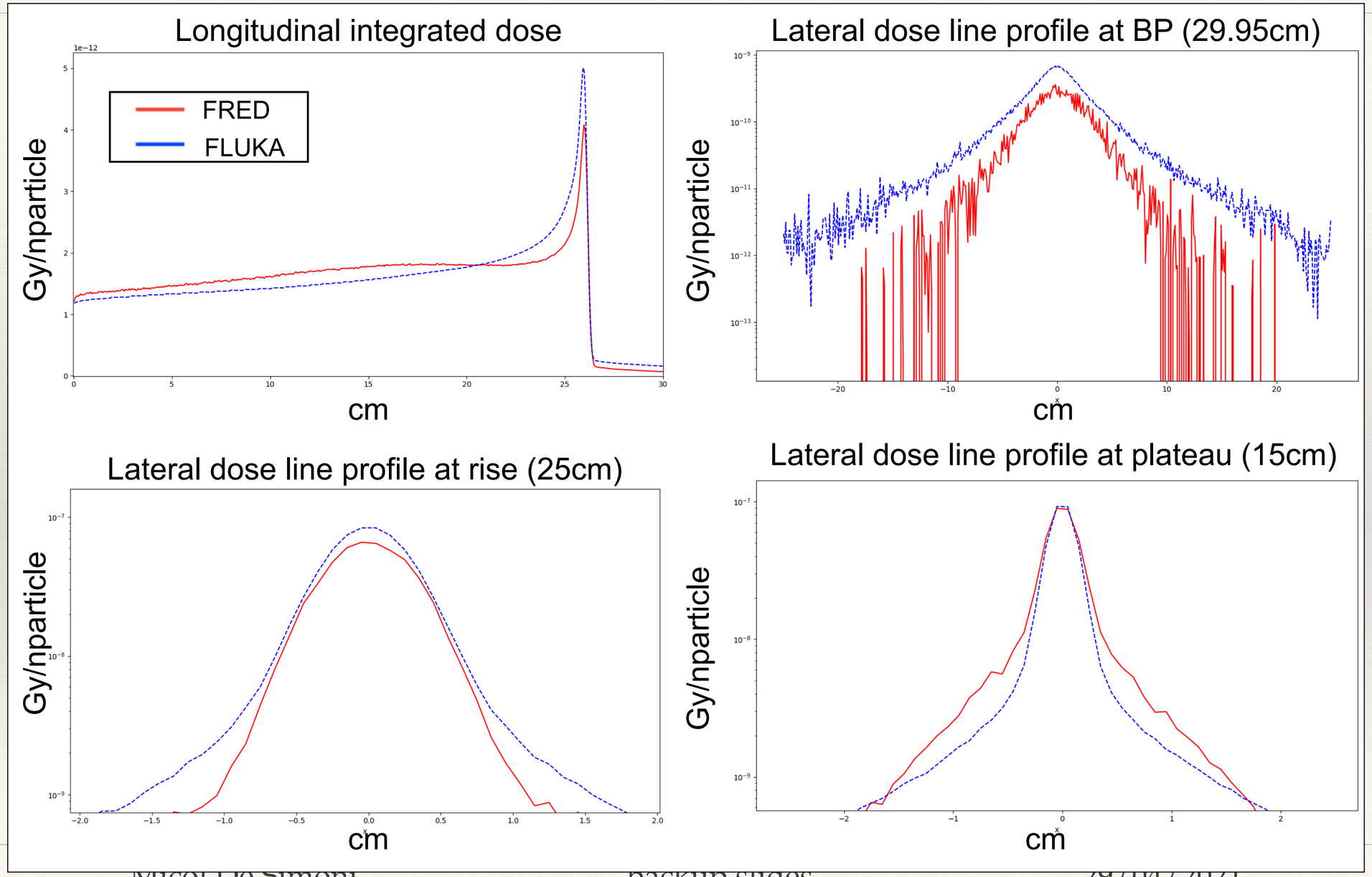

6Li->H2O @200MeV/u

Longitudinal integrated dose

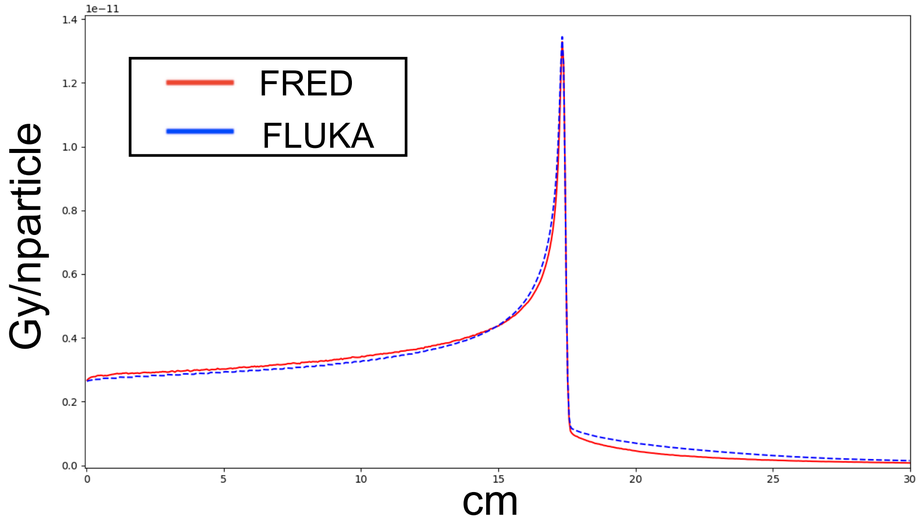

Lateral dose line profile at BP (17.3 cm)

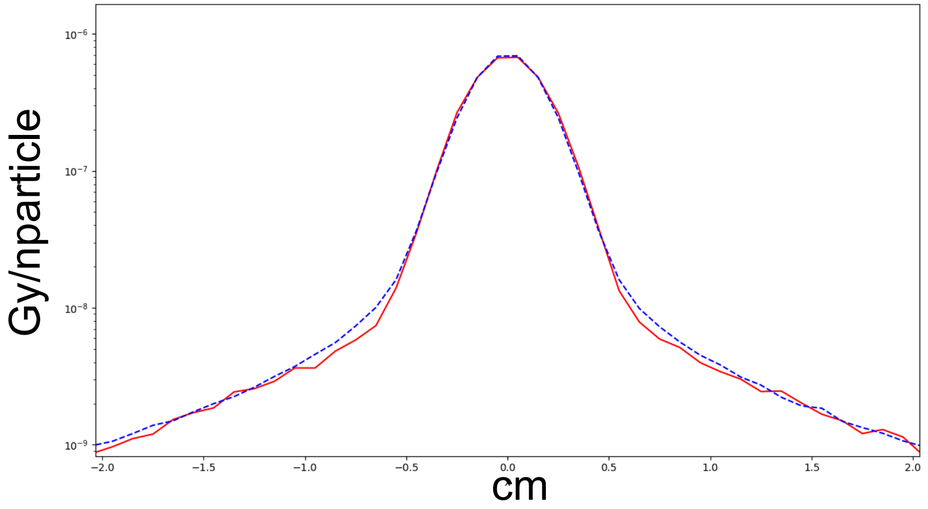

Lateral dose line profile at rise (16cm)

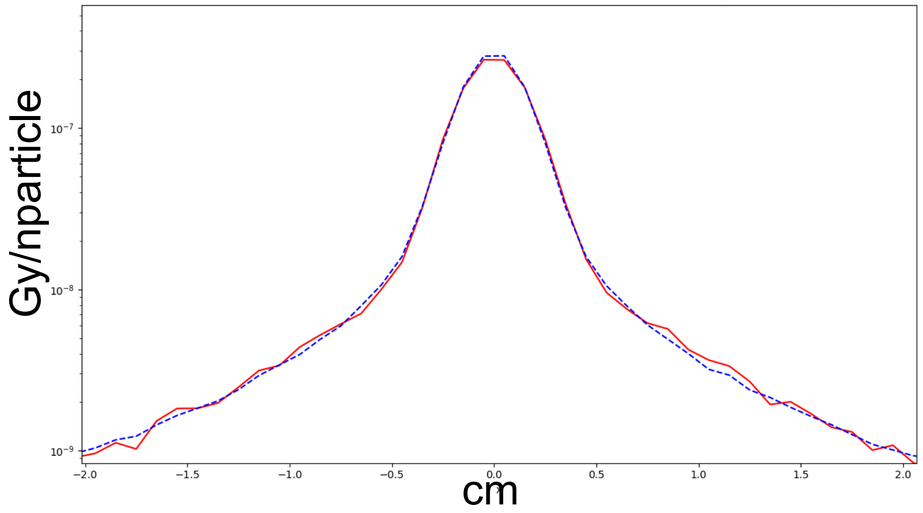

Lateral dose line profile at plateau (7cm)

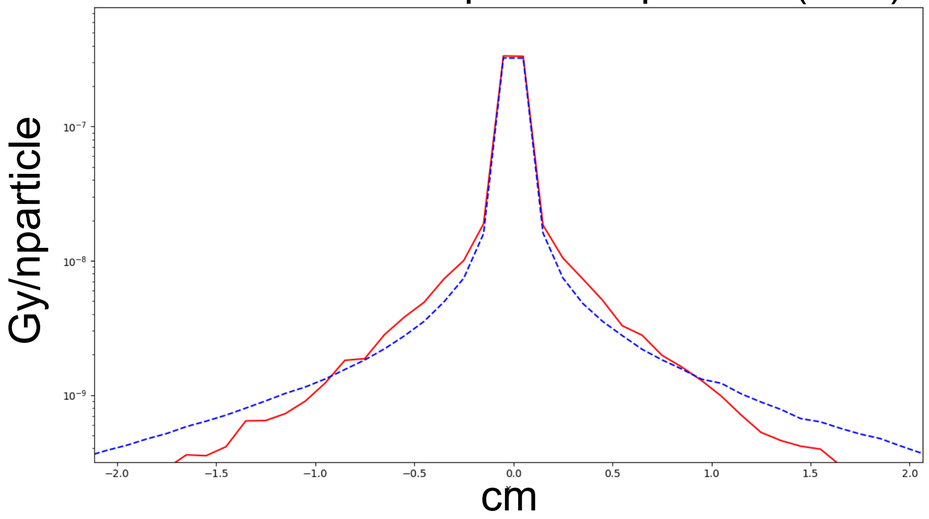

7Be->H2O @200MeV/u

Longitudinal integrated dose

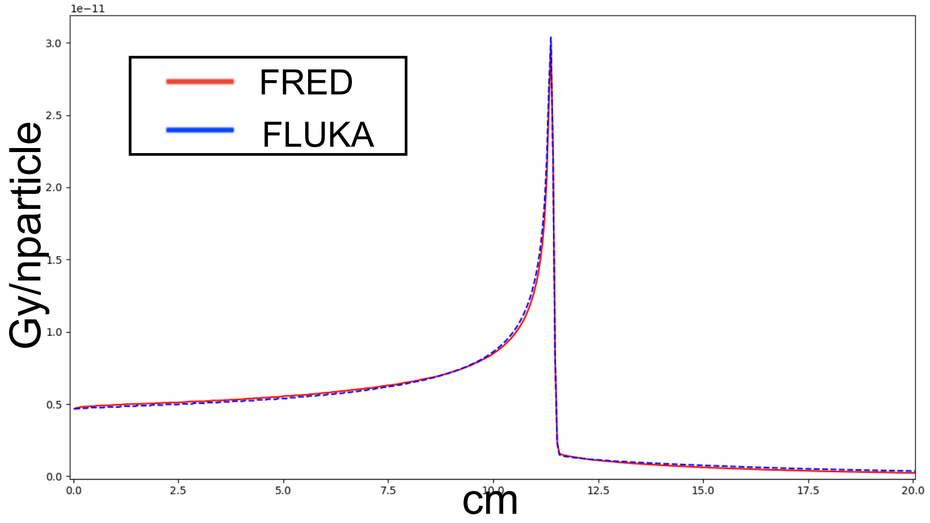

Lateral dose line profile at BP (11.37 cm)

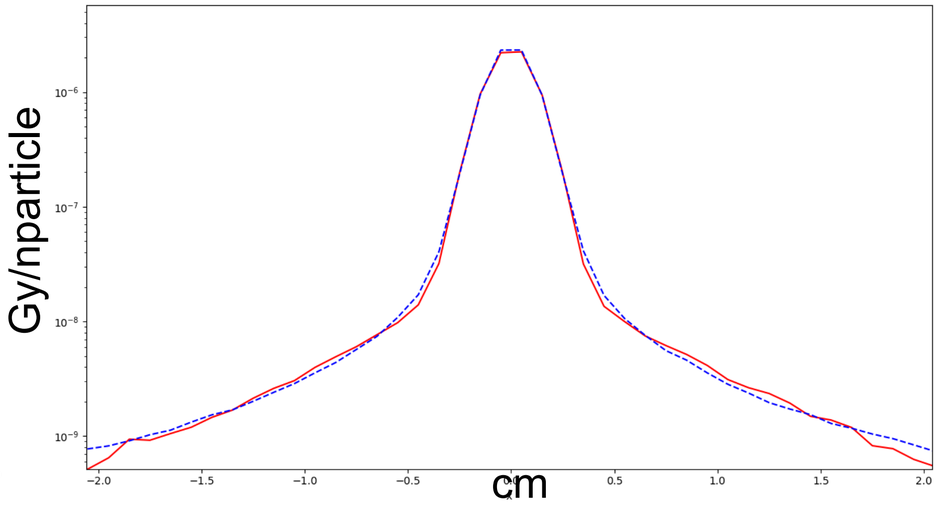

Lateral dose line profile at rise (11cm)

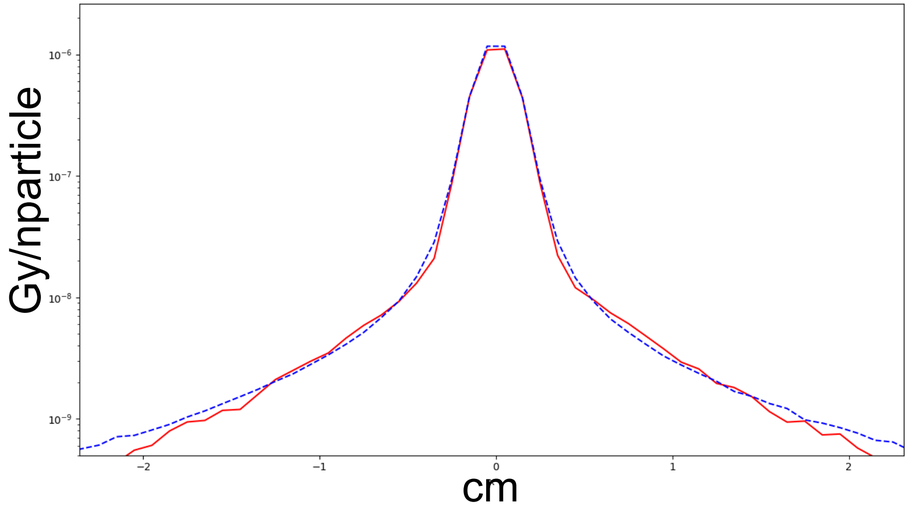

Lateral dose line profile at plateau (4cm)

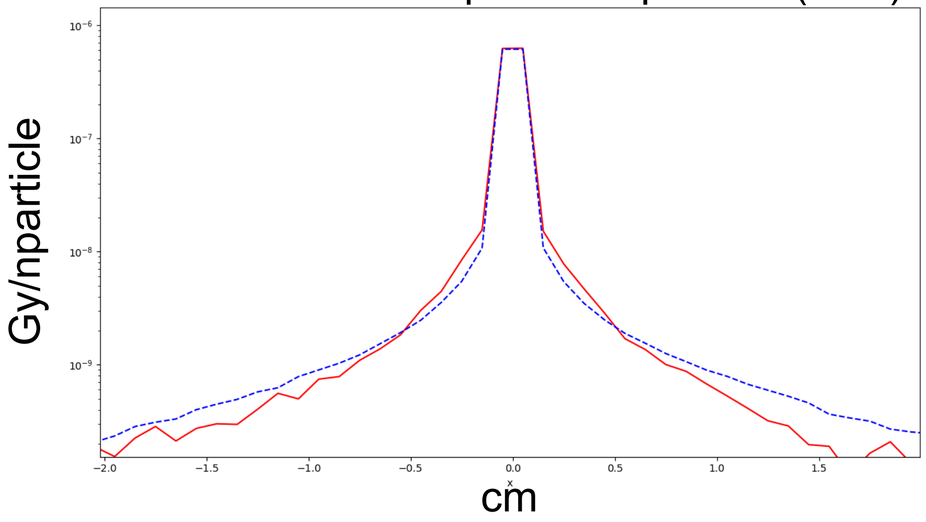

10B->H2O @200MeV/u

Longitudinal integrated dose

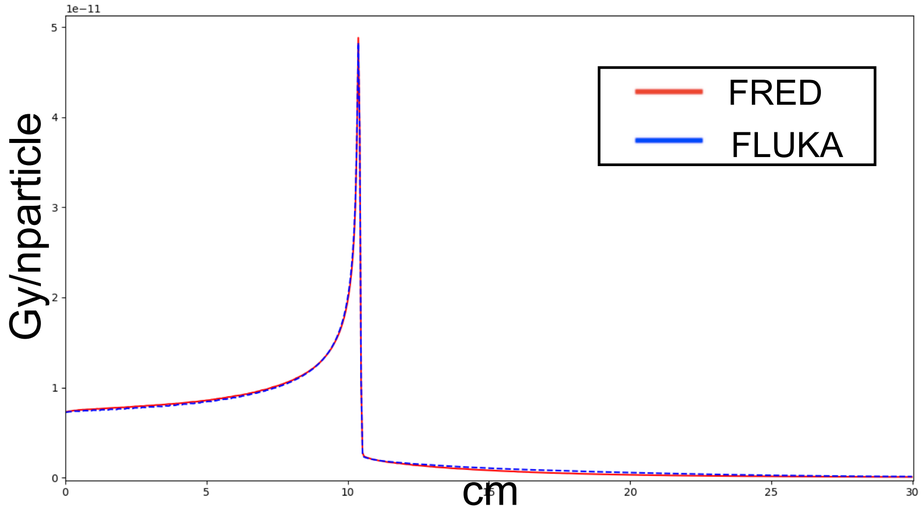

Lateral dose line profile at BP (10.35 cm)

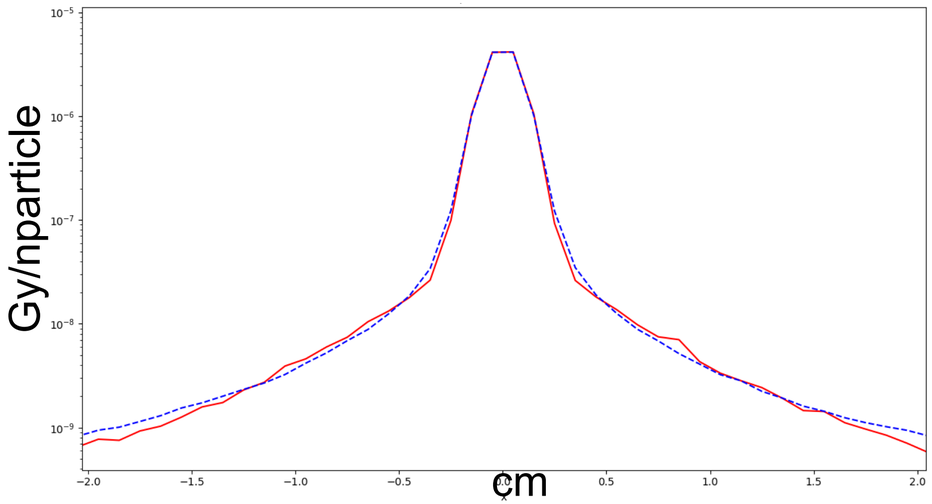

Lateral dose line profile at plateau (4cm)

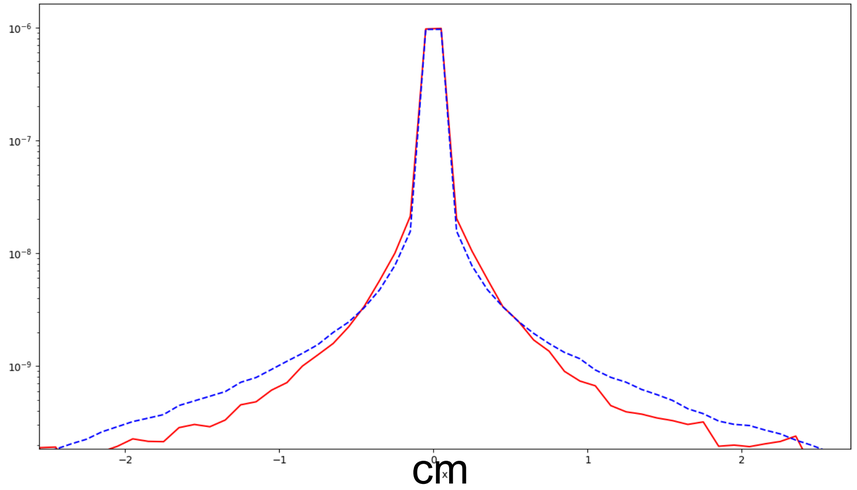

Heattner experiment

Study of the angular distribution and energy spectra of secondary fragments emitted by a 400 MeV/u beam of ^{12}C in water.

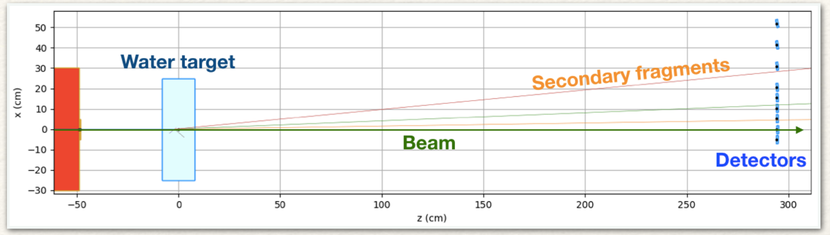

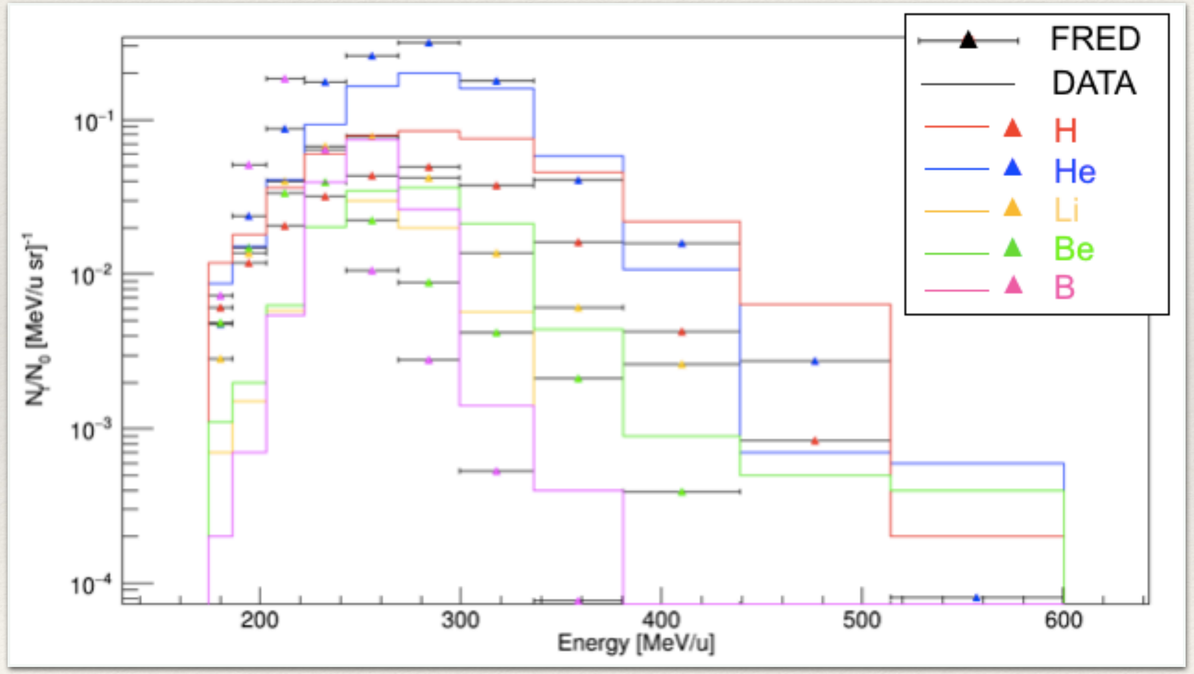

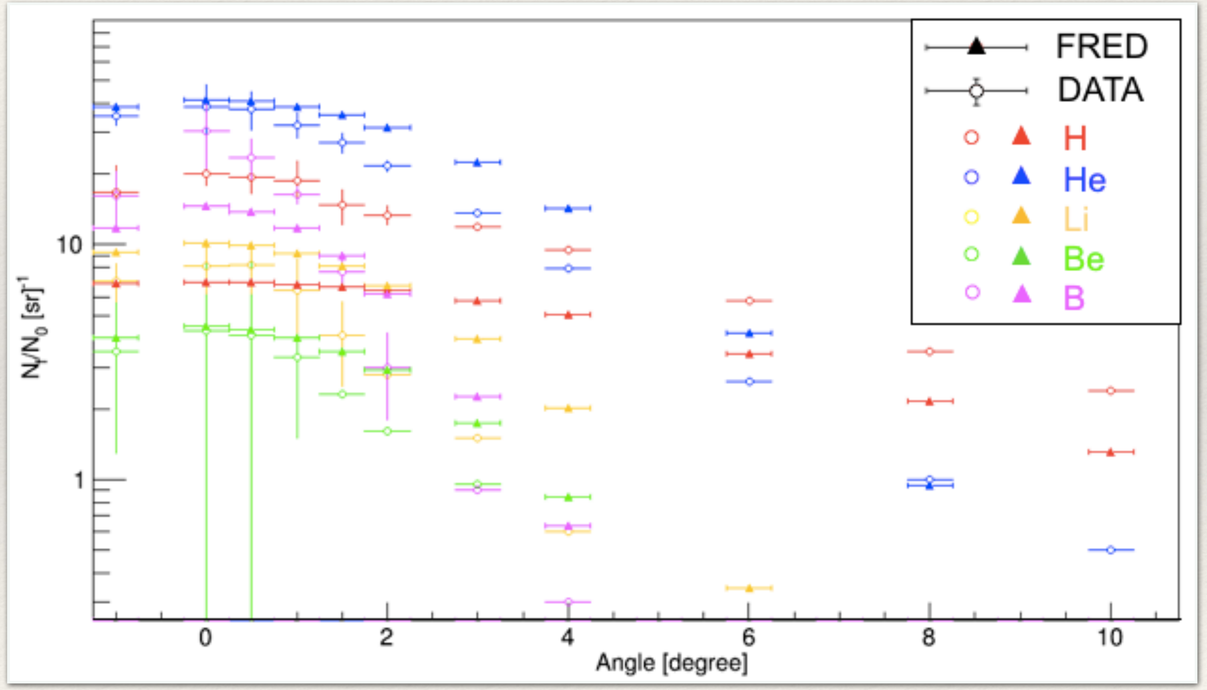

FLUKA

FLUKA can reproduce the position of the Bragg peaks of proton and carbon ion beams with a single ionization potential on average within the experimental uncertainties of about 100 μm. The average dose-weighted dose difference (D/D) is below 1% for protons and below 1.5% for carbon ions.

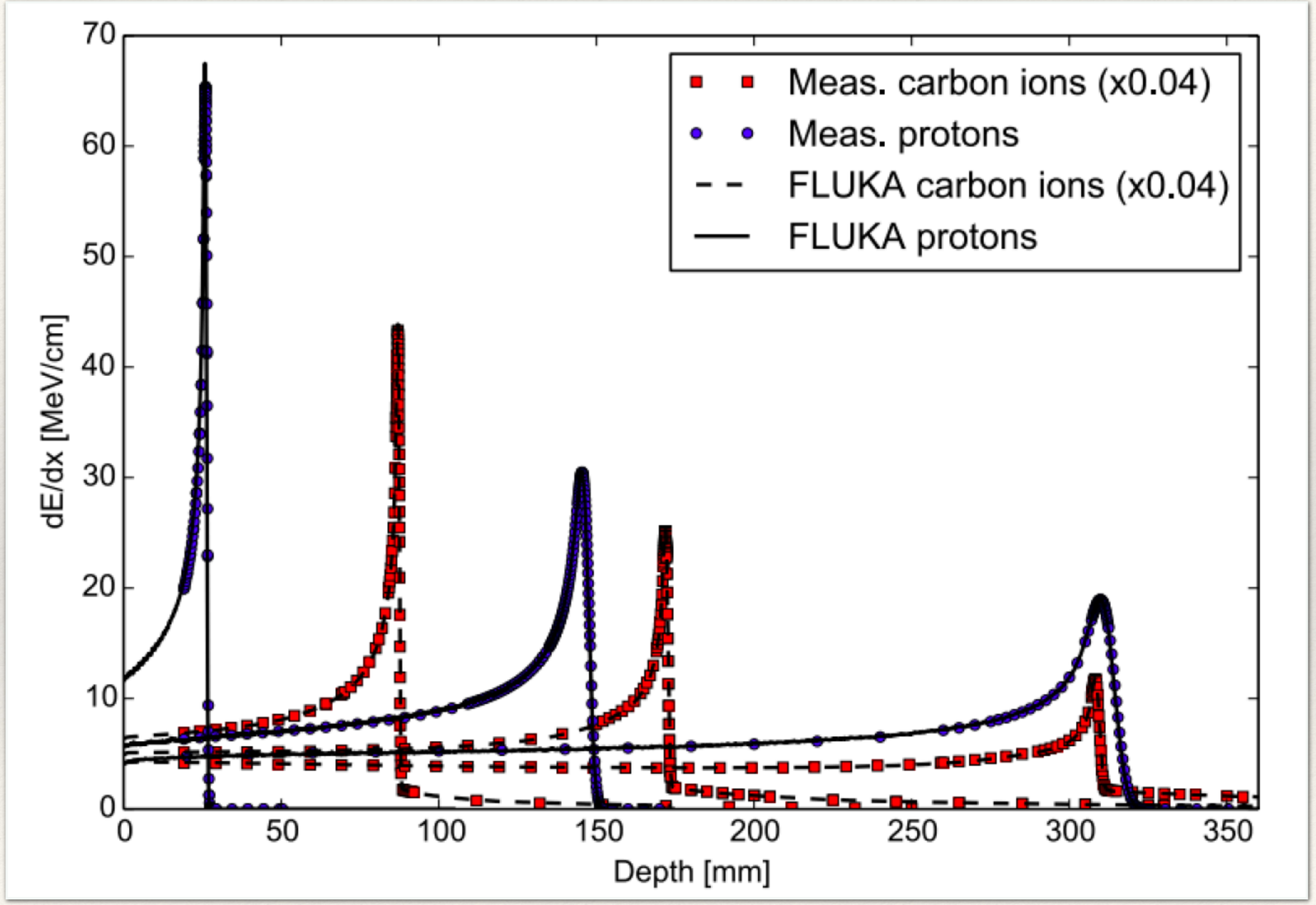

Battistoni G et al. Frontiers in Oncology 6 (2016)

Ganil experiment

$$\frac{d\sigma}{d\Omega}({}^{A}_{Z}X) = \frac{N_{{}^{A}_{Z}X} \times A_{target}}{N_{primary} \times \Omega \times \rho \times th \times N_A}$$

$$\frac{d\sigma}{d\Omega}({}^{A}_{Z}X, \theta) = \frac{N_{{}^{A}_{Z}X,\theta} \times A_{target}}{N_{primary} \times \Omega \times \rho \times th \times N_A \times \Delta E}$$

Ω =6.6

$\rho \times th = 0.04\grave{1}1$ g/cm^2

$\Delta E = 5$ MeV

Ganil experiment - FLUKA

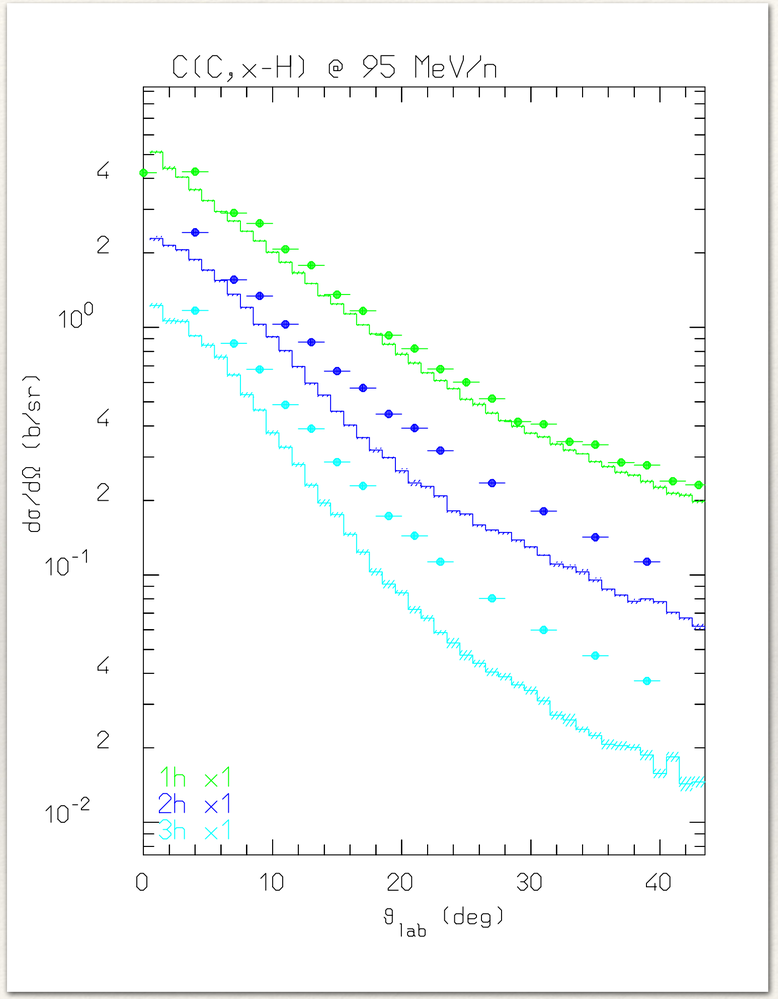

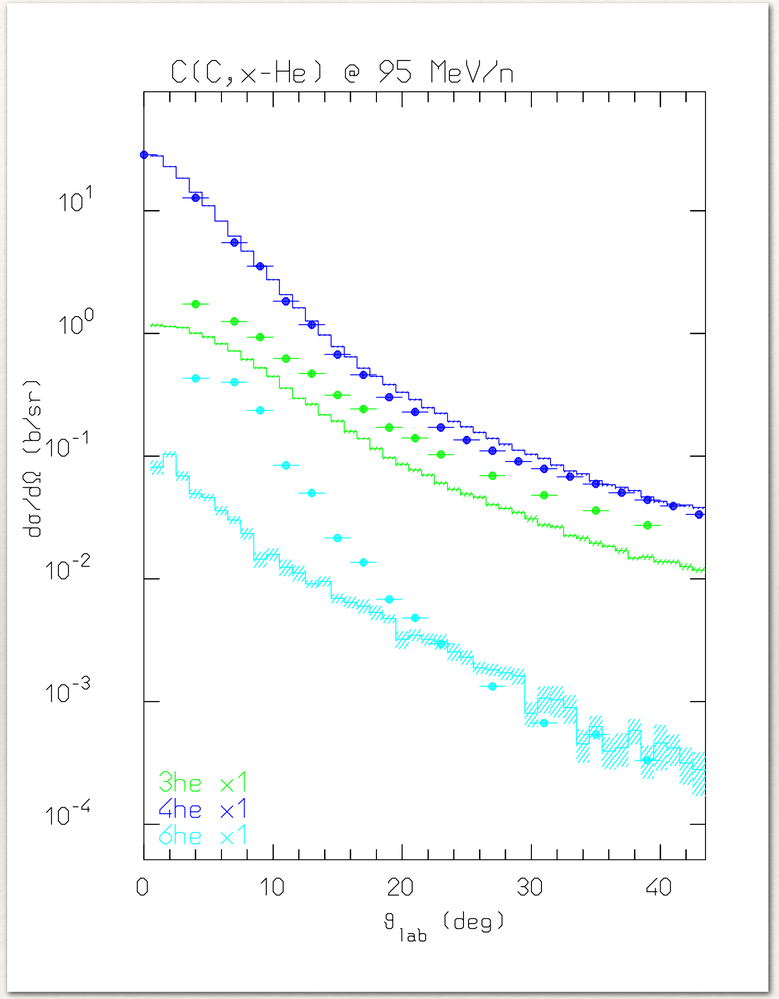

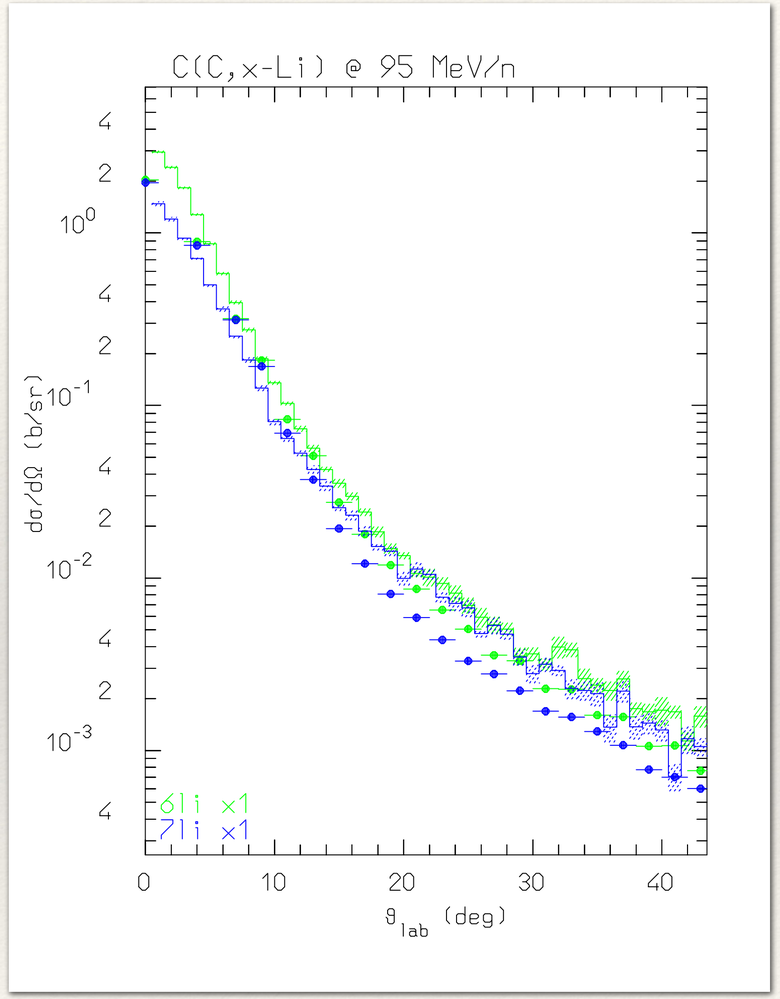

Ganil experiment - FLUKA